



University of Venda

**Multi-scale modelling of soil-transmitted
Helminths infections in humans**

by

MULALO MAKHUVHA

A Thesis Presented to the

UNIVERSITY OF VENDA

In Partial Fulfilment of the Requirements for the Degree

of

Master of science

in

APPLIED MATHEMATICS

Supervisor: Dr D. Mathebula

Co-Supervisor: Prof W. Garira

Declaration of Authorship

I, MULALO MAKHUVHA, declare that the dissertation titled, 'Multi-scale modelling of soil transmitted Helminths infection in humans' is my own work and it has never been submitted before for any degree or examination in any other university. Where I have quoted from the work of others, the source is always given.

Signed:

Date:

Abstract

In this study, we develop a multiscale model of soil transmitted helminths in humans with a special reference to hookworm infection. Firstly, we develop a single scale model that comprises of five between host scale populations namely; susceptible humans, infected humans, eggs in the physical environment, non-infective worms in the physical environment and infective worms in the physical environment. Secondly, we extend the single scale model to incorporate within-host scales namely; infective larvae within-host, immature worms in small intestine, mature worm population and within-host egg population which resulted to a multiscale model. The models are analysed both numerically and analytically. The models are epidemiologically and mathematically well posed. Numerical simulation results show that there is a bi-directional relationship between the between-host and within-host scales. This is in agreement with the sensitivity analysis results, we noted that the same parameters that reduce reproductive number R_0 are the same parameters that reduce the infective worms endemic equilibrium point. From the comparative effectiveness of hookworm interventions analysis results, we notice that any intervention combination that include wearing shoes controls and reduces the spread of the infection. The modelling framework developed in this study is vigorous to be applicable to other soil transmitted helminths infections.

Acknowledgements

I thank God almighty for granting me this great opportunity to write this work. Special thanks to my supervisors, Prof W. Garira and Dr D. Mathebula who accepted my plea to work with them as a masters student and through their guidance and support made my work reach this point. I cannot forget the modelling health and environmental linkages research group (MHELRG) for all their support, encouragement and our fights were not in vain. My parents, siblings, my children and my closest friends for the unconditional love and support and sacrifices you showed. I would like to express my sincere gratitude to Prof S. Shateyi for his endless prayers during the hard times and fruitful workshops that helped to complete this work. Many thanks to everybody who supported me either directly or indirectly in achieving the work presented here. I acknowledge with thanks the financial support from the DST-NRF Centre of Excellence in Mathematical and Statistical Sciences (CoE-MASS) Ref: BA2018/034.

Contents

Declaration of Authorship	i
Abstract	ii
Acknowledgements	iii
Contents	iv
List of Figures	vii
1 INTRODUCTION	1
1.1 Background on soil-transmitted helminths	1
1.2 The life cycle of soil-transmitted helminths of humans	2
1.2.1 Ascaris	2
1.2.2 Trichuris trichiura	3
1.2.3 Hookworm	4
1.3 Multiscale modelling of infectious diseases	8
1.4 Preventative and Treatment Measures	10
1.5 Problem statement of the study	10
1.6 Aim and Objectives of the Study	11
2 SINGLE-SCALE FRAMEWORK OF HOOKWORM INFECTION	13
2.1 Mathematical model	13

2.2	Human population	15
2.2.1	Susceptible human population	15
2.2.2	Infected human population	16
2.3	Physical environment parasite dynamics	16
2.3.1	Eggs populations	16
2.3.2	Worm population	16
2.4	Basic properties	17
2.4.1	Positivity of Solutions	18
2.4.2	Feasible Region	19
2.5	Determination of Disease free Equilibrium and its stability	21
2.5.1	Reproductive number of the model system	21
2.5.2	Local stability of DFE	23
2.5.3	Global stability of DFE	26
2.6	Endemic Equilibrium state and its stability	27
2.6.1	Endemic equilibrium	28
2.6.1.1	Existence of Endemic Equilibrium state	29
2.6.2	Global stability of Endemic Equilibrium state	30
2.7	Numerical solutions	35
2.7.1	Sensitivity analysis	35
2.7.2	Numerical solutions of the between-host dynamics of Hookworm infection	38
3	MULTISCALE MODELLING OF HOOKWORM INFECTION	43
3.1	Multi-scale model	43
3.2	Human population	45
3.3	Within-host dynamics	46
3.4	Physical sand environment dynamics	47
3.5	Basic properties	48
3.5.1	Positivity of Solution	49
3.5.2	Feasible Region	50

3.6	Disease free equilibrium and its stability(DFE)	53
3.6.1	Reproductive Number R_0	54
3.6.2	Local stability of DFE	56
3.6.3	Global Stability DFE	61
3.7	Endemic state and its stability	63
3.7.1	The Endemic equilibrium state	64
3.7.2	Existence of endemic equilibrium state	66
3.7.3	Local stability of Endemic equilibrium points	69
3.8	Numerical solutions	76
3.8.1	Sensitivity analysis	76
3.9	Results	81
3.9.1	The influence of between-host scale on within-host scale of the hookworm infection	81
3.10	The influence of With-host scale parameters on between-host scale variables	86
4	HOOKWORM MULTI-SCALE MODEL WITH INTERVENTION	90
4.1	The Multi-scale model for hookworm with health intervention combinations	90
4.2	Endemic points	93
4.3	Evaluation of the comparative effectiveness of Hookworm interventions	95
4.4	Comparative effectiveness of Hookworm intervention using R_{0E} as indicator	96
4.5	Comparative effectiveness of Hookworm intervention using \tilde{L}_M as indicator	98
5	DISCUSSION AND CONCLUSION	101

List of Figures

1.1	Life cycle of Ascaris [4].	3
1.2	Life cycle of Trichuris trichiura [4].	4
1.3	Life cycle of Hookworm [28].	5
2.1	A schematic representation of the epidemiological model of Hookworm infection.	14
2.2	Graphs of numerical solutions of the model system (2.3.8). Top left to right showing propagation of Infected humans in population level I_H , worms in the physical environment E_L , and from bottom left to right showing propagation of Non-infective worms L_H and Infective worms L_M , respectively. The solutions are presented for different values for average eggs produced in a day rate, N_H : $N_H = 10$, $N_H = 100$ and $N_H = 1000$	39
2.3	Graphs of numerical solutions of the model system (2.3.8). Top left to right showing propagation of Infected humans in population level I_H , worms in the physical environment E_L and from bottom left to right showing propagation of non-infective worms L_H and Infective worms L_M , respectively. The solutions are presented for different values of the infective contact rate, β_H : $\beta_H = 0.01$, $\beta_H = 0.1055$ and $\beta_H = 0.55$	40
2.4	Graphs of numerical solutions of the model system (2.3.8). Top left to right showing propagation of Infected humans in population level I_H , worms in the physical environment E_L and from bottom left to right showing propagation of non-infective worms L_H and Infective worms L_M , respectively. The solutions are presented for different values for hatching rate: α_L : $\alpha_L = 0.0055$, $\alpha_L = 0.05$ and $\alpha_L = 0.5$	41
2.5	Graphs of numerical solutions of the model system (2.3.8). Top left to right showing propagation of Infected humans in population level I_H , worms in the physical environment E_L and from bottom left to right showing propagation of non-infective worms L_H and Infective worms L_M , respectively. The solutions are presented for different values of the rate of being infective, α_H : $\alpha_H = 0.0055$, $\alpha_H = 0.05$ and $\alpha_H = 0.5$	42
3.1	A schematic representation of the transmission-cycle of Hookworm infection.	44
3.2	Graphs of numerical solutions of the model system (3.4.9). Top left to right showing propagation of Infective larvae within a human host L_w and worms in the small intestine L_s , respectively. Bottom left to right showing propagation of matured worms and hookworm eggs within the human host, respectively. The solutions are presented for different values of the infective contact rate, β_H : $\beta_H = 0.6$, $\beta_H = 0.06$ and $\beta_H = 0.006$	82

3.3	Graphs of numerical solutions of the model system (3.4.9). Top left to right showing propagation of Infective larvae within a human host L_w and worms in the small intestine L_s , respectively. Bottom left to right showing propagation of matured worms and hookworm eggs within the human host, respectively. The solutions are presented for different values of recruitment rate of new susceptible humans, Λ_H : $\Lambda_H = 10$, $\Lambda_H = 100$ and $\Lambda_H = 1000$	83
3.4	Graphs of numerical solutions of the model system (3.4.9). Top left to right showing propagation of Infective larvae within a human host L_w and worms in the small intestine L_s , respectively. Bottom left to right showing propagation of matured worms and hookworm eggs within the human host, respectively. The solutions are presented for different values of recruitment rate of new susceptible humans, N_H : $N_H = 300$, $N_H = 1200$ and $N_H = 2000$	84
3.5	Graphs of numerical solutions of the model system (3.4.9). Top left to right showing propagation of Infective larvae within a human host L_w and worms in the small intestine L_s , respectively. Bottom left to right showing propagation of matured worms and hookworm eggs within the human host, respectively. The solutions are presented for different values of recruitment rate of new susceptible humans, α_H : $\alpha_H = 0.0006$, $\alpha_H = 0.05$ and $\alpha_H = 0.005$	85
3.6	Graphs of numerical solutions of the model system (3.4.9). Top left to right showing propagation of Infected individuals I_H and hookworm eggs in the environment E_L , respectively. Bottom left to right showing propagation of immature worms in the environment E_L and infective larvae in the environment L_M , respectively. The solutions are presented for different values of migration rate of infective worm to small intestine, α_w : $\alpha_w = 0.5$, $\alpha_w = 0.05$ and $\alpha_w = 0.001$	86
3.7	Graphs of numerical solutions of the model system (3.4.9). Top left to right showing propagation of Infected individuals I_H and Hookworm eggs in the environment E_L , respectively. Bottom left to right showing propagation of immature worms in the environment E_L and infective larvae in the environment L_M , respectively. The solutions are presented for different values of excretion rate of hookworm eggs to the environment, α_h : $\alpha_h = 0.5$, $\alpha_h = 0.01$ and $\alpha_h = 0.003$	87
3.8	Graphs of numerical solutions of the model system (3.4.9). Top left to right showing propagation of Infected individuals I_H and hookworm eggs in the environment E_L , respectively. Bottom left to right showing propagation of immature worms in the environment E_L and Infective larvae in the environment L_M , respectively. The solutions are presented for different values of natural death of eggs in within-host, μ_h : $\mu_h = 0.0005$, $\mu_h = 0.003$ and $\mu_w = 0.05$	88
3.9	Graphs of numerical solutions of the model system (3.4.9). Top left to right showing propagation of infected individuals I_H and Hookworm eggs in the environment E_L , respectively. Bottom left to right showing propagation of immature worms in the environment E_L and infective larvae in the environment L_M , respectively. The solutions are presented for different values of average number of hookworm eggs produced within the human host, N_m : $N_m = 600$, $N_m = 1200$ and $N_m = 2000$	89

Chapter 1

INTRODUCTION

1.1 Background on soil-transmitted helminths

Soil-transmitted helminths are nematode worms that infect humans. They are transmitted by eggs present in human faeces which contaminate the soil, hence they can be called environmentally transmitted infections. These infections are prevalent in tropics and subtropic areas because of poor hygiene and sanitation facilities [7]. Bethony et al. (2006) suggested that some hosts harbour more parasites, hence this work incorporates the within-host dynamics. In the context of soil-transmitted helminths, disease severity increases proportionally to parasite burden. According to the World Health Organisation (WHO) approximately 1.5 billion people are infected with soil-transmitted helminths, of which one-third of the population are children [5]. A large part of the world's population is infected with one or more of these species: Ascaris, Whipworm and Hookworm [4]. They are transmitted either by physical penetration through the skin or ingesting of eggs with food. These soil helminths are often called intestinal infections due to the fact that the small intestine is the site of infection. Intestinal infections may result in malnutrition, iron-deficiency anaemia, malabsorption, stunting of growth and cognitive development.

The three parasitic worms namely: Ascaris, Whipworm and Hookworm are studied using similar approaches because they have common life cycles; reside in the intestines, their eggs get deposited in the physical environment and they are environmentally transmitted. There exists no vector in the transmissions. Soil-transmitted helminths remain a health burden in tropical regions with warm and moist climates. Over 267 million preschool-age children and over 568 million school-age children live in areas where these parasites are intensively transmitted and are in need of treatment and preventive interventions [6]. Soil-transmitted helminths impair the nutritional status of humans. These worms feed on host tissues and blood, hence infected people suffer from loss of iron and protein.

1.2 The life cycle of soil-transmitted helminths of humans

This section outlines the life cycles of the three soil-transmitted helminths of humans namely: Ascaris, Whipworm and Hookworm.

1.2.1 Ascaris

Ascaris lumbricoides is the largest nematode in the human intestine. This parasite live in the lumen of the small intestine. An infected human passes *Ascaris* eggs into the physical environment therefore contaminating the physical environment. In this study, physical environment refers to sandy soil. The eggs in the physical environment are unfertilised and not infective. They undergo some developmental changes to become infective. Infective eggs are swallowed by individuals through consumption of contaminated food that has not been carefully cooked, washed or peeled. The infective eggs hatch worms which invade the intestinal mucosa. From the mucosa the worms get carried to the lungs. These worms go through developmental stages which take 10 to 14 days to mature further in the lungs. Worms in the lungs penetrate through the alveolar walls, ascend to the bronchial tube to the throat and are swallowed. These worms develop into adult worms upon reaching the small intestine. Both female and male worms are present in the small intestine, each female worm produces approximately 200 000 eggs per day. The female worms are larger than the males and can be measured to 40cm in length and 60cm in diameter. The eggs are excreted in the faeces and get deposited in the physical environment. Adult worms do not multiply in the human host and they can live 1 to 2 years in the human body.

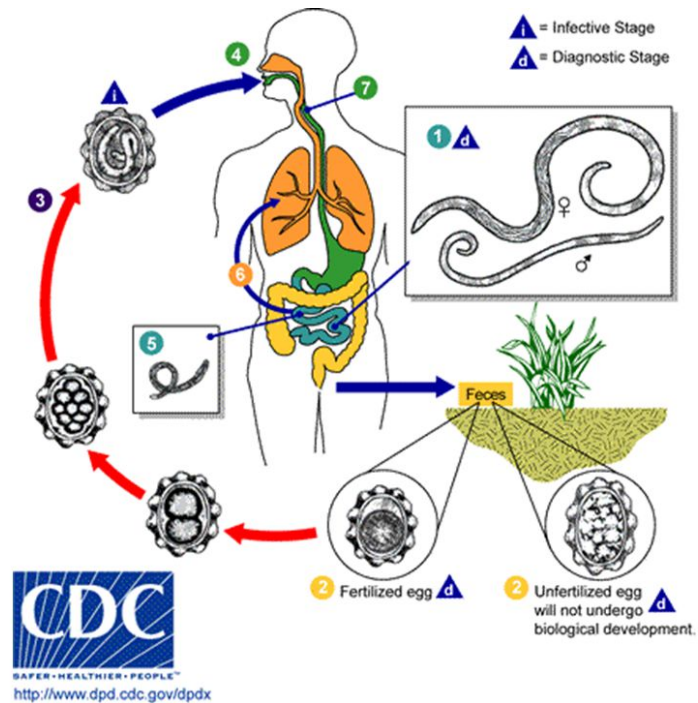


Figure 1.1: Life cycle of *Ascaris* [4].

The life cycle for *Ascaris* is represented in Figure (1.1).

1.2.2 *Trichuris trichiura*

Trichuris trichiura parasite is also known as human whipworm and its cycle is quite similar to *Ascaris*. This parasite is transmitted via contaminated soil, food or water contaminated by faeces from an infected host. Individuals are only infected through ingestion of the infective eggs. The eggs hatch in the small intestine and release larvae which develop into adult worms in the colon. The females lay between 3000 and 20 000 eggs per day. The eggs are then excreted to the physical environment, therefore contaminating the physical environment. *Trichuris* can cause diarrhoea and dysentery.

The life cycle of *Trichuris trichiura* is represented by Figure (1.2).

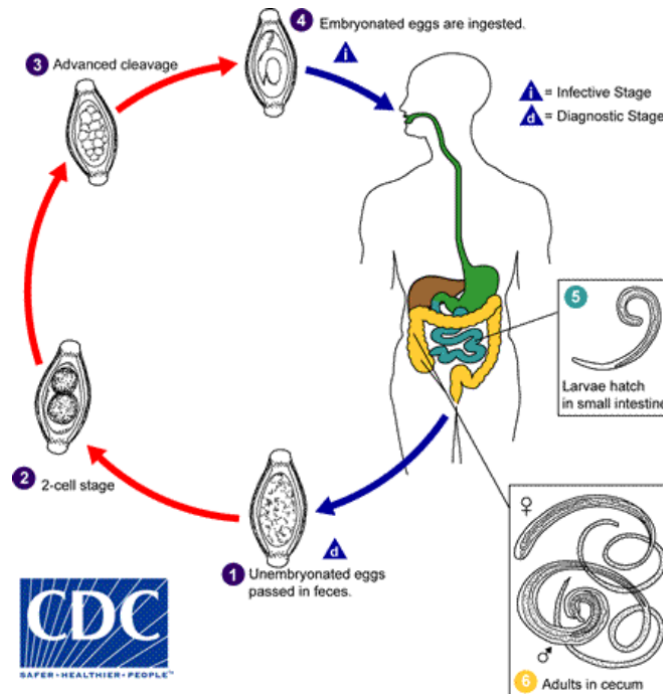


Figure 1.2: Life cycle of *Trichuris trichiura* [4].

1.2.3 Hookworm

Hookworm is little different from the first two nematodes because the larvae penetrate through the human skin. The first stage of eggs in the physical environment is to release immature worms. These worms mature into infective larvae which then penetrate through the skin of humans. The worms that have penetrated into the human body circulates through the blood system to the lungs. It then moves from lungs to Trachea, from there it then moves to pharynx. It then gets swallowed and arrive at the small intestine. Both the male and female worms are present in the small intestine, where they mature into adult worms. While there are still in the small intestine, the female worms produce hookworm eggs. These eggs are then excreted to the physical environment.

The life cycle of hookworm is represented by Figure (1.3).

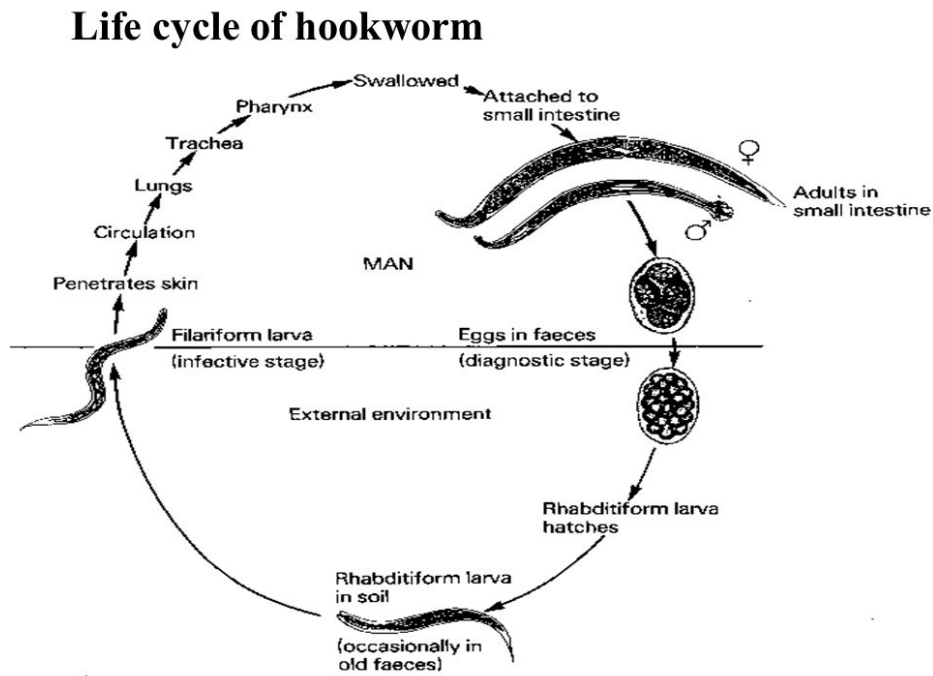


Figure 1.3: Life cycle of Hookworm [28].

For the purpose of understanding the disease dynamics of soil-transmitted helminths infection, hookworm was chosen in this study as an example for linking within-host and between-host hookworm infection dynamics. Hookworm infection was chosen due to the fact that it collaborates all the transmission dynamics for all the three parasites at the within-host and between-host scale.

Hookworm infection is caused by the Helminth nematode parasite, *Ancylostoma duodenale* and *Necator americanus*. This infection remains a huge burden since it is transmitted through contact with contaminated soil. The soil is one of the principal substrates of life on earth serving as a reservoir of water and nutrients. Hookworm is infamous for causing chronic intestinal blood loss that can result in anaemia. One of the many reasons we still study this infection is because, amongst other serious health problem, it remains one of the most common chronic infections causing anaemia, malnutrition and developmental delays in children. Bleakly (2003) suggests that the infection is not only a health problem but also one of the factors that contributed to slow economic development during the early 20th century in southern United States of America. Recently, there have been developments in improving our understanding of modelling infectious diseases. Even with these developments, hookworm infection remains an unexpected phenomenon. Our approach is to use multi-scale mathematical modelling to explain the

hookworm infection dynamics. Throughout the years, modelling infections has been considered based on disciplinary separation of immunology, epidemiology and environmental health which has hindered progress in treatment and prevention of infectious diseases [10].

In this study, we develop a multiscale model following hookworm transmission dynamics. This multiscale model will be used to evaluate health interventions for public health purposes. The model captures the disease dynamics at different scales at host level. Many mathematical models for hookworm transmission dynamics have been developed over the years but yet the mechanism of hookworm transmission has been explored in a single scale manner [8], [11],[12], [15],[24],[25]. The Viewing of every complex system (disease) in a single scale manner hinders the model from exhibiting multiple interactions in various transmission pathways. Multiscale modelling offers new insights in the different interactions between host, pathogen and physical environment for hookworm infection. There has been no attempt to link the within-host scale and between-host scale for the hookworm infection. Hotez et al. (2004) looked at the life cycle of the parasites, *Necator Americanus* and *Ancylostoma duodenale* and did not focus on how the hosts interact and how they influence each other. This approach explored the life cycle in a single scale manner. Sabatelli et al. (2008) went further to model the heterogeneity and impact of chemotherapy and vaccination against human hookworm. The study describes a stochastic individual-based model and uses the model to assess the impact of vaccination and chemotherapy against the infection. Furthermore, Sabatelli et al.(2008) demonstrated that if the risk of infection and vaccine protection are correlated there exists a direct correspondence between the reduction in worm burden and morbidity. The model tracks the establishment and removal of parasites in the host within a community. The limitation in such an approach is that vaccination and chemotherapy treatment are viewed as separate compartments, that is, single scale viewing. With the knowledge gathered from [13] on categorising framework for multiscale models of infectious disease systems it then narrows down the knowledge gap on linking models.

Chan et al. (1997) investigated the transmission patterns that suggested that the differences in levels of hookworm infection in adults and children are due to exposure differences. They further used the three models to investigate the transmission patterns of hookworm infection. The three models presented had an environmentally transmitted pathogen on the age-dependent model. The first model focuses on transmission on one site where-in the model assumes that adults and children are infected from the same transmission site. This is basically similar to what we assume in our model. The first model assumes

the adults and children are randomly mixed and are equally infected with worms. The second model separates the transmission rates, assuming different sites for adults and children. Unlike the first model, there is no mixing between adults and children. The third model has transmission occurring on two sites with one group being able to use both sites. The three models were developed following the work done by Anderson(1991), which describes the mean worm burden on the first model given by the following differential equation:

$$\frac{dW}{dt} = \mu R_0 f(w) - \mu W \quad (1.2.1)$$

where μ is the mortality rate of worms, R_0 being the reproductive number and $f(w)$ is a density-dependent fecundity function. Model 2 and model 3 extends Equation (1.2.1) by taking into account the different mean worm burden (W_C, W_A) and basic reproductive number (R_{0C}, R_{0A}) for worms in each group with the subscripts C for children and A for adults. The stochastic model was designed to study the effect of chemotherapy and vaccination. I then discovered that there is a mismatch on the application of intervention on the model which then gives rise to questions like where does the intervention operate?. The model is modelled in a single scale manner because it does not take into consideration the fact that before each group deposits eggs into the environment there exist dynamics within an infected human which play a big role in the environment transmission of the infection. The pathogen load in the environment is determined by the within-host dynamics, which is fed by information from the between-host dynamics.

A more recent study modelled the spread of the hookworm disease with the view to design optimal chemotherapy programs and to test the effectiveness of other prevention strategies [15]. The work done by Pawelek et al. (2016) motivated this work to model the infection at different scales because, infectious diseases are complex system and there is a lot of interactions occurring. Pawelek et al. (2016) developed an SEIR model with seven variables: susceptible individuals (S), exposed individuals (E), infected humans (I), humans being administered chemotherapy (R), Larva eggs (F), second stage not infective called the Rhabditiform larvae (L), and third stage infective Filariform larvae (A) which penetrates through the skin of susceptible humans. In our study, we model the newly infected humans by a term that shows the disease is bounded unlike having it to persist infinitely by the term βAS in model system (1.2.2). The model in Sabatelli et al. (2008) suggest that chemotherapy is administered at the between-host scale whereas the treatment operate at the within-host level. The model developed in this study has one group

of susceptible humans and there exist no reinfection of humans. The model presented below from [12] explains the epidemiological dynamics without within-host dynamics.

$$\left\{ \begin{array}{l} \frac{dS(t)}{dt} = \Lambda - \beta AS + \rho I - \delta S, \\ \frac{dI(t)}{dt} = \beta AS - (\rho + \delta)I_H, \\ \frac{dF(t)}{dt} = \kappa I - \psi F - \lambda F, \\ \frac{dA}{dt} = \psi F - \omega A. \end{array} \right. \quad (1.2.2)$$

The models developed in this study considers the second stage of the worms which still undergoes developmental stages in the environment to become infective.

In our study, the within-host model was then added to the epidemiological model to produce a multiscale model which will be used to evaluate health interventions for public health purposes. Our model captures the disease dynamics at different scales in each host level for hookworm.

1.3 Multiscale modelling of infectious diseases

There existed a wide knowledge gap in modelling infectious diseases until recently when Garira(2017) presented a complete categorization of multiscale models of infectious disease systems [13]. Multiscale modelling of infectious disease system is any representation of an infectious disease system at more than one scale. This concept is used in modelling infectious diseases due to the fact that infectious diseases are complex systems. The transmission properties of each type of entity (host, disease, transmission agent) and the interactions among the entities may also be affected by various factors, ranging from a microscopic scale to a macroscopic scale, including, but not limited to biological, human behavioral, demographic, socio-economic, environmental and ecological factors [17]. Complex system model incorporates many interacting components which are associated with four main levels whereby infectious

diseases systems are sub-partitioned into levels and scales. There are four main levels of organisation of infectious disease system which are: (a) the host level, (b) pathogen level, (c) health interventions level, (d) the environmental level [13]. We define each level as follows:

- (a) The host level: refers to either animals, humans, plants or vectors or a combination of two or three species.
- (b) The pathogen level: This can be any of the six different types; virus, prion, helminth, protozoa, bacteria and fungus.
- (c) The health intervention level: includes medical health and public health intervention levels. Medical interventions are applied at the within host level and public health interventions are those applied outside the host.
- (d) The environmental level: includes the geographical and the physical environment level.

Each one of these levels is resolved into a number of scales. As the scales of each level increase they converge towards the microscale and macroscale. After having the infectious disease system being appropriately partitioned into levels and scales based on the transmission dynamics then the submodels need to be linked using the appropriate integrating framework. There exists five categories of multiscale models of infectious disease system that integrate the within-host scale and between-host scale of an infectious system [13]. The different categories of multiscale models are individual-based multiscale models; nested multiscale models; embedded multiscale models; hybrid multiscale models and coupled multiscale. In this study, we follow the embedded framework to develop the multiscale model that represents hookworm transmission dynamics due to the fact that the within-host scale for hookworm infection cannot be represented independently and there exist an exchange of information between the two scales directly.

- Embedded multiscale models-Embedded model are defined as models where both the lower/micro scale submodel and the upper/macro scale influence each other in a reciprocal way. The lower/micro scale submodel is embedded within the upper/macro scale [16].

1.4 Preventative and Treatment Measures

The reduction in the number of fatal cases associated with hookworm infection imply or prove the effectiveness of both the preventative and treatment measures. In order to determine the effectiveness of both the treatment and preventative measures we perform comparative effectiveness of these measures. To be more specific, for hookworm infection, we have the following preventative and treatment measures: include surveillance, sanitation and hygiene, social mobilisation, chemotherapy and vaccines.

- (a) Sanitation- entails the provision of clean water and adequate sewage disposal. Hookworm infection is an environmentally transmitted infection preventative measures should target reducing contamination of the soil which can be achieved by construction of safe sewage systems and proper sanitation facilities.
- (b) Intervention for within the human host (chemotherapy and vaccines): Chemotherapy involves provision of different drugs for treatment of infected humans. Drug treatment imply temporal/permanent reduction of reproductive capacity of female worms and adult worms in the host. Vaccine is a biological preparation of the human system for disease prevention, it provides immunity to a particular disease. A vaccine contains an agent that resembles a disease causing micro-organism and is often made from weakened or killed forms of the microbe, its toxin or one of its surface protein. A vaccine is given to susceptible individuals to prevent humans from being infected.
- (c) Health education: This involves educating community members about hookworm infection and ensuring that they adopt and maintain behavioral practices that aim to reduce cases of hookworm. These may include wearing shoes, washing hands and foods before cooking.

1.5 Problem statement of the study

This study, seeks to bring in a different inputs in the modelling of soil-transmitted helminths infections. Hookworm infection is a huge health problem, it is estimated between 576 and 740 million individuals are infected with hookworm (see [1], [3]). The main questions are:

- To what extent does the within-host dynamics influence the disease dynamics at the population level?
- What effect does the population dynamics of disease transmission have on pathogen dynamics at the individual level?
- Which health intervention combinations eliminates the burden of hookworm infection.

1.6 Aim and Objectives of the Study

The main aim of this study is to develop a multi-scale model that represents the transmission dynamics of hookworm infection, in both within-host and between-host scales with a view of establishing new mathematical frameworks that can be used to illustrate the comparative effectiveness of hookworm infection treatment and preventative. Specific objectives of the study are as follows:

- To develop a between-host model for hookworm infection. The between-host model is sometimes called epidemiological model.
- To link the within host dynamics with the epidemiological model and have a multiscale model for hookworm infection.
- To evaluate health interventions of this linked multiscale model for hookworm infection, in order to assess which intervention combination would best help in the elimination and eradication of the infection.

It is to advance research and development in health interventions and suggest qualitative tools to understand effective ways to control, eliminate and even eradicate STHs infections. This type of work informs different stakeholders in informing policymakers which important aspects to pay attention to when implementing certain policy/law. The study will also help with assessing the effectiveness of applied interventions in reducing infection and transmission of hookworm.

The study is laid out as follows;

- Chapter 2 presents the single-scale model (epidemiological model). The model represents the transmission dynamics of hookworm infection at the between-host scale.
- Chapter 3 presents the extension of the model in chapter 2 by linking the within-host scale, between-host scale and the physical environment dynamics. The linked model is referred to as the multiscale model. Thereafter present the numerical solutions of the multiscale model.
- Chapter 4 presents the extension of the multiscale model in chapter 3 by incorporating the preventative and treatment measures of hookworm infection.
- Chapter 5 provides the discussion and conclusion.

Chapter 2

SINGLE-SCALE FRAMEWORK OF HOOKWORM INFECTION



2.1 Mathematical model

In this chapter, we develop and analyse an epidemiological model for hookworm infection. The model describes the population dynamics of the hookworm infection transmission. The model traces transmission dynamics of the aggregated populations of hookworm causing pathogens between humans and in the physical environment. The hookworm model presented herein is based on the dynamics of five populations at any given time t , which are: susceptible humans $S_H(t)$, infected humans $I_H(t)$, eggs in the physical environment $E_H(t)$, non-infective worms in the physical environment $L_H(t)$ and infective worms in the physical environment $L_M(t)$. The schematic representation of hookworm infection transmission is presented in Figure (2.1) and Table (2.1) summarises the model variables with initial conditions. The model system (1.2.2) is developed with the following assumptions:

- i. There is no vertical transmission of the disease.

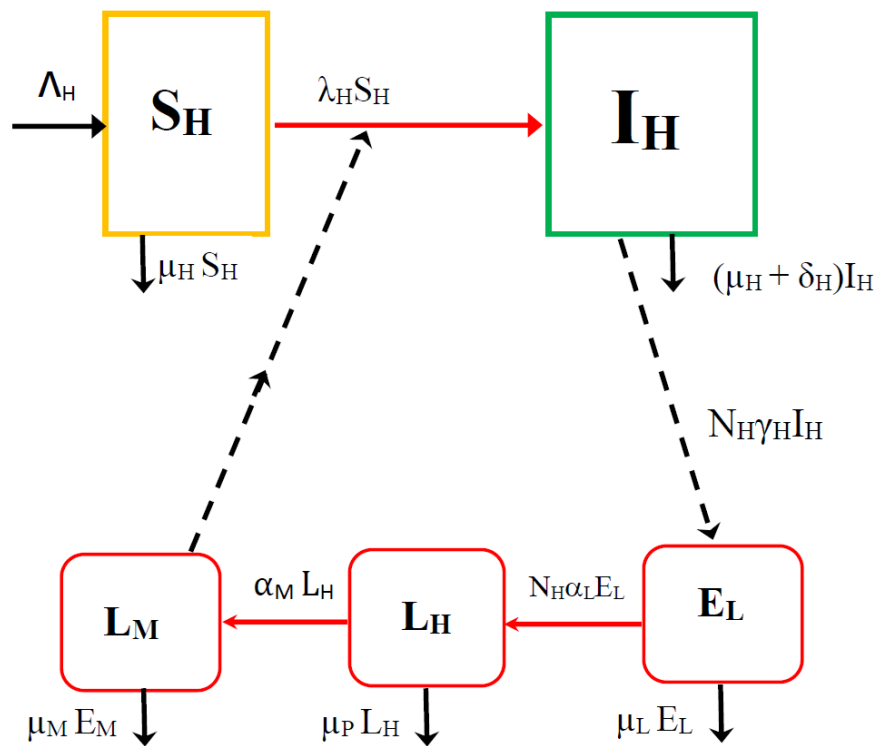


Figure 2.1: A schematic representation of the epidemiological model of Hookworm infection.

- ii. The transmission of the disease is only through contact with an average dose of hookworm infection pathogen load (L_M) in the physical environment.
- iii. There is no immigration of infectious humans.
- iv. The recruitment of humans is through birth and is constant.
- v. The model is based on an average person assumed to be healthy, the individual has not been previously exposed to the disease and therefore assumed to have acquired no immunity to the infection.
- vi. The eggs do not hatch inside an infected human.

Variables	Description	Initial	Source
$S_H(t)$	The susceptible population size	10 000	Assumed
$I_H(t)$	The infected human population size	0	Assumed
$E_L(t)$	The eggs in the physical environment	0	Assumed
$L_H(t)$	The non-infective worms in the physical environment	0	Assumed
$L_M(t)$	The infective worm in sand environment	1000	Assumed

Table 2.1: Description of the state variables of the model.

Based on the flow diagram shown in Figure (2.1) and assumptions made for the model, the following system of equations are formulated.

2.2 Human population

The total human population $N_H(t)$ comprises of susceptible $S_H(t)$ and infected $I_H(t)$ class, which is given by;

$$N_H(t) = S_H(t) + I_H(t). \quad (2.2.1)$$

2.2.1 Susceptible human population

The susceptible population over time t has new recruits entering the susceptible populations through birth at a constant rate Λ_H . The susceptible population decrease due to natural death rate μ_H . The infection rate is represented by $\lambda_H(t)$, with β_H being the contact rate of human with the environmental pathogen load and L_0 being the half saturation constant of the hookworm-causing pathogen population. The susceptible population over time t is given by:

$$\frac{dS_H}{dt} = \Lambda_H - \lambda_H S_H - \mu_H S_H \quad (2.2.2)$$

where,

$$\lambda_H = \frac{\beta_H L_M}{L_0 + L_M}. \quad (2.2.3)$$

2.2.2 Infected human population

The newly infected individuals move from being susceptible to the infected class. The movement is defined by $\lambda_H S_H(t)$ with $\lambda_H S_H(t)$ having the same meaning as above. The infected population decrease due to constant natural death rate μ_H and disease-induced death rate δ_H . The infected population is described by the following equation;

$$\frac{dI_H}{dt} = \lambda_H S_H - (\mu_H + \delta_H) I_H. \quad (2.2.4)$$

2.3 Physical environment parasite dynamics

As stated previously, the physical environment refers to the sandy soil wherein we have the population of eggs and worms for hookworm infection.

2.3.1 Eggs populations

The hookworm egg population is described by the average number of eggs excreted by an infected individual into the physical environment, contaminating the environment at an excretion rate, γ_H . An average number of eggs, N_H , are released into the physical environment every day. The eggs decay naturally at a constant rate μ_L . The egg population is modelled by the following equation:

$$\frac{dE_L}{dt} = N_H \gamma_H I_H - \mu_L E_L. \quad (2.3.5)$$

2.3.2 Worm population

In the worm population, there is non-infective and infective worms. The non-infective worms are produced when the eggs hatch in the physical environment at a constant rate α_L . An Average number of

non-infective worms N_L are hatched. The non-infective worm population decrease due to the natural death at a rate μ_P . The non-infective worms become infective at a rate α_H . The non-infective worm population is given by the following equation:

$$\frac{dL_H}{dt} = N_L \alpha_L E_L - (\mu_P + \alpha_H) L_H. \quad (2.3.6)$$

The infective worms are generated through developmental stages of the non-infective worms at the rate α_H and we assume that the infective worms die naturally at a constant rate μ_M . The infective worms is given by the following equation:

$$\frac{dL_M}{dt} = \alpha_H L_H - \mu_M L_M. \quad (2.3.7)$$

From the above equations and the diagram in Figure (2.1) we formulated the following system of equation:

$$\left\{ \begin{array}{l} \frac{dS_H}{dt} = \Lambda_H - \frac{\beta_H L_M}{L_0 + L_M} S_H - \mu_H S_H, \\ \frac{dI_H}{dt} = \frac{\beta_H L_M}{L_0 + L_M} S_H - (\mu_H + \delta_H) I_H, \\ \frac{dE_L}{dt} = N_H \gamma_H I_H - \mu_L E_L, \\ \frac{dL_H}{dt} = N_L \alpha_L E_L - (\mu_P + \alpha_H) L_H, \\ \frac{dL_M}{dt} = \alpha_H L_H - \mu_M L_M. \end{array} \right. \quad (2.3.8)$$

2.4 Basic properties

In this section, we study the mathematical properties of the system (2.3.8). We start by showing that all the solutions of the model (2.3.8) will remain positive. After showing that the solutions are non-negative given non-negative initial conditions, we will also show that the model is mathematically well-posed.

2.4.1 Positivity of Solutions

The positivity of the solution of the model (2.3.8) is shown by using the non-negative initial conditions $(S_H(0), I_H(0), E_L(0), L_H(0), L_M(0))$ such that the solutions S_H, I_H, E_L, L_H, L_M of the model remain positive for all $t \geq 0$, and not violate the basic aspect of the biological reality.

Theorem 2.1. *Given the initial conditions of the model (2.3.8) $(S_H(0) \geq 0, I_H(0) \geq 0, E_L(0) \geq 0, L_H(0) \geq 0, L_M(0) \geq 0)$, the resulting solution S_H, I_H, E_L, L_H, L_M are all positive for all $t \geq 0$*

Proof: Consider the first equation of the model system (2.3.8)

$$\frac{dS_H}{dt} = \Lambda_H - \lambda_H S_H - \mu_H S_H. \quad (2.4.9)$$

There exist a differential inequality describing the susceptible human population over time given by

$$\frac{dS_H}{dt} \geq -(\lambda_H + \mu_H)S_H. \quad (2.4.10)$$

The above expression can be solved by separation of variables as follows

$$\frac{dS_H}{S_H} \geq -(\lambda_H + \mu_H)dt. \quad (2.4.11)$$

After integration, we thus have

$$\ln S_H(t) \geq -\int_0^t \lambda_H(s)dt - \mu_H t. \quad (2.4.12)$$

The solution for susceptible human population is then given by

$$S_H(t) \geq S_H(0)e^{-(\mu_H t + \int_0^t \lambda_H(s)dt)} \geq 0. \quad (2.4.13)$$

Hence,

$$\lim_{t \rightarrow \infty} S_H(t) \geq 0. \quad (2.4.14)$$

Now consider the second equation of the system (2.3.8)

$$\frac{dI_H}{dt} = \frac{\beta_H L_M}{L_0 + L_M} S_H - (\mu_H + \delta_H) I_H. \quad (2.4.15)$$

We thus have,

$$\frac{dI_H}{dt} \geq -(\mu_H + \delta_H) I_H. \quad (2.4.16)$$

So that

$$I_H(t) \geq I_H(0) e^{-(\mu_H + \delta_H)t} \geq 0. \quad (2.4.17)$$

This implies that

$$\lim_{t \rightarrow \infty} I_H(t) \geq 0. \quad (2.4.18)$$

Similarly, it can be shown that $E_L \geq 0$, $L_H \geq 0$, $L_M \geq 0$ for all $t \geq 0$. Thus, in conclusion the solutions of the model will remain positive for all $t \geq 0$ when we start with non-negative initial value conditions in the model system (2.3.8).

2.4.2 Feasible Region

Having $N_H(t)$ denote the total number of human population add the first and the second term of the model system (2.3.8). We obtain the following

$$\frac{dS_H}{dt} + \frac{dI_H}{dt} = \Lambda_H - \mu_H(S_H + I_H) - \delta_H I_H. \quad (2.4.19)$$

Such that

$$\frac{dN_H}{dt} = \Lambda_H - \mu_H N_H - \delta_H I_H. \quad (2.4.20)$$

Which then follows that

$$\frac{dN_H}{dt} \leq \Lambda_H - \mu_H N_H. \quad (2.4.21)$$

After solving we get that

$$N(t) \leq \frac{\Lambda_H}{\mu_H} + c e^{-\mu_H t}, \quad \lim_{t \rightarrow \infty} N_H(t) \leq \frac{\Lambda_H}{\mu_H}. \quad (2.4.22)$$

This implies that the human population is bounded by $\frac{\Lambda_H}{\mu_H}$, which means that each human state variable is less or equal to $\frac{\Lambda_H}{\mu_H}$.

Using Equation (2.4.22) similar expressions can be derived for the remaining model variables as follows

$$\left\{ \begin{array}{l} \lim_{t \rightarrow \infty} E_L(t) \leq \frac{N_H \gamma_H \Lambda_H}{\mu_H \mu_L}, \\ \lim_{t \rightarrow \infty} L_H(t) \leq \frac{N_L \alpha_L}{(\alpha_H + \mu_P)} \frac{N_H \gamma_H \Lambda_H}{\mu_H \mu_L}, \\ \lim_{t \rightarrow \infty} L_M(t) \leq \frac{\alpha_H N_L \alpha_L}{\mu_M (\alpha_H + \mu_P)} \frac{N_H \gamma_H \Lambda_H}{\mu_H \mu_L}. \end{array} \right. \quad (2.4.23)$$

We let the invariant region of the model be denoted by ω_1 ,

$$\omega_1 = ((S_H, I_H, E_L, L_H, L_M) : 0 \leq S_H + I_H \leq M_1, 0 \leq E_L \leq M_2, \quad (2.4.24)$$

$$0 \leq L_H \leq M_3, 0 \leq L_M \leq M_4)$$

where,

$$\left\{ \begin{array}{l} M_1 = \frac{\Lambda_H}{\mu_H}, \\ M_2 = \frac{N_H \gamma_H \Lambda_H}{\mu_H \mu_L}, \\ M_3 = \frac{N_L \alpha_L}{(\alpha_H + \mu_P)} \frac{N_H \gamma_H \Lambda_H}{\mu_H \mu_L}, \\ M_4 = \frac{\alpha_H N_L \alpha_L}{\mu_M (\alpha_H + \mu_P)} \frac{N_H \gamma_H \Lambda_H}{\mu_H \mu_L}. \end{array} \right. \quad (2.4.25)$$

This implies that ω_1 is a positive invariant and attracting region, since all solution that will start in ω_1 will remain in ω_1 for all $t \geq 0$. Hence, the model system is mathematically and epidemiologically well posed.

2.5 Determination of Disease free Equilibrium and its stability

The equilibrium at disease free is obtained by setting the right-hand side of the model system (2.3.8) to zero. There exist two equilibrium states which are the disease-free equilibrium (DFE) and the endemic equilibrium point (EEP). At DFE there exist no infection, which means there is no larvae and eggs. Thus the model (2.3.8) has the DFE given by

$$E = (S_H^0, I_H^0, E_L^0, L_H^0, L_M^0), \quad (2.5.26)$$

$$= \left(\frac{\Lambda_H}{\mu_H}, 0, 0, 0, 0 \right). \quad (2.5.27)$$

2.5.1 Reproductive number of the model system

The reproductive number R_0 is the average number of secondary infections by a single infected host that is exposed to a totally susceptible population. We use R_0 to analyse the disease outbreak whereby $R_0 < 1$ tells us that the outbreak will disappear with time and $R_0 > 1$ suggests that the outbreak will persist at endemic levels. This has been an important threshold parameter that has been used to measure a disease transmission cycle in many epidemic models. However, for infectious diseases like soil-transmitted helminths the basic reproductive number is defined as the average number of eggs produced by a single adult female parasite that has reached maturity, because they do not replicate within the hosts. We determine the basic reproductive number for the system by using the next generation operator approach [26]. The model can be written in the form

$$\begin{cases} \frac{dX}{dt} = f(X, Y, Z), \\ \frac{dY}{dt} = g(X, Y, Z), \\ \frac{dZ}{dt} = h(X, Y, Z), \end{cases} \quad (2.5.28)$$

where,

- i. $X = (S_H)$ represents all compartments of individuals that are not infected,
- ii. $Y = (I_H, E_L, L_H)$ represents all compartments of infected individuals that are not capable of infecting others,
- iii. $Z = (L_M)$ represents all compartments of infected individuals who are capable of infecting.

$$\tilde{g}(X^*, Z) = (\tilde{g}_1(X^*, Z), \tilde{g}_2(X^*, Z), \tilde{g}_3(X^*, Z)), \quad (2.5.29)$$

$$E = \left(\frac{\Lambda_H}{\mu_H}, 0, 0, 0, 0 \right),$$

where,

$$\begin{cases} \tilde{g}_1(X^*, Z) = \frac{\beta_H \Lambda_H L_M}{\mu_H L_0 (\mu_H + \delta_H)}, \\ \tilde{g}_2(X^*, Z) = \frac{N_H \gamma_H}{\mu_L} \frac{\beta_H \Lambda_H L_M}{\mu_H L_0 (\mu_H + \delta_H)}, \\ \tilde{g}_3(X^*, Z) = \frac{N_L \alpha_L}{\mu_H L_0 (\alpha_H + \alpha_P)} \frac{N_H \gamma_H}{\mu_L} \frac{\beta_H \Lambda_H L_M}{(\mu_H + \delta_H)}. \end{cases} \quad (2.5.30)$$

and

$$A = D_Z h(X^*, \tilde{g}(X^*, 0), 0). \quad (2.5.31)$$

Using the above equation (2.5.31) on the model system (2.3.8) we then have the following expression

$$A = \frac{\alpha_H N_L \alpha_L}{\mu_H \mu_L L_0 (\mu_P + \alpha_H)} \frac{N_H \gamma_H \beta_H \Lambda_H}{(\mu_H + \delta_H)} - \mu_M. \quad (2.5.32)$$

From these expression we then deduce that

$$M = \frac{\alpha_H N_L \alpha_L}{\mu_H \mu_L L_0 (\mu_P + \alpha_H)} \frac{N_H \gamma_H \beta_H \Lambda_H}{(\mu_H + \delta_H)} \quad (2.5.33)$$

and

$$D = \mu_M.$$

Since $R_0 = MD^{-1}$, it then follows

$$R_0 = \frac{N_L \alpha_L N_H \alpha_H \gamma_H \beta_H \Lambda_H}{\mu_M \mu_H \mu_L L_0 (\mu_P + \alpha_H) (\mu_H + \delta_H)}. \quad (2.5.34)$$

2.5.2 Local stability of DFE

In this section, we determine the local stability of DFE for the model system (2.3.8) by linearizing the model system (2.3.8). The Jacobian matrix obtained is evaluated at disease-free equilibrium E_0 . The disease free equilibrium is given by:

$$E_0 = \left(\frac{\Lambda_H}{\mu_H}, 0, 0, 0, 0 \right). \quad (2.5.35)$$

The Jacobian matrix of the model system (2.3.8) evaluated at the DFE is given by

$$J(E_0) = \begin{pmatrix} -\mu_H & 0 & 0 & 0 & -\frac{\beta_H \Lambda_H}{L_0 \mu_H} \\ 0 & -a_0 & 0 & 0 & \frac{\beta_H \Lambda_H}{L_0 \mu_H} \\ 0 & N_H \gamma_H & -\mu_L & 0 & 0 \\ 0 & 0 & N_L \alpha_L & -a_1 & 0 \\ 0 & 0 & \alpha_H & -\mu_M & 0 \end{pmatrix}. \quad (2.5.36)$$

We test for stability of DFE by calculating the eigenvalues λ of the above Jacobian matrix. The eigenvalues are calculated by finding the determinant of the Jacobian matrix.

$$\det(J(E_0) - \lambda) = (-\mu_H - \lambda) \begin{vmatrix} -a_0 - \lambda & 0 & 0 & \frac{\beta_H \Lambda_H}{\mu_H L_0} \\ N_H \gamma_H & -\mu_l - \lambda & 0 & 0 \\ 0 & N_L \alpha_L & -a_1 - \lambda & 0 \\ 0 & 0 & \alpha_H & -\mu_M - \lambda \end{vmatrix}$$

$$\frac{\beta_H \Lambda_H}{\mu_H L_0} \begin{vmatrix} -a_0 - \lambda & 0 & 0 & \frac{\beta_H \Lambda_H}{\mu_H L_0} \\ N_H \gamma_H & -\mu_l - \lambda & 0 & 0 \\ 0 & N_L \alpha_L & -a_1 - \lambda & 0 \\ 0 & 0 & \alpha_H & -\mu_M - \lambda \end{vmatrix} = 0,$$

$$(-\mu_H - \lambda)(-a_0 - \lambda) \begin{vmatrix} -\mu_l - \lambda & 0 & 0 \\ N_L \alpha_L & -a_1 - \lambda & 0 \\ 0 & \alpha_H & -\mu_M - \lambda \end{vmatrix} - (-\mu_H - \lambda) \frac{\beta_H \Lambda_H}{\mu_H L_0} \begin{vmatrix} N_H \gamma_H & -\mu_l - \lambda & 0 \\ 0 & N_L \alpha_L & -a_1 - \lambda \\ 0 & 0 & \alpha_H \end{vmatrix} = 0,$$

$$(-\mu_H - \lambda)(-a_0 - \lambda)(-\mu_L - \lambda) \begin{vmatrix} -a_1 - \lambda & 0 \\ \alpha_H & -\mu_M - \lambda \end{vmatrix} - (-\mu_H - \lambda) \frac{\beta_H \Lambda_H N_H \gamma_H}{\mu_H L_0} \begin{vmatrix} N_L \alpha_L & -a_1 - \lambda \\ 0 & \alpha_H \end{vmatrix} = 0,$$

which reduces to

$$(-\mu_H - \lambda)(-a_0 - \lambda)(-\mu_L - \lambda)(-a_1 - \lambda)(-\mu_M - \lambda) - (-\mu_H - \lambda) \frac{\beta_H \Lambda_H N_H \gamma_H N_L \alpha_L \alpha_H}{\mu_H L_0} = 0. \quad (2.5.37)$$

After solving the above equation we get the simplified form

$$(-\mu_H - \lambda)[\lambda^4 + \phi_1 \lambda^3 + \phi_2 \lambda^2 + \phi_3 \lambda + \phi_4] = 0, \quad (2.5.38)$$

where,

$$\begin{cases} \phi_1 = a_0 + a_1 + \mu_M + \mu_L, \\ \phi_2 = a_0\mu_L + a_1\mu_M + (a_0 + \mu_L)(a_1 + \mu_M), \\ \phi_3 = a_0\mu_L(a_1 + \mu_M) + a_1\mu_M(a_0 + \mu_L), \\ \phi_4 = a_0a_1\mu_L\mu_M(1 - R_0). \end{cases} \quad (2.5.39)$$

It can be clearly seen that the characteristic equation has one of the eigenvalues being $\lambda = -\mu_H$. Now to determine the remaining eigenvalues of the polynomial of degree 4 is as follows

$$P(\lambda) = \lambda^4 + \phi_1\lambda^3 + \phi_2\lambda^2 + \phi_3\lambda + \phi_4. \quad (2.5.40)$$

We use the Routh-Hurwitz criteria. We define the matrices whose elements are the coefficients (ϕ_s) of the characteristic polynomial $P(\lambda)$ in equation (2.5.40) as follows

$$H_1 = \begin{pmatrix} \phi_1 \end{pmatrix}, \quad H_2 = \begin{pmatrix} \phi_1 & 1 \\ \phi_3 & \phi_2 \end{pmatrix}, \quad (2.5.41)$$

$$H_3 = \begin{pmatrix} \phi_1 & 1 & 0 \\ \phi_3 & \phi_2 & \phi_1 \\ 0 & \phi_4 & \phi_3 \end{pmatrix}, \quad H_4 = \begin{pmatrix} \phi_1 & 1 & 0 & 0 \\ \phi_3 & \phi_2 & \phi_1 & 1 \\ 0 & \phi_4 & \phi_3 & \phi_2 \\ 0 & 0 & 0 & \phi_4 \end{pmatrix}. \quad (2.5.42)$$

Evaluating the determinant of matrices, we obtain

$$\begin{cases} \det(H_1) = \phi_1, \\ \det(H_2) = \phi_1\phi_2 - \phi_3, \\ \det(H_3) = \phi_1(\phi_3\phi_2 - \phi_4\phi_1) + \phi_3^2, \\ \det(H_4) = \phi_1\phi_2\phi_3\phi_4 + \phi_3\phi_4. \end{cases} \quad (2.5.43)$$

It can be observed that all the coefficients $\phi_1, \phi_2, \phi_3, \phi_4$ of the polynomial are greater than zero whenever $R_0 < 1$. The determinant of the matrices H_1, H_2, H_3, H_4 are positive whenever $\phi_1\phi_2 > \phi_3; \phi_3\phi_2 > \phi_4\phi_1$ will be positive if and only if $R_0 < 1$. Hence all the roots of $P(\lambda)$ are negative or have negative real numbers. This is summarised in the following theorem.

Theorem 2.2. *The disease free equilibrium point E_0 of the model system 2.3.8 is locally asymptotically stable whenever $R_0 < 1$ and unstable otherwise.*

2.5.3 Global stability of DFE

Theorem 2.3. *The fixed point $E_0 = \left(\frac{\Lambda_H}{\mu_H}, 0, 0, 0, 0\right)$, is a globally asymptotically stable (g.a.s) equilibrium of system 2.3.8 if $R_0 > 1$.*

PROOF : Consider the Volterra-type Lyapunov function[23], linear equations and $S_0 = \frac{\Lambda_H}{\mu_H}$.

The Lyapunov function is given by:

$$L_0 = a_1(S_H - S_0 \ln S_H) + a_2I_H + a_3E_L + a_4L_H + a_5L_M, \quad (2.5.44)$$

that satisfies

$$\left\{ \begin{aligned} \frac{dL_0}{dt} &= a_1 \frac{dS_H}{dt} \left(1 - \frac{S_0}{S_H}\right) + a_2 \frac{dI_H}{dt} + a_3 \frac{dE_L}{dt} + a_4 \frac{dL_H}{dt} + a_5 \frac{dL_M}{dt}, \\ &= a_1 \left(1 - \frac{S_0}{S_H}\right) [\Lambda_H - \lambda_H S_H - \mu_H S_H] + a_2 [\lambda_H S_H - (\mu_H + \delta_H) I_H] + a_3 [N_H \gamma_H I_H - \mu_L E_L] \\ &+ a_4 [N_L \alpha_L E_L - (\alpha_H + \mu_P) L_H] + a_5 [\alpha_H L_H - \mu_M L_M], \\ &= -a_1 \frac{\mu_H}{S_H} (S_H - S_0)^2 + a_1 \lambda_H S_0 + \lambda_H S_H (a_2 - a_1) + I_H [a_3 N_H \gamma_H - a_2 (\mu_H + \delta_H)] \\ &+ E_L (a_4 N_L \alpha_L - a_3 \mu_L) + L_H [\alpha_H a_5 - a_4 (\alpha_H + \mu_P)] - a_5 \mu_M L_M. \end{aligned} \right. \quad (2.5.45)$$

Constants are defined by:

$$\left\{ \begin{array}{l} a_1 = 1, \\ a_2 = 1, \\ a_3 = \frac{(\mu_H + \delta_H)}{N_H \gamma_H}, \\ a_4 = \frac{(\mu_H + \delta_H)}{N_H \gamma_H} \frac{\mu_L}{N_L \alpha_L}, \\ a_5 = \frac{(\mu_H + \delta_H) \mu_L (\alpha_H + \mu_P)}{N_H \gamma_H N_L \alpha_L \alpha_H}. \end{array} \right. \quad (2.5.46)$$

Therefore, the derivative becomes

$$\left\{ \begin{array}{l} \frac{dL_0}{dt} = -\frac{\mu_H}{S_H} (S_H - S_0)^2 + \lambda_H S_0 - \frac{(\mu_H + \delta_H) \mu_L (\alpha_H + \mu_P)}{N_H \gamma_H N_L \alpha_L \alpha_H} \mu_M L_M, \\ = -\frac{\mu_H}{S_H} (S_H - S_0)^2 + \frac{\beta_H L_M \Lambda_H}{\mu_H (L_0 + L_m)} - \frac{(\mu_H + \delta_H) \mu_L (\alpha_H + \mu_P)}{N_H \gamma_H N_L \alpha_L \alpha_H} \mu_M L_M, \\ = -\frac{\mu_H}{S_H} (S_H - S_0)^2 + \frac{(\mu_H + \delta_H) (\alpha_H + \mu_P) \mu_L \mu_M}{N_H \gamma_H N_L \alpha_L \alpha_H} L_M (R_0 - 1). \end{array} \right. \quad (2.5.47)$$

It is clear that $\frac{dL_0}{dt} \leq 0$ whenever $R_0 \leq 1$ for all $S_H, L_M > 0$. From Theorem (2.3) it can be concluded that the DFE is globally asymptotically stable wherever $R_0 < 1$.

2.6 Endemic Equilibrium state and its stability

The endemic equilibrium state is a state where the disease cannot be totally eradicated meaning it remains in the population. The endemic equilibrium point of the model system (2.3.8) is given by

$$E^* = (S_H^*, I_H^*, E_L^*, L_H^*, L_M^*) \quad (2.6.48)$$

which satisfies

$$0 = \Lambda_H - \frac{\beta_H L_M^*}{L_0 + L_M^*} S_H^* - \mu_H S_H^*, \quad (2.6.49)$$

$$0 = \frac{\beta_H L_M^*}{L_0 + L_M^*} S_H^* - (\mu_H + \delta_H) I_H^*, \quad (2.6.50)$$

$$0 = N_H \gamma_H I_H^* - \mu_L E_L^*, \quad (2.6.51)$$

$$0 = N_L \alpha_L E_L^* - (\mu_P + \alpha_H) L_H^*, \quad (2.6.52)$$

$$0 = \alpha_H L_H^* - \mu_M L_M^* \quad (2.6.53)$$

for all $S_H^*, I_H^*, E_L^*, L_H^*, L_M^* > 0$. We therefore obtain the following endemic values and prove the existence of the points in the sections below.

2.6.1 Endemic equilibrium

The endemic equilibrium expressions of the model system (2.3.8) are given as follows. The endemic value of susceptible humans is defined by

$$S_H^* = \frac{\Lambda_H}{\mu_H + \lambda_H^*}. \quad (2.6.54)$$

The endemic value of infected humans is defined as

$$I_H^* = \frac{\lambda_H^* \Lambda_H}{(\mu_H + \delta_H)(\mu_H + \lambda_H^*)}. \quad (2.6.55)$$

The endemic value of the eggs in the environment is given by

$$E_H^* = \frac{N_H \gamma_H \lambda_H^* \Lambda_H}{\mu_L (\mu_H + \delta_H) (\mu_H + \lambda_H^*)}. \quad (2.6.56)$$

The endemic value for non-infective worms in the environment is given by

$$L_H^* = \frac{N_L \alpha_L}{(\mu_P + \alpha_H)} \frac{N_H \gamma_H \lambda_H^* \Lambda_H}{\mu_L (\mu_H + \delta_H) (\mu_H + \lambda_H^*)}. \quad (2.6.57)$$

The endemic value for infective worms in the environment is given by

$$L_M^* = \frac{N_L \alpha_L \alpha_H}{\mu_M (\mu_P + \alpha_H)} \frac{N_H \gamma_H \lambda_H^* \Lambda_H}{\mu_L (\mu_H + \delta_H) (\mu_H + \lambda_H^*)}. \quad (2.6.58)$$

2.6.1.1 Existence of Endemic Equilibrium state

In this section, we prove the existence of the endemic equilibrium point or constant solutions for the model system (2.3.8) making use of the reproductive number R_0 .

Theorem 2.4. *The model system (2.3.8) has positive unique endemic equilibrium point given by*

$$E^* = (S_H^*, I_H^*, E_L^*, L_H^*, L_M^*) \quad (2.6.59)$$

with $S_H^*, I_H^*, E_L^*, L_H^*, L_M^*$ all non-negative, whose existence and properties are determined by the threshold parameter R_0 where

$$R_0 = \frac{N_L \alpha_L N_H \alpha_H \gamma_H \beta_H \Lambda_H}{\mu_M \mu_H \mu_L L_0 (\mu_P + \alpha_H) (\mu_H + \delta_H)}. \quad (2.6.60)$$

Proof. Let $E^* = (S_H^*, I_H^*, E_L^*, L_H^*, L_M^*)$ be a constant solution of the model system (2.3.8). We express the endemic values in terms of one variable, L_M^* which then yields the following

$$\left\{ \begin{array}{l} S_H^* = \frac{\Lambda_H (L_0 + L_M^*)}{\beta_H L_M^* + \mu_H (L_0 + L_M^*)}, \\ I_H^* = \frac{\beta_H \Lambda_H L_M^*}{(\mu_H + \delta_H) [\beta_H L_M^* + \mu_H (L_0 + L_M^*)]}, \\ E_L^* = \frac{\beta_H \Lambda_H N_H \gamma_H L_M^*}{\mu_L (\mu_H + \delta_H) (\mu_P + \alpha_H) [\beta_H L_M^* + \mu_H (L_0 + L_M^*)]}, \\ L_H^* = \frac{\beta_H \Lambda_H N_H \gamma_H N_L \alpha_L L_M^*}{\mu_L (\mu_H + \delta_H) (\mu_P + \alpha_H) [\beta_H L_M^* + \mu_H (L_0 + L_M^*)]}. \end{array} \right. \quad (2.6.61)$$

Substitute the above expressions into the last equation of the model given by

$$\frac{dL_M^*}{dt} = \alpha_h L_H - \mu_M L_M. \quad (2.6.62)$$

Which is true that

$$L_M^* [AL_M^* + B] = 0. \quad (2.6.63)$$

$L_M^* = 0$ or $AL_M^* + B = 0$ of which we can conclude that

$$L_M^* = -\frac{B}{A}. \quad (2.6.64)$$

Where,

$$\begin{cases} A = \beta_H \mu_M \mu_L (\mu_H + \delta_H) (\mu_P + \alpha_H) + \mu_M \mu_H \mu_L (\mu_H + \delta_H) (\mu_P + \alpha_H), \\ B = \mu_H \mu_M \mu_L (\mu_P + \alpha_H) (\mu_H + \delta_H) - \beta_H \Lambda_H N_H \gamma_H N_L \alpha_L \alpha_H. \end{cases} \quad (2.6.65)$$

Since $L_M^* = -\frac{B}{A}$ it can then be written in terms of R_0 as follows

$$L_M^* = \frac{(R_0 - 1)}{\beta_H + \mu_H}. \quad (2.6.66)$$

We can deduce that equation (2.6.66) is positive for $R_0 > 1$ and equation (2.6.63) gives $L_M^* = 0$, which corresponds with the disease free equilibrium. We can conclude from the Theorem (2.4) that there exist a unique endemic equilibrium point for the model system (2.3.8). \square

2.6.2 Global stability of Endemic Equilibrium state

In this subsection we establish the stability the endemic equilibrium solutions for the model system (2.3.8).

Theorem 2.5. *If the basic reproductive number $R_0 > 1$ then the positive equilibrium points given by*

$$E^* = (S_H^*, I_H^*, E_L^*, L_H^*, L_M^*) \quad (2.6.67)$$

is globally asymptotically stable.

Proof. Consider the Volterra-type Lyapunov function[23] of the form

$$\left\{ \begin{array}{l} L_1 = L(S_H, I_H, E_L, L_H, L_M), \\ \\ = a_1(S_H - S_H^* \ln S_H) + a_2(I_H - I_H^* \ln I_H) + a_3(E_L - E_L^* \ln E_L) \\ \\ + a_4(L_H - L_H^* \ln L_H) + a_5(L_M - L_M^* \ln L_M). \end{array} \right. \quad (2.6.68)$$

Then the Lie derivative of L_1 in the direction of the vector field give the right hand side of the multiscale model system (??EQN:1) is

$$\left\{ \begin{array}{l} \frac{dL_1}{dt} = a_1 \left(1 - \frac{S_H^*}{S_H}\right) \frac{dS_H}{dt} + a_2 \left(1 - \frac{I_H^*}{I_H}\right) \frac{dI_H}{dt} + a_3 \left(1 - \frac{E_L^*}{E_L}\right) \frac{dE_L}{dt} \\ \\ + a_4 \left(1 - \frac{L_H^*}{L_H}\right) \frac{dL_H}{dt} + a_5 \left(1 - \frac{L_M^*}{L_M}\right) \frac{dL_M}{dt}, \\ \\ = a_1 \left(1 - \frac{S_H^*}{S_H}\right) [\Lambda_H - \lambda_H S_H - \mu_H S_H] + a_2 \left(1 - \frac{I_H^*}{I_H}\right) [\lambda_H S_H - (\mu_H + \delta_H) I_H] \\ \\ + a_3 \left(1 - \frac{E_L^*}{E_L}\right) [N_H \gamma_H I_H - \mu_L E_L] + a_4 \left(1 - \frac{L_H^*}{L_H}\right) [N_L \alpha_L E_L - (\alpha_H + \delta_P) L_H] \\ \\ + a_5 \left(1 - \frac{L_M^*}{L_M}\right) [\alpha_H L_H - \mu_M L_M]. \end{array} \right. \quad (2.6.69)$$

Since E^* is an equilibrium point, the following relations hold:

$$\left\{ \begin{array}{l} \Lambda_H = \lambda_H^* S_H^* + \mu_H S_H^*, \\ (\mu_H + \delta_H) = \frac{\lambda_H^* S_H^*}{I_H^*}, \\ \mu_L = \frac{N_H \gamma_H I_H^*}{E_L^*}, \\ (\alpha_H + \mu_P) = \frac{N_L \alpha_L E_L^*}{L_H^*}, \\ \alpha_H = \frac{\mu_M L_M^*}{L_H^*}. \end{array} \right. \quad (2.6.70)$$

Therefore; substitute the endemic equilibrium points on the derivative lyapunov equation:

$$\left\{ \begin{aligned}
 \frac{dL_1}{dt} &= a_1 \left(1 - \frac{S_H^*}{S_H}\right) [\lambda_H^* S_H^* + \mu_H S_H^* - \lambda_H S_H - \mu_H S_H] \\
 &+ a_2 \left(1 - \frac{I_H^*}{I_H}\right) \left[\lambda_H S_H - \lambda_H^* S_H^* \frac{I_H}{I_H^*}\right] + a_3 \left(1 - \frac{E_L^*}{E_L}\right) \left[N_H \gamma_H I_H - N_H \gamma_H I_H^* \frac{E_L}{E_L^*}\right] \\
 &+ a_4 \left(1 - \frac{L_H^*}{L_H}\right) \left[N_L \alpha_L E_L - N_L \alpha_L E_L^* \frac{L_H}{L_H^*}\right] + a_5 \left(1 - \frac{L_M^*}{L_M}\right) \left[\mu_M L_M^* \frac{L_H}{L_M^*} - \mu_M L_M\right], \\
 &= -a_1 \frac{\mu_H}{S_H} (S_H - S_H^*)^2 + \lambda_H^* S_H^* \left(a_1 - a_1 \frac{S_H^*}{S_H} - a_2 \frac{I_H}{I_H^*} + a_2\right) \\
 &+ \lambda_H S_H \left(a_2 \frac{S_H^*}{S_H} - a_2 \frac{I_H}{I_H^*} - a_1 + a_2\right) \\
 &+ E_L^* \left[a_4 N_L \alpha_L - a_4 N_L \alpha_L \frac{L_H}{L_H^*} - a_4 N_L \alpha_L \frac{E_L}{E_L^*} \frac{L^*}{L_H} - a_3 N_H \gamma_H \frac{I_H}{E_L}\right] \\
 &+ I_H \left[a_3 N_H \gamma_H - a_3 N_H \gamma_H \frac{I_H^*}{I_H} \frac{E_L}{E_H^*} + a_4 N_L \alpha_L \frac{E_L}{I_H} + a_3 N_H \gamma_H \frac{I_H^*}{I_H}\right] \\
 &+ L_M^* \left[a_5 \mu_M \frac{L_H}{L_H^*} - a_5 \mu_M \frac{L_M}{L_M^*} - a_5 \mu_M \frac{L_M^*}{L_M} \frac{L_H}{L_H^*} + a_5 \mu_M\right].
 \end{aligned} \right. \tag{2.6.71}$$

We choose the constants a_1, a_2, a_3 and a_5 as

$$\left\{ \begin{aligned}
 a_1 &= 1, \\
 a_2 &= 1, \\
 a_3 &= \frac{a_4}{N_H \gamma_H \frac{I_H}{E_L}} \left(N_L \alpha_L - N_L \alpha_L \frac{L_H}{L_H^*} - N_L \alpha_H \frac{E_L}{E_L^*} \frac{L_H^*}{L_H}\right), \\
 a_5 &= 1.
 \end{aligned} \right.$$

We then substitute the constants above to obtain the following results

$$\left\{ \begin{aligned}
 \frac{dL_1}{dt} &= -\frac{\mu_H}{S_H}(S_H - S_H^*)^2 + \lambda_H^* S_H^* \left(2 - \frac{S_H^*}{S_H} - \frac{I_H}{I_H^*}\right) + \lambda_H S_H \left(\frac{S_H^*}{S_H} - \frac{I_H^*}{I_H}\right) \\
 &\quad + \left(\mu_H \frac{L_H}{L_H^*} - \mu_M \frac{L_M}{L_M^*} - \mu_M \frac{L_M}{L_M^*} \frac{L_H}{L_H^*} + \mu_M\right), \\
 &= -\frac{\mu_H}{S_H}(S_H - S_H^*)^2 + \lambda_H^* S_H^* \left(2 - \frac{S_H^*}{S_H} - \frac{I_H}{I_H^*}\right) \\
 &\quad + \lambda_H S_H \left(\frac{S_H^*}{S_H} - \frac{I_H^*}{I_H}\right) + \mu_M \frac{L_H}{L_H^*} \left(1 - \frac{L_M^*}{L_M}\right) + \mu_H \left(1 - \frac{L_M}{L_M^*}\right), \\
 &\leq -\frac{\mu_H}{S_H}(S_H - S_H^*)^2 + \lambda_H^* S_H^* \left(2 - \frac{S_H^*}{S_H} - \frac{I_H}{I_H^*}\right) + \lambda_H S_H \left(\frac{S_H^*}{S_H} - \frac{I_H^*}{I_H}\right) + \mu_H \left(1 - \frac{L_M}{L_M^*}\right).
 \end{aligned} \right. \quad (2.6.72)$$

Using the arithmetic mean inequality and the condition $S_H^* < S_H; I_H^* > I_H; E_L^* > E_L; L_H^* > L_H$ and $L_M > L_M^*$ we get

$$2 \leq \sqrt{\frac{S_H^* I_H}{S_H I_H^*}}. \quad (2.6.73)$$

It is clear that from the stated conditions for S_H, I_H, L_M we have

$$\left\{ \begin{aligned}
 \frac{S_H^*}{S_H} - \frac{I_H}{I_H^*} &\leq 0, \\
 1 - \frac{L_M}{L_M^*} &\leq 0.
 \end{aligned} \right. \quad (2.6.74)$$

Then we can conclude that $\frac{dL_1}{dt} \leq 0$. Thus L_1 is indeed the Lyapunov function of the model system (2.3.8). Since

$$\dot{L}_1 \leq 0 \iff (S_H^*, I_H^*, E_L^*, L_H^*, L_M^*) = E^*,$$

then it can be concluded that the endemic equilibrium is globally asymptotically stable. \square

2.7 Numerical solutions

In this section, we plot the solutions of the epidemiological model for hookworm infection but we first look at how sensitive are the between host parameters and how they influence the reproductive number and endemic point.

2.7.1 Sensitivity analysis

In this section, we conduct the sensitivity analysis for the model system (2.3.8). Sensitivity analysis is an estimate of which parameters are most influential in affecting the behavior of the simulation, this is crucial when looking for which parameters to target when implementing intervention measures. The analysis measure which parameters are most sensitive. These information will help in estimating which parameters to focus on when controlling the infection. We use the nomarlised forward sensitivity index of both R_0 and L_M^* to each of the model parameters defined by

$$N_{J_i}^I = \frac{\partial J_i}{\partial I} \times \frac{I}{J_i}, \quad i = 1, 2, \quad (2.7.75)$$

where

$$\begin{cases} J_1 = R_0, \\ J_2 = L_M^*. \end{cases} \quad (2.7.76)$$

The sensitive index is derived for all the parameters and is represented in Table (2.3) and all the parameters are sensitive to R_0 and L_M^* . In Table (2.3), it can be noticed that some indices have either a positive or negative sign. The index value indicates when the parameters are increased what happens to the element J_1 and J_2 . For instance, increasing saturation rate L_0 reduces R_0 and L_M^* and also increasing β_H increases both R_0 and L_M^* .

The reproductive number and the endemic point are most sensitive to changes in natural death rate of humans, μ_H . For instance, when $N_{\mu_H}^{R_0} = -1.42$ means increasing μ_H by 10% decreases the reproductive number by 14.2 %. The killing of people to reduce the transmission dynamics goes against research ethics.

From the Table (2.3) we notice that the increase in β_H increases the reproductive number meaning it is one of the parameters to target when introducing any intervention measures to reduce the hookworm infection transmission. The use of vaccine can reduce secondary infections and the persistence of the infection is significantly important.

From Table (2.3), we observe that δ_H is the least sensitive with respect to R_0 meaning increasing this parameter has minimal effect to reduce R_0 . The parameters that are capable of reducing the secondary infections are saturation constant L_0 , death rate μ_L and natural death rate of matured worms μ_M . When we introduce intervention measures these are parameters we have to target in reducing R_0 . The same parameters are capable of reducing the persistence of the infections, L_M^* .

Furthermore we can deduce that:

- (i) The use of drugs as treatment to reduce the induced death rate has the least effect to reduce the secondary infection maybe because there exist no human-human transmission directly.
- (ii) The increase of death rate of infective worms μ_M can reduce L_M^* , that means there killing of infective worms can reduce persistence of the infection.

Parameter	Description	Initial value value	Units	Source
β_H	Exposure rate of humans	0.028	day^{-1}	[29]
Λ_H	Human birth rate	0.5	humans day^{-1}	Estimated
L_0	Saturation constant	2×10^6	—	Estimated
μ_H	Human natural death rate	0.0000384	day^{-1}	[30]
δ_H	Death induced rate	0.0013699	day^{-1}	[10]
γ_H	Eggs excretion rate	0.25	day^{-1}	Estimated
N_L	Number of hatched non-infective worms	1000	day^{-1}	Estimated
α_L	Hatching rate of eggs in the physical environment	0.009	day^{-1}	Estimated
μ_L	Natural decay of eggs	0.0025	day^{-1}	[31]
N_H	Number of eggs excreted	1000	day^{-1}	[31]
α_H	Rate at which immature worms become infective worms	0.005	day^{-1}	Estimated
μ_P	Natural decay of immature worms in environment	0.0.000685	day^{-1}	Estimated
μ_M	Natural decay of infective larvae	0.05	day^{-1}	Estimated

Table 2.2: Within-host parameter values used in simulation

Number	Parameter	Sensitivity index(R_0)	Sensitivity index(L_M^*)
1	Λ_H	1	1.01
2	γ_H	1	1.01
3	L_0	-1	-1.01
4	α_H	0.99	1
5	δ_H	-0.58	0.59
6	β_H	1	0.05
7	μ_H	-1.42	-1.47
8	N_L	1	1.01
9	α_L	1	1.01
10	μ_L	-1	-1.01
11	N_H	1	1.01
12	α_H	0.99	0.99
13	μ_P	-0.99	-1
14	μ_M	-1	-1.01

Table 2.3: Sensitivity indeces

2.7.2 Numerical solutions of the between-host dynamics of Hookworm infection

In this subsection, we plot the solution of the model system (2.3.8) using the values of the model parameter in Table (2.1) and Table (2.2).

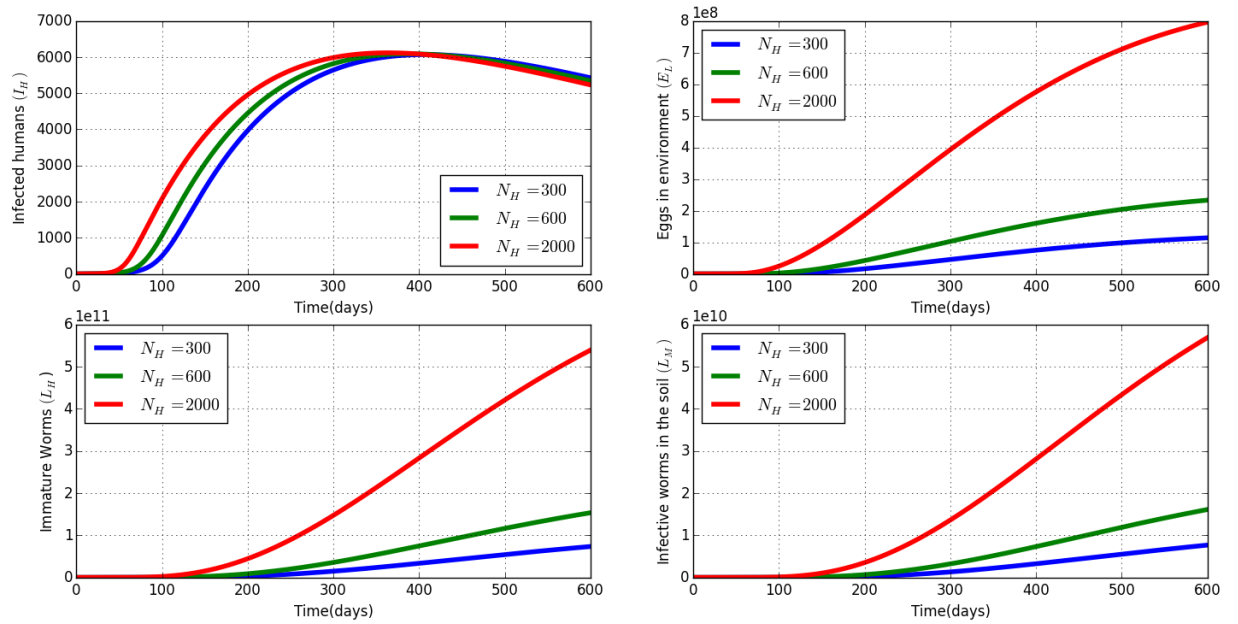


Figure 2.2: Graphs of numerical solutions of the model system (2.3.8). Top left to right showing propagation of Infected humans in population level I_H , worms in the physical environment E_L , and from bottom left to right showing propagation of Non-infective worms L_H and Infective worms L_M , respectively. The solutions are presented for different values for average eggs produced in a day rate, N_H :

$$N_H = 10, N_H = 100 \text{ and } N_H = 1000.$$

In Figure (2.2), we can deduce that the reduction of average eggs produced per day has chances of reducing the number of infected individuals, eggs in the physical environment, immature worms and infective worms in the physical environment.

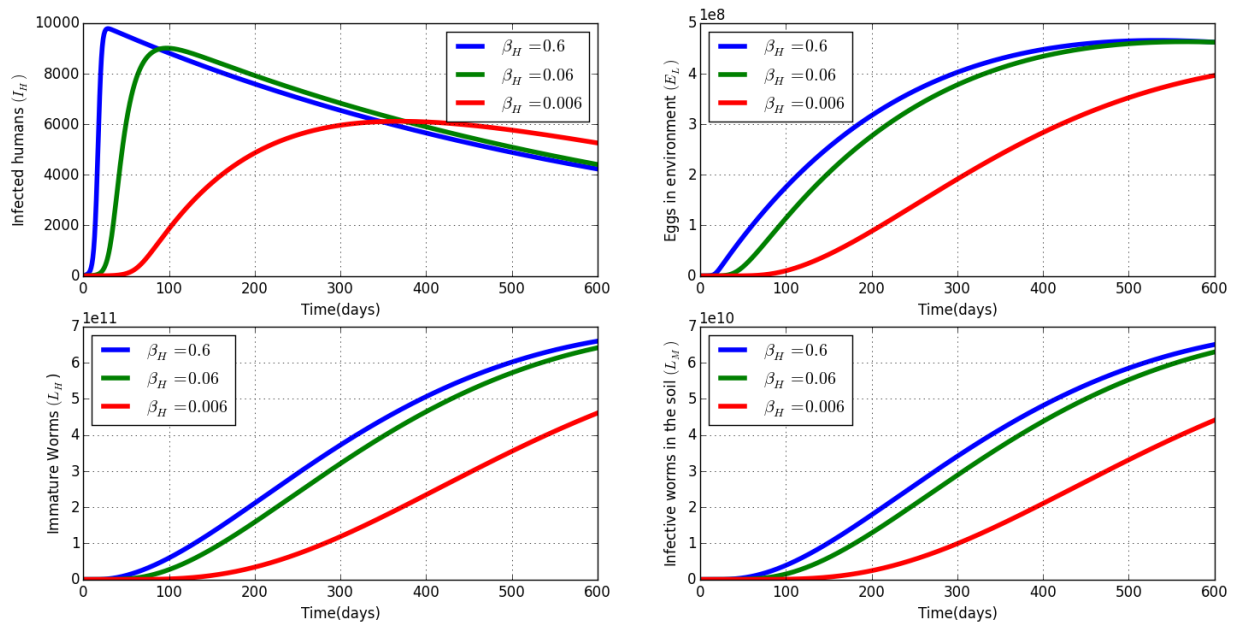


Figure 2.3: Graphs of numerical solutions of the model system (2.3.8). Top left to right showing propagation of Infected humans in population level I_H , worms in the physical environment E_L and from bottom left to right showing propagation of non-infective worms L_H and Infective worms L_M , respectively. The solutions are presented for different values of the infective contact rate, β_H : $\beta_H = 0.01$, $\beta_H = 0.1055$ and $\beta_H = 0.55$.

Figure (2.3) shows that the different values for β_H converge to a constant value after 8 months. This figure also illustrate that the infected humans, eggs in the physical environment, immature worms and infective worms class to grow faster when the contact rate is higher. This kind of results gave rise to questions like, what can be done to reduce the contact rate between humans and pathogen.

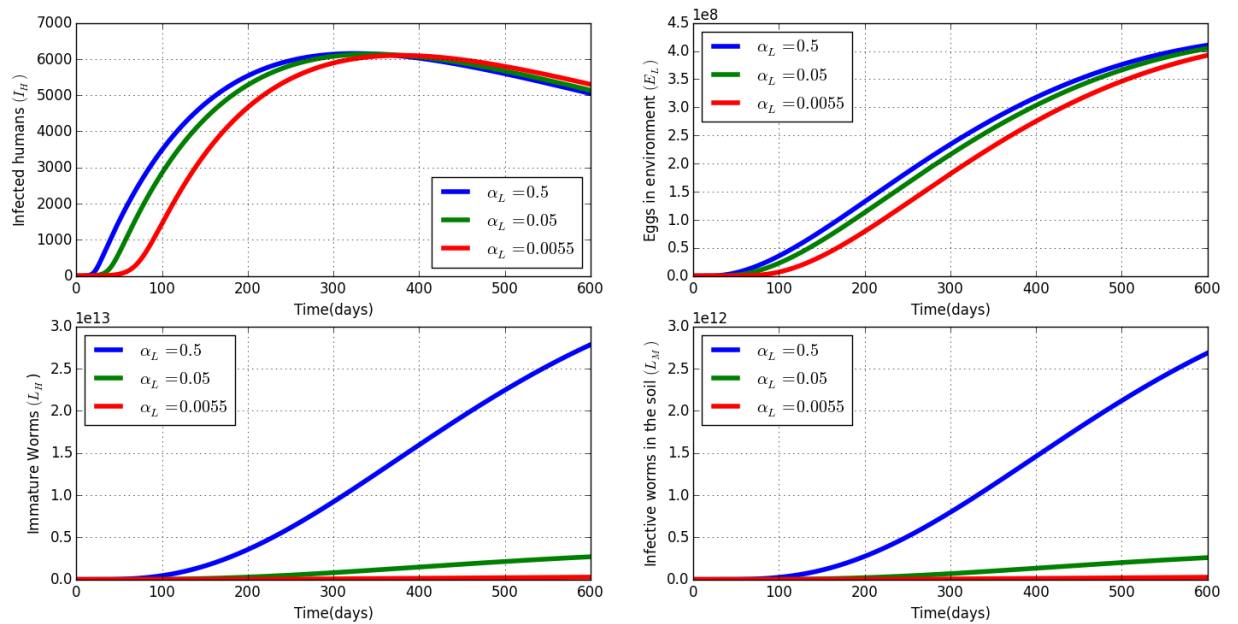


Figure 2.4: Graphs of numerical solutions of the model system (2.3.8). Top left to right showing propagation of Infected humans in population level I_H , worms in the physical environment E_L and from bottom left to right showing propagation of non-infective worms L_H and Infective worms L_M , respectively. The solutions are presented for different values for hatching rate: α_L : $\alpha_L = 0.0055$, $\alpha_L = 0.05$ and $\alpha_L = 0.5$.

Furthermore, in Figure (2.4) we can deduce that the rate at which the eggs hatch in the physical environment has little difference on the number of infected humans and the eggs deposited in the physical environment but has a huge difference in the number of immature and infective worms. The more we have more eggs hatching we have more worms in the physical environment.

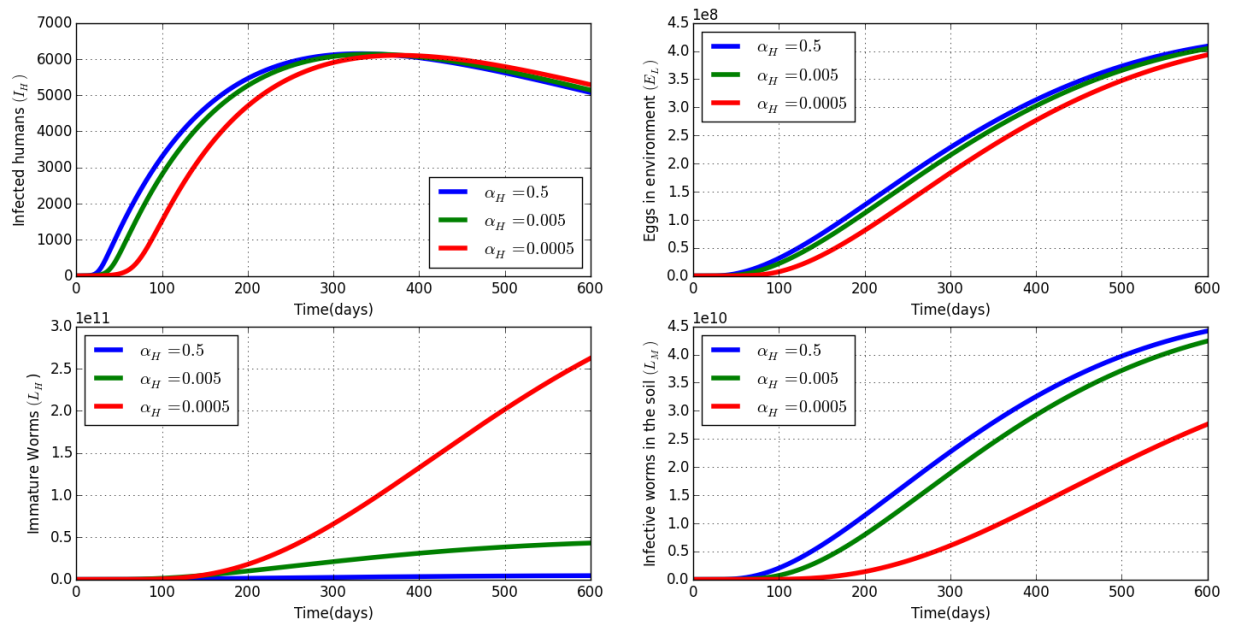


Figure 2.5: Graphs of numerical solutions of the model system (2.3.8). Top left to right showing propagation of Infected humans in population level I_H , worms in the physical environment E_L and from bottom left to right showing propagation of non-infective worms L_H and Infective worms L_M , respectively. The solutions are presented for different values of the rate of being infective, α_H : $\alpha_H = 0.0055$, $\alpha_H = 0.05$ and $\alpha_H = 0.5$.

In Figure (2.5) illustrates the rate at which the non infective worms become infective. The rate has little effect on the number of infected humans and eggs in the physical environment. The figure also suggest that when the rate at which non-infective worms become infective is high then immature worms gets reduced and the immature worms face an increment if the rate of change of the infective stage is less. It can be further deduced that when the rate of change in infective stage is high it gives rise in the number of infective worms in the physical environment.

Chapter 3

MULTISCALE MODELLING OF HOOKWORM INFECTION

3.1 Multi-scale model

In this chapter, a multi-scale model for hookworm infection is presented together with the analysis of the model. The model traces the transmission life cycle of hookworm infection, linking the dynamics occurring in within-host, between-host and environmental scale. The multiscale model for hookworm in humans is based on 9 populations at any given time t . In this study, we will use the multi-scale mathematical modelling approach as represented in Figure (3.1). Multi-scale will explicitly capture the dependence of epidemics on the transmission dynamics, and also the dependency of the within-host scale on the between-host scale and vice versa. Multi-scale modelling is a promising scientific methodology that can provide a more holistic approach to disease modelling. The interaction between pathogen, host, and the environment consist of dynamical processes that often occur at a distinct temporal, spatial, and biological scales ranging from molecular events and pathogen-host immune system interactions to global epidemiology and public health.

Following the disease dynamics of hookworm infection using multiscale modelling Figure (3.1) is used to illustrate the dynamics.

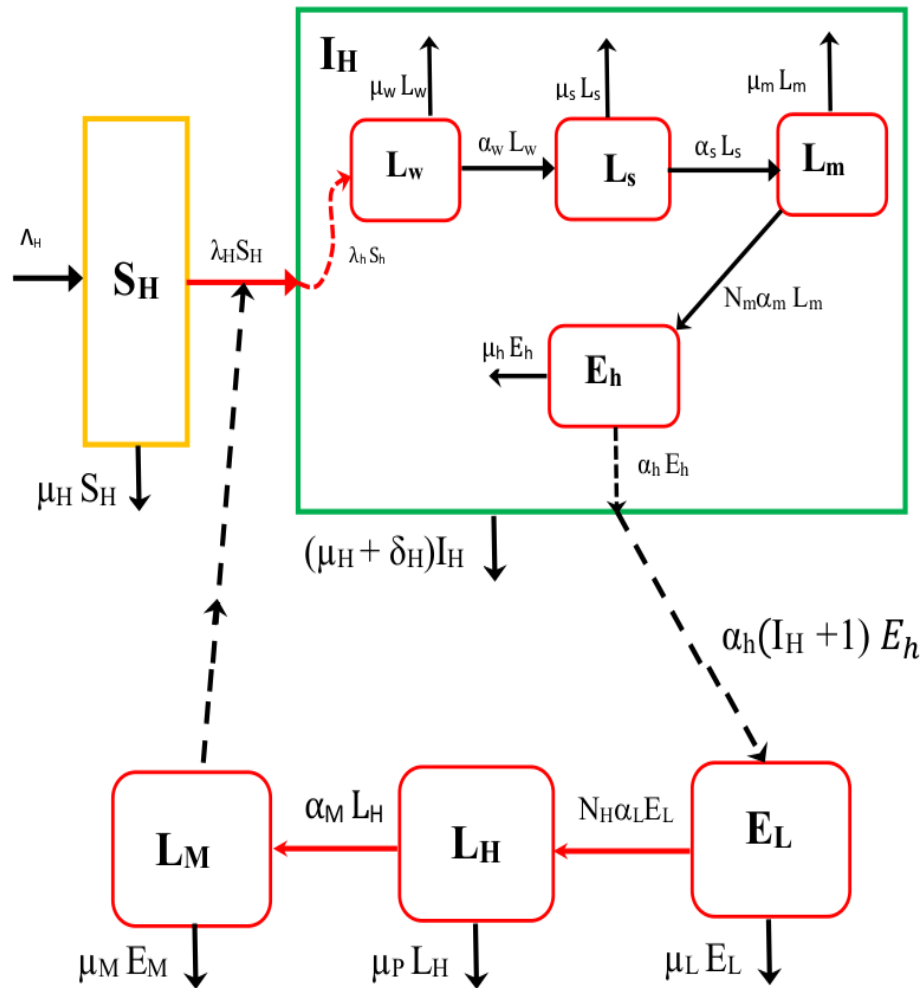


Figure 3.1: A schematic representation of the transmission-cycle of Hookworm infection.

The variables shown in Figure (3.1) summarised in Table (3.1).

Variables	Description	Initial value
$S_H(t)$	The susceptible population size in the behavioral human environment	10000
$I_H(t)$	The infected human population size in the behavioral human environment	0
$L_w(t)$	The infective larvae population in the biological environment	800
$L_s(t)$	The immature worms in the small intestine	0
$L_m(t)$	The mature worm in the biological human environment	0
$E_h(t)$	The eggs in the biological human environment	0
$E_L(t)$	The eggs in the physical environment	0
$L_H(t)$	The non-infective larvae population in the physical environment	0
$L_M(t)$	The infective larvae population in physical environment	1000

Table 3.1: Description of the state variables for the multiscale model

The development of the multiscale model in this chapter is based on the approach developed in [10] for environmentally transmitted infectious diseases.

3.2 Human population

As mentioned previously, the human population has two compartments which are the susceptible population and infected population. A susceptible population is a group of people that are vulnerable to the disease these individuals have not been exposed to any vaccination against it and have not developed immunity. The infected population is all the individuals that have been infected by the hookworm infection. The susceptible population at any time t , have new recruits though birth at a constant rate Λ_H . There is a constant death rate of the human population at μ_H . The susceptible humans acquire hookworm infection by infective larvae found in the physical environment at a rate $\lambda_H(t)$ where

$$\lambda_H(t) = \frac{\beta_H L_M}{L_0 + L_M}, \quad (3.2.1)$$

with β_H being the maximum rate of exposure, L_0 is the half saturation constant of the hookworm-causing pathogen population. The infected host have natural death and mortality rate at constant rate μ_H and δ_H , respectively. The susceptible individual population is given by:

$$\frac{dS_H}{dt} = \Lambda_H - \lambda_H S_H - \mu_H S_H, \quad (3.2.2)$$

and the infected individual population is defined by:

$$\frac{dI_H}{dt} = \lambda_H S_H - (\mu_H + \delta_H) I_H. \quad (3.2.3)$$

3.3 Within-host dynamics

Average hookworm population within a single infected human host L_w , larvae that has penetrated through the human skin. The force of infection is given by $\lambda_H(t)S_H(t)$. Following the approach in [10], multiscale modelling of environmentally transmitted infectious disease systems, the uptake of pathogen by a single human host through super-infection is given by:

$$\frac{\lambda_H(t)S_h(t)}{\eta I_h(t)} = \lambda_h(t)S_h(t) = \frac{\beta_H L_M (S_H - 1)}{\eta (L_0 + L_M) (I_H + 1)}. \quad (3.3.4)$$

Skin penetration of the larvae causes itchy rash then fever, coughing, wheezing or abdominal pain, loss of appetite and diarrhoea. The worm population in a human is assumed to die naturally at a rate μ_w and exit to the small intestine through blood vessels at a rate α_w , where they undergo developmental changes to become immature worms. The immature worms attach to the wall of the small intestine. The immature worm population in the small intestine, L_s , decays at a constant death rate μ_s and the immature worms develop into mature worms at a rate α_s . The female worms produce eggs, the mean population of the mature worms $L_m(t)$, within a single infected human host is generated following developmental changes undergone by immature worms to become mature at a rate $\frac{\alpha_s}{2}$. The developmental changes result in reaching sexual maturity. The matured worms die at a constant death rate μ_m . The mean population of hookworm eggs $E_h(t)$, produced within a single infected human when worms lay an average of N_m eggs per day, the eggs are produced at a rate α_m and the eggs decay naturally inside the human body at a

rate μ_h . The eggs get excreted by the human host into the physical environment at a rate α_h . The worm population within an infected human is given by

$$\frac{dL_w}{dt} = \lambda_h S_h - (\mu_w + \alpha_w)L_w. \quad (3.3.5)$$

The worm population in the small intestine is defined by

$$\frac{dL_s}{dt} = \alpha_w L_w - (\mu_s + \alpha_s)L_s. \quad (3.3.6)$$

The matured worm population is given by

$$\frac{dL_m}{dt} = \frac{\alpha_s}{2} L_s - \mu_m L_m. \quad (3.3.7)$$

The eggs produced inside the human is defined

$$\frac{dE_h}{dt} = N_m \alpha_m L_m - (\mu_h + \alpha_h)E_h. \quad (3.3.8)$$

3.4 Physical sand environment dynamics

The population of hookworm eggs, $E_L(t)$ contaminates the physical environment and is generated from excreted hookworm eggs from within an infected human in faeces. Each infected human host excretes these eggs at a rate $\alpha_h E_h(t)$ and for a total of $I_h(t)$ infected humans, with the rate of contamination of the physical environment by hookworm eggs becomes $I_h(t)\alpha_h E_h$ where $I_h = I_H + 1$. The hookworm eggs die naturally at a constant death rate μ_L . The eggs hatch non-infective larvae (rhabditiform) at a rate α_L . The mean population of the eggs hatch an average of N_H larvae per day and the larvae undergo developmental changes and become infective at a rate α_H . The population of infective larvae $L_M(t)$, die at a constant death rate μ_M .

The model system (3.4.9) portrays the dynamics of the hookworm infection illustrated in the Figure (3.1).

$$\left\{ \begin{array}{l}
 \frac{dS_H}{dt} = \Lambda_H - \lambda_H S_H - \mu_H S_H, \\
 \frac{dI_H}{dt} = \lambda_H S_H - (\mu_H + \delta_H) I_H, \\
 \frac{dL_w}{dt} = \lambda_h S_h - (\mu_w + \alpha_w) L_w, \\
 \frac{dL_s}{dt} = \alpha_w L_w - (\mu_s + \alpha_s) L_s, \\
 \frac{dL_m}{dt} = \frac{\alpha_s}{2} L_s - \mu_m L_m, \\
 \frac{dE_h}{dt} = N_m \alpha_m L_m - (\mu_h + \alpha_h) E_h, \\
 \frac{dE_L}{dt} = (I_H + 1) \alpha_h E_h - (\mu_L + \alpha_L) E_L, \\
 \frac{dL_H}{dt} = N_H \alpha_L E_L - (\mu_P + \alpha_H) L_H, \\
 \frac{dL_M}{dt} = \alpha_H L_H - \mu_M L_M.
 \end{array} \right. \quad (3.4.9)$$

where,

$$\left\{ \begin{array}{l}
 \lambda_H = \frac{\beta_H L_M}{L_0 + L_M}, \\
 \lambda_h S_h = \frac{\beta_H L_M (S_H - 1)}{\eta (L_0 + L_M) (I_H + 1)}.
 \end{array} \right. \quad (3.4.10)$$

3.5 Basic properties

In this section, we study the mathematical properties of the model (3.4.9).

3.5.1 Positivity of Solution

Considering positivity of the model system (3.4.9), we assume that all state variables and parameters for the model (3.4.9) are non-negative for all $t \geq 0$, so that they should not violate the basic aspect of the biological reality. We will show that the solutions of model system (3.4.9) with positive initial conditions will remain non-negative for all $t \geq 0$. Consider the first equation of the multiscale model for hookworm:

$$\frac{dS_H}{dt} = \Lambda_H - \lambda_H S_H - \mu_H S_H. \quad (3.5.11)$$

Which is true that

$$\frac{dS_H}{dt} \leq -(\lambda_H + \mu_H)S_H. \quad (3.5.12)$$

After solving equation (3.5.12) by separation of variables we get

$$\int \frac{dS_H}{S_H} \leq \int -(\lambda_H + \mu_H)dt \quad (3.5.13)$$

By letting

$$\hat{t} = \sup\{t > 0 : S_H > 0, I_H > 0, L_w > 0, L_s > 0, L_m > 0, E_H > 0, E_L > 0, L_H > 0\} \in [0, t]. \quad (3.5.14)$$

Integrate inequality (3.5.13), we thus have

$$\ln S_H \geq -\mu_H t - \int_0^t \lambda_H(t)dt + c. \quad (3.5.15)$$

Hence,

$$S_H \geq S_0 e^{-\mu_H t - \int_0^t \lambda_H(t)dt} > 0. \quad (3.5.16)$$

Now, consider the second equation of the model system (3.4.9):

$$\frac{dI_H}{dt} = \lambda_H S_H - (\mu_H + \delta_H)I_H, \quad (3.5.17)$$

We thus have

$$\frac{dI_H}{dt} \geq -(\mu_H + \delta_H)I_H. \quad (3.5.18)$$

Therefore,

$$I_H \geq I_H(0)e^{-(\mu_H + \delta_H)t} > 0. \quad (3.5.19)$$

Similarly, it can be shown that solutions of $L_w > 0$, $L_s > 0$, $L_m > 0$, $E_h > 0$, $E_L > 0$, $L_H > 0$, $L_M > 0$ for all $t > 0$.

3.5.2 Feasible Region

All parameters and state variables are assumed to be positive. It follows from the previous chapter that the solutions of the model are always positive given initial non-negative conditions, now we verify that non-negative solutions remain bounded and non-negative. Let

$$N_H = S_H + I_H \quad (3.5.20)$$

and add equation (1) and equation (2) of the model system (3.4.9) it then follows that

$$\frac{dN_H}{dt} = \Lambda_H - \mu_H N_H - \delta_H I_H. \quad (3.5.21)$$

It continues to be

$$\left\{ \begin{array}{l} \frac{N_H}{dt} \leq \Lambda_H - \mu_H N_H, \\ \frac{N_H}{dt} + \mu_H N_H \leq \Lambda_H. \end{array} \right. \quad (3.5.22)$$

The integrating factor is $e^{\mu_H t}$, multiply both sides with the integrating factor as follows

$$\frac{d}{dt}(N_H e^{\mu_H t}) \leq \Lambda_H e^{\mu_H t}. \quad (3.5.23)$$

Integrating equation (3.5.23) yields

$$N_H e^{\mu_H t} \leq \frac{\Lambda_H}{\mu_H} e^{\mu_H t} + c. \quad (3.5.24)$$

So that

$$N_H(t) \leq \frac{\Lambda_H}{\mu_H} + c e^{-\mu_H t}. \quad (3.5.25)$$

This implies that

$$\lim_{t \rightarrow \infty} \sup(N_H(t)) \leq \frac{\Lambda_H}{\mu_H}. \quad (3.5.26)$$

Now, using the same method of solving ordinary differential equation we then have the third equation as

$$\frac{d}{dt}(L_w e^{(\mu_w + \alpha_w)t}) \leq \frac{\beta_H L_M (\Lambda_H - \mu_H)}{\phi_w (L_0 + L_M) (\Lambda_H + \mu_H)} e^{(\mu_w + \alpha_w)t}, \quad (3.5.27)$$

integrate both sides

$$L_w e^{(\mu_w + \alpha_w)t} \leq \frac{1}{(\mu_w + \alpha_w)} \frac{\beta_H L_M (\Lambda_H - \mu_H)}{\phi_w (L_0 + L_M) (\Lambda_H + \mu_H)} e^{(\mu_w + \alpha_w)t} + C. \quad (3.5.28)$$

Which then implies that

$$\lim_{t \rightarrow \infty} L_w \leq \frac{1}{(\mu_w + \alpha_w)} \frac{\beta_H L_M (\Lambda_H - \mu_H)}{\phi_w (L_0 + L_M) (\Lambda_H + \mu_H)}. \quad (3.5.29)$$

Similar expressions can be derived using the above approach

$$\left\{ \begin{array}{l} \lim_{t \rightarrow \infty} L_s \leq \frac{1}{(\mu_w + \alpha_w)} \frac{1}{(\mu_s + \alpha_s)} \frac{\beta_H L_M \alpha_w (\Lambda_H - \mu_H)}{\phi_w(L_0 + L_M)(\Lambda_H + \mu_H)}, \\ \lim_{t \rightarrow \infty} L_m \leq \frac{1}{\mu_m(\mu_w + \alpha_w)} \frac{1}{(\mu_s + \alpha_s)} \frac{\beta_H L_M \alpha_w (\Lambda_H - \mu_H)}{2\phi_w(L_0 + L_M)(\Lambda_H + \mu_H)}, \\ \lim_{t \rightarrow \infty} E_h \leq \frac{N_m \alpha_m}{\mu_m(\mu_w + \alpha_w)} \frac{1}{(\mu_s + \alpha_s)} \frac{1}{(\mu_h + \alpha_h)} \frac{\beta_H L_M \alpha_w \alpha_s (\Lambda_H - \mu_H)}{\phi_w(L_0 + L_M)(\Lambda_H + \mu_H)}, \\ \lim_{t \rightarrow \infty} E_L \leq \frac{N_m \alpha_m \alpha_h}{\mu_m \mu_H (\mu_w + \alpha_w)} \frac{1}{(\mu_s + \alpha_s)} \frac{1}{(\mu_h + \alpha_h)} \frac{1}{(\mu_L + \alpha_L)} \frac{\beta_H L_M \alpha_w \alpha_s (\Lambda_H - \mu_H)}{2\phi_w(L_0 + L_M)}, \\ \lim_{t \rightarrow \infty} L_H \leq \frac{N_m \alpha_m N_H \alpha_L \alpha_h}{\mu_m \mu_H (\mu_w + \alpha_w)} \frac{1}{(\mu_s + \alpha_s)} \frac{1}{(\mu_h + \alpha_h)} \frac{1}{(\mu_L + \alpha_L)} \frac{1}{(\mu_P + \alpha_H)} \frac{\beta_H L_M \alpha_w \alpha_s (\Lambda_H - \mu_H)}{2\phi_w(L_0 + L_M)}. \end{array} \right. \quad (3.5.30)$$

The expression for L_M is as follows;

$$\left\{ \begin{array}{l} L_M \leq \frac{N_m \alpha_m N_H \alpha_L \alpha_h \alpha_H \beta_H \alpha_w \alpha_s (\Lambda_H - \mu_H)}{2\eta \mu_m \mu_H \mu_M (\mu_w + \alpha_w) (\mu_s + \alpha_s) (\mu_h + \alpha_h) (\mu_L + \alpha_L) (\mu_P + \alpha_H)} - L_0, \\ \leq L_0 (\mu_H + \delta_H) (R_0 - 1). \end{array} \right. \quad (3.5.31)$$

Therefore, when we substitute the expression for L_M into equation (3.5.30) we get the region Ω defined by

$$\Omega = \{(S_H, I_H, L_w, L_s, L_m, E_h, E_L, L_H, L_M) \in \mathbb{R}_+^9 : 0 \leq S_H + I_H \leq Z_1, 0 \leq L_w \leq Z_2, 0 \leq L_s \leq Z_3, 0 \leq L_m \leq Z_4, 0 \leq E_h \leq Z_5, 0 \leq E_L \leq Z_6, 0 \leq L_H \leq Z_7, 0 \leq L_M \leq Z_8\} \quad (3.5.32)$$

where,

$$\left\{ \begin{array}{l}
 Z_1 = \frac{\Lambda_H}{\mu_H}, \\
 Z_2 = \frac{\beta_H(R_0 - 1)(\Lambda_H - \mu_H)}{\eta R_0(\mu_w + \alpha_w)(\Lambda_H + \mu_H)}, \\
 Z_3 = \frac{\alpha_w \beta_H L_0(R_0 - 1)(\Lambda_H - \mu_H)}{\eta L_0 R_0(\mu_w + \alpha_w)(\mu_s + \alpha_s)(\Lambda_H + \mu_H)}, \\
 Z_4 = \frac{\beta_H \alpha_w \alpha_s L_0(R_0 - 1)(\Lambda_H - \mu_H)}{2\eta \mu_m L_0 R_0(\mu_w + \alpha_w)(\mu_s + \alpha_s)(\Lambda_H + \mu_H)}, \\
 Z_5 = \frac{N_m \alpha_m \alpha_s \alpha_w \beta_H L_M(\Lambda_H - \mu_H)}{2\eta L_0 R_0 \mu_m(\mu_s + \alpha_s)(\mu_h + \alpha_h)(\mu_w + \alpha_w)(\Lambda_H + \mu_H)}, \\
 Z_6 = \frac{N_m \alpha_m \alpha_h \alpha_w \alpha_s \beta_H L_0(R_0 - 1)(\Lambda_H - \mu_H)}{2\eta \mu_m \mu_H L_0 R_0(\mu_s + \alpha_s)(\mu_w + \alpha_w)(\mu_h + \alpha_h)(\mu_L + \alpha_L)}, \\
 Z_7 = \frac{N_m \alpha_h \alpha_s \alpha_m N_H \alpha_w \alpha_L \beta_H L_M(\Lambda_H - \mu_H)}{2\eta \mu_m \mu_H L_0 R_0(\mu_s + \alpha_s)(\mu_w + \alpha_w)(\mu_P + \alpha_H)(\mu_h + \alpha_h)(\mu_L + \alpha_L)}, \\
 Z_8 = L_0(\mu_H + \delta_H)(R_0 - 1).
 \end{array} \right. \quad (3.5.33)$$

This implies that Ω is a positively invariant region since all solutions that will start in Ω will remain in Ω for all $t \geq 0$. Hence the model system (3.4.9) is mathematically and epidemiologically well posed.

3.6 Disease free equilibrium and its stability(DFE)

The equilibrium states of the model are obtained by setting the right-hand side of the model system (3.4.9) to zero and solve for the variables. Disease-free equilibrium suggests that there is no disease, therefore, no worms, eggs and therefore no human infection. The multiscale model (3.4.9) has a disease-free equilibrium is given by

$$E_0 = (S_H, I_H, L_w, L_s, L_m, E_h, E_L, L_H, L_M), \quad (3.6.34)$$

$$= \left(\frac{\Lambda_H}{\mu_H}, 0, 0, 0, 0, 0, 0, 0, 0 \right), \quad (3.6.35)$$

where E_0 denotes the disease-free equilibrium of the model system (3.4.9).

3.6.1 Reproductive Number R_0

Similarly to the previous chapter, we use the next generation operator approach as follows. We determine the basic reproductive number for the system by using the next generation operator approach [26]. The multiscale model can be written in the form

$$\begin{cases} \frac{dX}{dt} = f(X, Y, Z), \\ \frac{dY}{dt} = g(X, Y, Z), \\ \frac{dZ}{dt} = h(X, Y, Z), \end{cases} \quad (3.6.36)$$

where,

- i. $X = (S_H)$ represents all compartments of individuals that are not infected,
- ii. $Y = (I_H, L_w, L_s, L_m, E_h, E_L, L_H)$ represents all compartments of infected individuals that are not capable of infecting others,
- iii. $Z = (L_M)$ represents all compartments of infected individuals who are capable of infecting.

$$\tilde{g}(X^*, Z) = (\tilde{g}_1(X^*, Z), \tilde{g}_2(X^*, Z), \tilde{g}_3(X^*, Z), \tilde{g}_4(X^*, Z), \tilde{g}_5(X^*, Z), \tilde{g}_6(X^*, Z), \tilde{g}_7(X^*, Z)) \quad (3.6.37)$$

where,

$$\left\{ \begin{array}{l} \tilde{g}_1(X^*, Z) = \frac{\beta_H L_M \Lambda_H}{\mu_H (\mu_H + \delta_H) (L_0 + L_M)}, \\ \tilde{g}_2(X^*, Z) = \frac{\beta_H L_M (\Lambda_H - \mu_H)}{\eta \mu_H (\mu_H + \delta_H) (\mu_w + \alpha_w) (L_0 + L_M) (I_H + 1)}, \\ \tilde{g}_3(X^*, Z) = \frac{\beta_H \alpha_w L_M (\Lambda_H - \mu_H)}{\eta \mu_H (\mu_H + \delta_H) (\mu_w + \alpha_w) (\mu_s + \alpha_s) (L_0 + L_M) (I_H + 1)}, \\ \tilde{g}_4(X^*, Z) = \frac{1}{2} \frac{\alpha_h \alpha_w \beta_H (\Lambda_H - \mu_H) L_M}{\eta \mu_m \mu_H (\mu_H + \delta_H) (\mu_s + \alpha_s) (\mu_w + \alpha_w) (L_0 + L_M) (I_H + 1)}, \\ \tilde{g}_5(X^*, Z) = \frac{1}{2} \frac{N_m \alpha_s \alpha_m \alpha_w \beta_H (\Lambda_H - \mu_H) L_M}{\eta \mu_m \mu_H (\mu_H + \delta_H) (\mu_h + \alpha_h) (\mu_s + \alpha_s) (\mu_w + \alpha_w) (L_0 + L_M) (I_H + 1)}, \\ \tilde{g}_6(X^*, Z) = \frac{1}{2} \frac{N_m \alpha_m \alpha_s \alpha_h \alpha_w \beta_H (\Lambda_H - \mu_H) L_M}{\eta \mu_m \mu_H (\mu_H + \delta_H) (\mu_L + \alpha_L) (\mu_h + \alpha_h) ((\mu_s + \alpha_s) (\mu_w + \alpha_w) (L_0 + L_M))}, \\ \tilde{g}_7(X^*, Z) = \frac{1}{2} \frac{N_H N_m \alpha_L \alpha_m \alpha_s \alpha_w \alpha_h \beta_H L_M (\Lambda_H - \mu_H)}{\eta \mu_m \mu_H (\mu_H + \delta_H) (\mu_P + \alpha_H) (\mu_L + \alpha_L) (\mu_h + \alpha_h) (\mu_s + \alpha_s) (\mu_w + \alpha_w) (L_0 + L_M)}. \end{array} \right. \quad (3.6.38)$$

Now, we use the following equation

$$\frac{dL_M}{dt} = \alpha_H L_H - \mu_R L_M. \quad (3.6.39)$$

Let $A = D_z h(X^*, \tilde{g}(X^*, 0), 0)$ and further assume that A can be written in the form $A = M - D$, where $M \geq 0$ and $D > 0$, is a diagonal matrix. Then A becomes

$$A = \frac{1}{2} \frac{N_H N_m \alpha_L \alpha_H \alpha_m \alpha_s \alpha_w \alpha_h \beta_H (\Lambda_H - \mu_H)}{\eta \mu_m \mu_H (\mu_H + \delta_H) (\mu_P + \alpha_H) (\mu_L + \alpha_L) (\mu_h + \alpha_h) (\mu_s + \alpha_s) (\mu_w + \alpha_w) L_0} - \mu_M. \quad (3.6.40)$$

From the above equation we can deduce that

$$M = \frac{1}{2} \frac{N_H N_m \alpha_L \alpha_H \alpha_m \alpha_s \alpha_w \alpha_h \beta_H (\Lambda_H - \mu_H)}{\eta \mu_m \mu_H \mu_M (\mu_H + \delta_H) (\mu_P + \alpha_H) (\mu_L + \alpha_L) (\mu_h + \alpha_h) (\mu_s + \alpha_s) (\mu_w + \alpha_w) L_0} \quad (3.6.41)$$

and $D = \mu_M$. Therefore the basic reproductive number is the spectral radius (dominant eigenvalue) of the matrix given by

$$T = MD^{-1} \quad (3.6.42)$$

that means that

$$R_0 = \rho(T). \quad (3.6.43)$$

We can then conclude that the basic reproductive number of the model (3.4.9) is given by

$$R_0 = \frac{1}{2} \frac{N_H N_m \alpha_L \alpha_H \alpha_h \alpha_m \alpha_s \alpha_w \beta_H (\Lambda_H - \mu_H)}{L_0 \mu_m \mu_M \mu_H \eta (\mu_H + \delta_H) (\mu_L + \alpha_L) (\mu_h + \alpha_h) (\mu_s + \alpha_s) (\mu_w + \alpha_w) (\mu_P + \alpha_H)} \quad (3.6.44)$$

$$(3.6.45)$$

$$= R_{0w} R_{0H}, \quad (3.6.46)$$

with R_{0w} being a partial within-host reproductive number and R_{0H} being a partial between-host reproductive number. Therefore, the basic reproductive number R_0 , given by

$$R_0 = R_{0w} R_{0H} \quad (3.6.47)$$

where,

$$\begin{cases} R_{0w} = \frac{N_m \alpha_m \alpha_s \alpha_w \alpha_h}{2\eta \mu_m (\mu_h + \alpha_h) (\mu_s + \alpha_s) (\mu_w + \alpha_w)}, \\ R_{0H} = \frac{N_H \alpha_H \alpha_L \beta_H (\Lambda_H - \mu_H)}{\mu_M \mu_H L_0 (\mu_H + \delta_H) (\mu_L + \alpha_L) (\mu_P + \alpha_H) L_0}. \end{cases} \quad (3.6.48)$$

It can be concluded that both the within-host and the between-host factors affect the transmission of hookworm infection.

3.6.2 Local stability of DFE

To determine the local stability of model system (3.4.9), we linearise equations of the model in order to obtain the Jacobian matrix. By pure inspection, it is nearly impossible to see the eigenvalues of the matrix (3.6.50). To prove the local stability of the model system (3.4.9), we then use the Gershgorin's

theorem [22]. The theorem is used on a strictly diagonally dominant matrices, first we check if each row satisfies the inequality $|A_{ij}| > \sum_{j \neq i} |A_{ij}|$.

Theorem 3.1. *The disease free equilibrium point E^0 , of model system (3.4.9) is locally asymptotically stable whenever $R_0 < 1$ and unstable otherwise.*

$$E^0 = \left(\frac{\Lambda_H}{\mu_H}, 0, 0, 0, 0, 0, 0, 0, 0, 0 \right), \quad (3.6.49)$$

The Jacobian matrix of the model system (3.4.9) evaluated at the DFE is given by

$$J(E^0) = \begin{pmatrix} -\mu_H & 0 & 0 & 0 & 0 & 0 & 0 & 0 & -\frac{\beta_H \Lambda_H}{L_0 \mu_H} \\ 0 & -b_0 & 0 & 0 & 0 & 0 & 0 & 0 & \frac{\beta_H \Lambda_H}{L_0 \mu_H} \\ 0 & 0 & -b_1 & 0 & 0 & 0 & 0 & 0 & \frac{\beta_H (\Lambda_H - \mu_H)}{\phi_w \mu_H L_0} \\ 0 & 0 & \alpha_w & -b_2 & 0 & 0 & 0 & 0 & 0 \\ 0 & 0 & 0 & \frac{\alpha_s}{2} & -\mu_m & 0 & 0 & 0 & 0 \\ 0 & 0 & 0 & 0 & N_m \alpha_m & -b_3 & 0 & 0 & 0 \\ 0 & 0 & 0 & 0 & 0 & \alpha_h & -b_4 & 0 & 0 \\ 0 & 0 & 0 & 0 & 0 & 0 & N_H \alpha_L & -b_5 & 0 \\ 0 & 0 & 0 & 0 & 0 & 0 & 0 & \alpha_H & -\mu_M \end{pmatrix}. \quad (3.6.50)$$

Where,

$$\left\{ \begin{array}{l} b_0 = (\mu_H + \delta_H), \\ b_1 = (\mu_w + \alpha_w), \\ b_2 = (\mu_s + \alpha_s), \\ b_3 = (\mu_h + \alpha_h), \\ b_4 = (\mu_L + \alpha_L), \\ b_5 = (\mu_P + \alpha_H). \end{array} \right. \quad (3.6.51)$$

Stability of the DFE is tested by using the Geshgorin's theorem [22] which states that the eigenvalues of A must always lie within the Geshgorin disks C_j corresponding to

$$|A_{ij}| > \sum_{j \neq i} |A_{ij}| \quad \text{for } i=1, 2, 3, \dots, n. \quad (3.6.52)$$

$$\left\{ \begin{array}{l}
 \text{row 1 : } | -\mu_H | > \left| -\frac{\beta_H \Lambda_H}{L_0 \mu_H} \right|, \\
 \text{row 2 : } | -a_0 | > \left| \frac{\beta_H \Lambda_H}{L_0 \mu_H} \right|, \\
 \text{row 3 : } | -a_1 | > \left| \frac{\beta_H (\Lambda_H - \mu_H)}{\phi_w L_0 \mu_H} \right|, \\
 \text{row 4 : } | -a_2 | > | \alpha_w |, \\
 \text{row 5 : } | -\mu_m | > \left| \frac{\alpha_s}{2} \right|, \\
 \text{row 6 : } | -a_3 | > | N_m \alpha_m |, \\
 \text{row 7 : } | -a_4 | > | \alpha_h |, \\
 \text{row 8 : } | -a_5 | > | N_H \alpha_L |, \\
 \text{row 9 : } | -\mu_M | > | \alpha_H |.
 \end{array} \right. \quad (3.6.53)$$

Which then follows that

$$\left\{ \begin{array}{l} \mu_H > \frac{\beta_H \Lambda_H}{L_0 \mu_H}, \\ a_0 > \frac{\beta_H \Lambda_H}{L_0 \mu_H}, \\ a_1 > \frac{\beta_H (\Lambda_H - \mu_H)}{\phi_w L_0 \mu_H}, \\ a_2 > \alpha_w, \\ \mu_m > \frac{\alpha_s}{2}, \\ a_3 > N_m \alpha_m, \\ a_4 > \alpha_h, \\ a_5 > N_H \alpha_L, \\ \mu_M > \alpha_H. \end{array} \right. \quad (3.6.54)$$

Which then mean that

$$\left\{ \begin{array}{l} a_1 a_2 \mu_m a_3 a_4 a_4 a_5 \mu_M > \frac{\beta_H (\Lambda_H - \mu_H)}{2 \mu_H L_0} \alpha_w \alpha_s N_m \alpha_m \alpha_h N_H \alpha_L \alpha_H, \\ 1 > \frac{\beta_H \alpha_w \alpha_s N_m \alpha_m \alpha_h N_H \alpha_L \alpha_H (\Lambda_H - \mu_H)}{2 \mu_H L_0 \mu_M \mu_m a_1 a_2 a_3 a_4 a_5}, \end{array} \right. \quad (3.6.55)$$

where,

$$R_0 = \frac{\beta_H \alpha_w \alpha_s N_m \alpha_m \alpha_h N_H \alpha_L \alpha_H (\Lambda_H - \mu_H)}{2 \mu_H L_0 \mu_M \mu_m a_1 a_2 a_3 a_4 a_5} \quad (3.6.56)$$

with the definition of a_1, a_2, a_3, a_4, a_5 mentioned above previously in this section therefore $R_0 < 1$.

3.6.3 Global Stability DFE

We use Theorem (3.2) to establish that the disease free equilibrium is globally asymptotically stable if $R_0 < 1$ whenever the two conditions (H_1, H_2) are satisfied [21].

Theorem 3.2. *The fixed point $E^0 = (\frac{\Lambda_H}{\mu_H}, 0, 0, 0, 0, 0, 0, 0, 0)$ is globally asymptotically stable (g.a.s) equilibrium of the system (3.4.9) if $R_0 < 1$ and the assumptions (H1) and (H2) are satisfied.*

$$\begin{cases} \frac{dX}{dt} = F(X, Z), \\ \frac{dZ}{dt} = G(X, Z). \end{cases} \quad (3.6.57)$$

where,

- i. $X = (S_H)$ represents all compartments of individuals that are not infected,
- ii. $Z = (I_H, L_w, L_s, L_m, E_h, E_L, L_H, L_M)$ represents all compartments which are infectious.

$$E^0 = (X^*, 0) = \left(\frac{\Lambda_H}{\mu_H}, 0, 0, 0, 0, 0, 0, 0, 0 \right),$$

denotes the disease free equilibrium of the system. These conditions should be met for global stability:

H1. $\frac{dX}{dt} = F(X, 0)$ where X^* is globally asymptotically stable,

H2. $G(X, Z) = AZ - \hat{G}(X, Z)$, $\hat{G}(X, Z) > 0$ for $(X, Z) \in \mathbb{R}_9^+$ where $A = D_Z G(X^*, 0)$ is an M -matrix and \mathbb{R}_9^+ is the region where the model makes biological sense.

Therefore,

$$F(X, 0) = [\Lambda_H - \mu_H S_H], \quad (3.6.58)$$

and

$$J(E_0) = \begin{pmatrix} -k_0 & 0 & 0 & 0 & 0 & 0 & 0 & \frac{\beta_H \Lambda_H}{L_0 \mu_H} \\ 0 & -k_1 & 0 & 0 & 0 & 0 & 0 & \frac{\beta_H (\Lambda_H - \mu_H)}{\phi_w \mu_H L_0} \\ 0 & \alpha_w & -k_2 & 0 & 0 & 0 & 0 & 0 \\ 0 & 0 & \frac{\alpha_s}{2} & -\mu_m & 0 & 0 & 0 & 0 \\ 0 & 0 & 0 & N_m \alpha_m & -k_3 & 0 & 0 & 0 \\ 0 & 0 & 0 & 0 & \alpha_h & -k_4 & 0 & 0 \\ 0 & 0 & 0 & 0 & 0 & N_H \alpha_L & -k_5 & 0 \\ 0 & 0 & 0 & 0 & 0 & 0 & \alpha_H & -\mu_M \end{pmatrix}, \quad (3.6.59)$$

where,

$$\begin{cases} k_0 = (\mu_H + \delta_H), \\ k_1 = (\mu_w + \alpha_w), \\ k_2 = (\mu_s + \alpha_s), \\ k_3 = (\mu_h + \alpha_h), \\ k_4 = (\mu_L + \alpha_L), \\ k_6 = (\mu_P + \alpha_H). \end{cases} \quad (3.6.60)$$

$$\tilde{G}(X, Z) = \begin{bmatrix} \beta_H L_M \left(\frac{\Lambda_H}{L_0 \mu_H} - \frac{S_H}{L_0 + L_M} \right) \\ \beta_H L_M \left(\frac{(\Lambda_H - \mu_H)}{\phi_w L_0 \mu_H} - \frac{(S_H - 1)}{(L_0 + L_M)(I_H + 1)} \right) \\ 0 \\ 0 \\ 0 \\ 0 \\ 0 \\ 0 \end{bmatrix}. \quad (3.6.61)$$

Since $(S_H^0 = \frac{\Lambda_H}{\mu_H}) \frac{1}{L_0} \geq \frac{S_H}{L_0 + L_M}$ and $\frac{(\Lambda_H - \mu_H)}{\phi_w L_0 \mu_H} \geq \frac{(S_H - 1)}{(L_0 + L_M)(I_H + 1)}$ therefore $\tilde{G}(X, Z) \geq 0$ for all $(X, Z) \in \mathbb{R}_9^+$. From the working we can clearly see that the matrix J is an M-matrix since the off diagonal elements of J are non-negative.

3.7 Endemic state and its stability

The model system (3.4.9) has two steady states : the disease free state $E^0 = \left(\frac{\Lambda_H}{\mu_H}, 0, 0, 0, 0, 0, 0, 0, 0 \right)$ and the infection steady state E_1^* . In this section, we determine the endemic equilibrium state. Following from [27] the endemic equilibrium state is the state where the disease cannot be totally eradicated but remaining in the population. For the disease to persist in the population, the susceptible class, infectious class, within-host infective worm class, matured worm class, small intestine worm class, within-host eggs, physical environment eggs class, non-infective worm class, physical environment infective worm class must not be zero at endemic equilibrium state. The endemic equilibrium states E_1^* given by

$$E_1^* = (S_H^*, I_H^*, L_w^*, L_s^*, L_m^*, E_h^*, E_L^*, L_H^*, L_M^*). \quad (3.7.62)$$

Endemic equilibrium expressions are shown with their interpretation and also prove its existence.

3.7.1 The Endemic equilibrium state

The infected steady state E_1^* exists if and only if $R_0 > 1$. Meaning that

$$E_1^* = (S_H^*, I_H^*, L_w^*, L_s^*, L_m^*, E_h^*, E_L^*, L_H^*, L_M^*) \neq \left(\frac{\Lambda_H}{\mu_H}, 0, 0, 0, 0, 0, 0, 0, 0 \right).$$

Then we solve the equations in the model system (3.4.9) simultaneously.

The susceptible human's endemic value is given by

$$S_H^* = \frac{\Lambda_H}{\lambda_H^* + \mu_H}. \quad (3.7.63)$$

From the above expression, the susceptible human population at the endemic equilibrium is proportional to the average time the susceptible stay in the compartment and the rate of supply of new susceptible recruited through birth. The point of exit this compartment is through natural death or infection.

The endemic value of infected humans is given by

$$I_H^* = \frac{\lambda_H^* S_H^*}{\mu_H + \delta_H}. \quad (3.7.64)$$

This expression shows that the infected population at endemic is directly proportional to the average rate of staying in infectious class, the rate of infection of the susceptible population and the number of susceptible individuals.

The endemic value of the infective larvae inside a single infected host is given by

$$L_w^* = \frac{\lambda_h^* S_h^*}{\mu_w + \alpha_w}. \quad (3.7.65)$$

From the above expression we deduce that the average hookworm parasite population inside a single human host at equilibrium is equal to the life-span of hookworm parasite within a single infected host and the rate at which a susceptible host to become an infected host.

At endemic, the population of immature worm in the small intestine is given by

$$L_s^* = \frac{\alpha_w L_w^*}{\mu_s + \alpha_s}. \quad (3.7.66)$$

The endemic value of the mature worms is

$$L_m^* = \frac{\alpha_s L_s^*}{2\mu_m}. \quad (3.7.67)$$

The above expression shows that the rate at which the immature become mature worms and the life-span of mature worms determine the endemic equilibrium within a human host. Therefore the natural decay of mature worms reduces the mature worms.

The average hookworm egg population within a single infected human host at endemic equilibrium is

$$E_h^* = \frac{N_m \alpha_m L_m^*}{\mu_h + \alpha_h}. \quad (3.7.68)$$

The expression implies that equilibrium of the average hookworm egg population within a host is directly proportional to the average egg and worm. Factors that destroy the eggs within an infected human host reduce the endemic equilibrium associated with worm eggs.

The population of hookworm eggs at the physical sand environment at endemic equilibrium is given by

$$E_L^* = \frac{(I_H^* + 1)\alpha_h E_h^*}{\mu_L + \alpha_L}. \quad (3.7.69)$$

It can be deduced that the life-span of eggs is the rate at which each infected human host excrete hookworm eggs total number of humans infected by larvae influence the endemic equilibrium associated with hookworm eggs in the physical sand environment.

$$L_H^* = \frac{N_H \alpha_L E_L^*}{\mu_p + \alpha_H}. \quad (3.7.70)$$

The endemic value for the infective larvae is given by

$$L_M^* = \frac{\alpha_H L_H^*}{\mu_H}. \quad (3.7.71)$$

The endemic value of infective larvae is influenced by non-infective larvae directly influence the endemic levels of larvae in physical sand environment.

3.7.2 Existence of endemic equilibrium state

In this section we look at the above results and prove its existence of endemic equilibrium for the model (3.4.9). Each variable is written in terms of L_M^* as follows:

$$\left\{ \begin{array}{l} S_H^*(L_M^*) = \frac{\Lambda_H(L_0 + L_M^*)}{\mu_H L_0 + (\beta_H + \mu_H)L_M^*}, \\ I_H^*(L_M^*) = \frac{\beta_H \Lambda_H L_M^*}{(\mu_H + \delta_H)[(\beta_H + \mu_H)L_M^* + \mu_H L_0]}, \\ L_w^*(L_M^*) = \frac{(\Lambda_H - \mu_H)\beta_H L_M^*(L_0 + L_M^*) - \beta_H^2 L_M^{*2}}{\eta(\mu_w + \alpha_w)(L_0 + L_M^*)[(\beta_H + \mu_H)L_M^* + \mu_H L_0](I_H^* + 1)}, \\ L_s^*(L_M^*) = \frac{(\Lambda_H - \mu_H)\beta_H \alpha_w L_M^*(L_0 + L_M^*) - \beta_H^2 \alpha_w L_M^{*2}}{\eta(\mu_w + \alpha_w)(\mu_s + \alpha_s)(L_0 + L_M^*)[(\beta_H + \mu_H)L_M^* + \mu_H L_0](I_H^* + 1)}, \\ L_m^*(L_M^*) = \frac{(\Lambda_H - \mu_H)\beta_H \alpha_w \alpha_s L_M^*(L_0 + L_M^*) - \beta_H^2 \alpha_w \alpha_s L_M^{*2}}{2\eta\mu_m(\mu_w + \alpha_w)(\mu_s + \alpha_s)(L_0 + L_M^*)[(\beta_H + \mu_H)L_M^* + \mu_H L_0](I_H^* + 1)}, \\ E_h^*(L_M^*) = \frac{(\Lambda_H - \mu_H)\beta_H \alpha_w \alpha_s N_m \alpha_m L_M^*(L_0 + L_M^*) - \beta_H^2 \alpha_w \alpha_s N_m \alpha_m L_M^{*2}}{2\eta\mu_m(\mu_w + \alpha_w)(\mu_s + \alpha_s)(\mu_h + \alpha_h)(L_0 + L_M^*)[(\beta_H + \mu_H)L_M^* + \mu_H L_0](I_H^* + 1)}, \\ E_L^*(L_M^*) = \frac{(\Lambda_H - \mu_H)\beta_H \alpha_w \alpha_s N_m \alpha_m \alpha_h L_M^*(L_0 + L_M^*) - \beta_H^2 \alpha_w \alpha_s N_m \alpha_m \alpha_h L_M^{*2}}{2\eta\mu_m(\mu_w + \alpha_w)(\mu_s + \alpha_s)(\mu_h + \alpha_h)(\mu_L + \alpha_L)(L_0 + L_M^*)[(\beta_H + \mu_H)L_M^* + \mu_H L_0]}, \\ L_H^*(L_M^*) = \frac{(\Lambda_H - \mu_H)\beta_H \alpha_w \alpha_s N_m \alpha_m \alpha_h N_H \alpha_L L_M^*(L_0 + L_M^*) - \beta_H^2 \alpha_w \alpha_s N_m \alpha_m \alpha_h N_H \alpha_L L_M^{*2}}{2\eta\mu_m(\mu_w + \alpha_w)(\mu_s + \alpha_s)(\mu_h + \alpha_h)(\mu_L + \alpha_L)(\mu_P + \alpha_H)(L_0 + L_M^*)e}, \end{array} \right. \quad (3.7.72)$$

where

$$e = [(\beta_H + \mu_H)L_M^* + \mu_H L_0].$$

Proof: Let

$$E_1 = (S_H^*, I_H^*, L_w^*, L_s^*, L_m^*, E_h^*, E_L^*, L_H^*, L_M^*) \quad (3.7.73)$$

be an endemic solution for the model system (3.4.9). We then express $S_H^*, I_H^*, L_w^*, L_s^*, L_m^*, E_h^*, E_L^*, L_H^*$ in terms of L_M^* as follows:

substitute the above expressions in the equation for L_M which is given by:

$$\frac{dL_M}{dt} = \alpha_H L_H^* - \mu_M L_M^*, \quad (3.7.74)$$

at the endemic we get :

$$L_M^*[AL_M^{*2} + BL_M^* + C] = 0. \quad (3.7.75)$$

Where,

$$\left\{ \begin{array}{l} A = 2\eta\mu_m\mu_H(\mu_s + \alpha_s)(\mu_w + \alpha_w)(\mu_h + \alpha_h)(\mu_L + \alpha_L)(\mu_P + \alpha_H), \\ B = \left[1 + \left(\frac{\beta_H}{\Lambda_H - \mu_H} - 1 \right) \frac{\mu_H(\mu_H + \delta_H)}{\beta_H + 2\mu_H} R_0 \right] 2\eta L_0 \mu_m \mu_M (\mu_s + \alpha_s)(\mu_w + \alpha_w)(\mu_h + \alpha_h) \\ \quad (\mu_L + \alpha_L)(\mu_P + \alpha_H)(\beta_H + 2\mu_H), \\ C = [1 - (\mu_H + \delta_H)R_0] 2\eta\mu_m\mu_H\mu_M L_0^2 (\mu_s + \alpha_s)(\mu_w + \alpha_w)(\mu_h + \alpha_h)(\mu_L + \alpha_L)(\mu_P + \alpha_H). \end{array} \right. \quad (3.7.76)$$

Equation (3.7.75) can be represented in the form:

$$A[L_M^{*2} + E_M L_M^* + F_M]L_M^* = 0, \quad (3.7.77)$$

where $E_M = \frac{B}{A}$ and $F_M = \frac{C}{A}$. Therefore,

$$\left\{ \begin{array}{l} E_M = \left[1 + \left(\frac{\beta_H}{\Lambda_H - \mu_H} - 1 \right) \frac{\mu_H(\mu_H + \delta_H)}{\beta_H + 2\mu_H} R_0 \right] (\beta_H + \mu_H), \\ F_M = [1 - (\mu_H + \delta_H)R_0] \mu_H L_0^2 \end{array} \right. \quad (3.7.78)$$

From equation (3.7.76) it is clear that A is positive for all $R_0 > 1$. Furthermore, $C < 0$ for $R_0 > 1$ while B can be both positive or negative for different values for $R_0 > 1$. Using equation (3.7.75) we can get

$L_M^* = 0$, which corresponds to disease-free equilibrium point or

$$L_M^* = \frac{1}{2} \left[-E_M \pm \sqrt{E_M^2 - 4F_M} \right] \quad (3.7.79)$$

for the endemic equilibrium point.

The following conditions have to hold for L_M^* to exist;

$$\begin{cases} E_M^2 - 4F_M \geq 0 \\ E_M^2 \geq 4F_M \\ E_M^* \geq \pm 2\sqrt{F_M} \end{cases} \quad (3.7.80)$$

and

$$\begin{cases} -E_M^2 \pm \sqrt{E_M^2 - 4F_M} > 0 \\ \pm \sqrt{E_M^2 - 4F_M} > E_M \\ E_M - 4F_M > E_M \\ F_M < 0. \end{cases} \quad (3.7.81)$$

For $F_M < 0$ to be true $1 - (\mu_H + \delta_H)R_0 < 0$ which therefore means $R_0 \geq \frac{1}{\mu_H + \delta_H}$ which also mean $\mu_H + \delta_H = 1$ for $R_0 \geq 1$. We can conclude that there exist only a single positive endemic point for $R_0 \geq 1$. Therefore, there exist only one unique endemic equilibrium point for the model system (3.4.9) whenever $R_0 > 1$.

Theorem 3.3. *The model system (3.4.9) formulated in terms of proportions has at least one endemic equilibrium solution given by*

$$E_1 = (S_H^*, I_H^*, L_w^*, L_s^*, L_m^*, E_h^*, E_L^*, L_H^*, L_M^*), \quad (3.7.82)$$

with S_H^* , I_H^* , L_w^* , L_s^* , L_m^* , E_h^* , E_L^* , L_H^* , L_M^* all non-negative whose existence and properties are determined by the threshold parameter R_0 where

$$R_0 = \frac{1}{2} \frac{N_H N_m \alpha_L \alpha_H \alpha_h \alpha_m \alpha_s \alpha_w \beta_H (\Lambda_H - \mu_H)}{L_0 \mu_m \mu_H \mu_M (\mu_H + \delta_H) (\mu_L + \alpha_L) (\mu_h + \alpha_h) (\mu_m + \alpha_m) (\mu_s + \alpha_s) (\mu_w + \alpha_w) (\mu_p + \alpha_H)}. \quad (3.7.83)$$

3.7.3 Local stability of Endemic equilibrium points

The endemic points exist and it has been determined and now we have to check its stability. The stability is addressed by using the bifurcation approach. Center manifold Theory is used to determine the local stability of a non-hyperbolic equilibrium.

In this case we apply the Center Manifold Theory to change our set of variables. Let $S_H = x_1$, $I_H = x_2$, $L_w = x_3$, $L_s = x_4$, $L_m = x_5$, $E_h = x_6$, $E_L = x_7$, $L_H = x_8$, $L_M = x_9$ so that $N_H = x_1 + x_2$. Furthermore, we let $\phi = \beta^*$, where β^* is considered as the bifurcation parameter. Letting $\beta^* = \beta_H$, if we consider $R_0 = 1$ and solve for β^* . The vector notation $\mathbf{x} = (x_1, x_2, x_3, x_4, x_5, x_6, x_7, x_8, x_9)^T$ and the model system can be written in the form $\frac{d\mathbf{x}}{dt} = F(\mathbf{x})$ where,

$$F(\mathbf{x}) = (f_1, f_2, f_3, f_4, f_5, f_6, f_7, f_8, f_9), \quad (3.7.84)$$

such that

$$\left\{ \begin{array}{l} \frac{dx_1}{dt} = \Lambda_H - \lambda_H x_1 - \mu_H x_1, \\ \frac{dx_2}{dt} = \lambda_H x_1 - (\mu_H + \delta_H) x_2, \\ \frac{dx_3}{dt} = \lambda_h S_h - (\mu_w + \alpha_w) x_3, \\ \frac{dx_4}{dt} = \alpha_w x_3 - (\mu_s + \alpha_s) x_4, \\ \frac{dx_5}{dt} = \frac{\alpha_s}{2} x_4 - \mu_m x_5, \\ \frac{dx_6}{dt} = N_m \alpha_m x_5 - (\mu_h + \alpha_h) x_6, \\ \frac{dx_7}{dt} = (x_2 + 1) \alpha_h x_6 - (\mu_l + \alpha_l) x_7, \\ \frac{dx_8}{dt} = N_H \alpha_L x_7 - (\mu_P + \alpha_H) x_8, \\ \frac{dx_9}{dt} = \alpha_H x_8 - \mu_M x_9, \end{array} \right. \quad (3.7.85)$$

where,

$$\lambda_H(t) = \frac{\beta_H x_9(t)}{L_0 + x_9(t)}, \quad \lambda_h(t) s_h(t) = \frac{\beta_H x_9(t) [x_9(t) - 1]}{\phi_w (L_0 + x_9(t)) [x_2(t) + 1]}. \quad (3.7.86)$$

$$J(E^0) = \begin{pmatrix} -\mu_H & 0 & 0 & 0 & 0 & 0 & 0 & 0 & -\frac{\beta_H \Lambda_H}{L_0 \mu_H} \\ 0 & d_1 & 0 & 0 & 0 & 0 & 0 & 0 & \frac{\beta_H \Lambda_H}{L_0 \mu_H} \\ 0 & 0 & d_2 & 0 & 0 & 0 & 0 & 0 & \frac{\beta_H (\Lambda_H - \mu_H)}{\phi_w \mu_H L_0} \\ 0 & 0 & \alpha_w & d_3 & 0 & 0 & 0 & 0 & 0 \\ 0 & 0 & 0 & \frac{\alpha_s}{2} & -\mu_m & 0 & 0 & 0 & 0 \\ 0 & 0 & 0 & 0 & N_m \alpha_m & d_4 & 0 & 0 & 0 \\ 0 & 0 & 0 & 0 & 0 & \alpha_h & d_5 & 0 & 0 \\ 0 & 0 & 0 & 0 & 0 & 0 & N_H \alpha_L & d_6 & 0 \\ 0 & 0 & 0 & 0 & 0 & 0 & 0 & \alpha_H & -\mu_M \end{pmatrix}, \quad (3.7.87)$$

where,

$$\begin{cases} d_1 = -(\mu_H + \delta_H), \\ d_2 = -(\mu_w + \alpha_w), \\ d_3 = -(\mu_s + \alpha_s), \\ d_4 = -(\mu_h + \alpha_h), \\ d_5 = -(\mu_L + \alpha_L), \\ d_6 = -(\mu_P + \alpha_H). \end{cases} \quad (3.7.88)$$

Theorem 3.4. Consider the following general system of ordinary differential equations with parameter ϕ :

$$\frac{dx}{dt} f(x, \phi), \quad f : \mathbb{R}^n \longrightarrow \mathbb{R}, \quad f : \mathbb{C}^2(\mathbb{R}^2 \times \mathbb{R}) \quad (3.7.89)$$

where 0 is an equilibrium point of the system (3.4.9), that is $f(0, \phi) = 0$ for all ϕ and assume

1. $A = D_x f(0, 0) = \left(\frac{\partial f_i(0, 0)}{\partial x_i} \right)$ is a linearization of the system around the equilibrium 0 with ϕ evaluated at 0. Zero is a simple eigenvalue of A and other eigenvalues of A have negative real part.
2. Matrix A has a left eigenvector denoted by \mathbf{u} and a right eigenvector denoted by \mathbf{v} , corresponding to the zero eigenvalue.

let f_k be the k th component of f and

$$\begin{cases} a = \sum_{k,i,j=1}^n u_k v_i v_j \frac{\partial^2 f_k}{\partial x_i \partial x_j}(0, 0), \\ b = \sum_{k,i,j=1}^n u_k v_i \frac{\partial^2 f_k}{\partial x_i \partial \phi}(0, 0). \end{cases} \quad (3.7.90)$$

The local dynamics of the system around the equilibrium point 0 is totally governed by the signs of a and b .

- i. $a > 0, b > 0$, when $\phi < 0$ with $|\phi| \ll 1$, 0 is locally asymptotically stable and there exists a positive unstable equilibrium; when $0 < \phi \ll 1$, 0 is unstable and there exists a negative and locally asymptotically stable equilibrium.
- ii. $a < 0, b < 0$, when $\phi < 0$ with $|\phi| \ll 1$, 0 is unstable; when $0 < \phi \ll 1$, 0 is a locally asymptotically stable, and there exists a positive unstable equilibrium point.
- iii. $a >, b < 0$, when $\phi < 0$ with $|\phi| \ll 1$, 0 is unstable and there exists a locally asymptotically stable negative equilibrium; when $0 < \phi \ll 1$, 0 is stable and a positive unstable equilibrium appear.
- iv. $a < 0, b > 0$, when ϕ changes from negative to positive, 0 changes its stability from stable to unstable. correspondingly a negative unstable equilibrium becomes positive and locally asymptotically stable.

The eigenvectors of the Jacobian matrix (3.7.87), when $R_0 = 1$ and $\beta_H = \beta^*$ has right eigenvectors associated with the zero eigenvalue given by $u = [u_1, u_2, u_3, u_4, u_5, u_6, u_7, u_8, u_9]^T$, where

$$\left\{ \begin{array}{l} u_1 = -\frac{\beta^*}{\mu_H L_0} \cdot \frac{\Lambda_H}{\mu_H}, \\ u_2 = \frac{\beta^*}{L_0 \mu_H} \cdot \frac{\Lambda_H}{(\mu_H + \delta_H)}, \\ u_3 = \frac{1}{(\mu_w + \alpha_w)} \cdot \frac{\beta^*(\Lambda_H - \mu_H)}{\phi_w \mu_H L_0}, \\ u_4 = \frac{1}{\mu_s + \alpha_s} \cdot \frac{\alpha_w}{(\mu_w + \alpha_w)} \cdot \frac{\beta^*(\Lambda_H - \mu_H)}{\phi_w \mu_H L_0}, \\ u_5 = \frac{1}{2} \cdot \frac{1}{\mu_m} \cdot \frac{\alpha_s}{\mu_s + \alpha_s} \cdot \frac{\alpha_w}{(\mu_w + \alpha_w)} \cdot \frac{\beta^*(\Lambda_H - \mu_H)}{\phi_w \mu_H L_0}, \\ u_6 = \frac{1}{2} \cdot \frac{1}{\mu_h + \alpha_h} \cdot \frac{N_m \alpha_m}{\mu_m} \cdot \frac{\alpha_s}{\mu_s + \alpha_s} \cdot \frac{\alpha_w}{(\mu_w + \alpha_w)} \cdot \frac{\beta^*(\Lambda_H - \mu_H)}{\phi_w \mu_H L_0}, \\ u_7 = \frac{1}{2} \cdot \frac{1}{\mu_L + \alpha_L} \cdot \frac{\alpha_h}{\mu_h + \alpha_h} \cdot \frac{N_m \alpha_m}{\mu_m} \cdot \frac{\alpha_s}{\mu_s + \alpha_s} \cdot \frac{\alpha_w}{(\mu_w + \alpha_w)} \cdot \frac{\beta^*(\Lambda_H - \mu_H)}{\phi_w \mu_H L_0}, \\ u_8 = \frac{1}{2} \cdot \frac{1}{\mu_P + \alpha_H} \cdot \frac{N_H \alpha_L}{\mu_L + \alpha_L} \cdot \frac{\alpha_h}{\mu_h + \alpha_h} \cdot \frac{N_m \alpha_m}{\mu_m} \cdot \frac{\alpha_s}{\mu_s + \alpha_s} \cdot \frac{\alpha_w}{(\mu_w + \alpha_w)} \cdot \frac{\beta^*(\Lambda_H - \mu_H)}{\phi_w \mu_H L_0}, \\ u_9 = 1. \end{array} \right. \quad (3.7.91)$$

Now, we also have to calculate the left eigenvectors of the matrix 3.7.87 associated with the zero eigen-vector at $\beta_H = \beta^*$. The left eigenvector is given by $v = [v_1, v_2, v_3, v_4, v_5, v_6, v_7, v_8, v_9]^T$, where

$$\left\{ \begin{array}{l} v_1 = 0, \\ v_2 = 0, \\ v_3 = \frac{\mu_M \phi_w \mu_H L_0}{\beta_H (\Lambda_H - \mu_H)}, \\ v_4 = \frac{\mu_w + \alpha_w}{\alpha_w} \cdot \frac{\mu_M \phi_w \mu_H L_0}{\beta_H (\Lambda_H - \mu_H)}, \\ v_5 = \frac{2(\mu_s + \mu_s)}{\alpha_s} \cdot \frac{\mu_w + \alpha_w}{\alpha_w} \cdot \frac{\mu_M \phi_w \mu_H L_0}{\beta_H (\Lambda_H - \mu_H)}, \\ v_6 = \frac{\mu_m}{N_m \alpha_m} \cdot \frac{2(\mu_s + \mu_s)}{\alpha_s} \cdot \frac{\mu_w + \alpha_w}{\alpha_w} \cdot \frac{\mu_M \phi_w \mu_H L_0}{\beta_H (\Lambda_H - \mu_H)}, \\ v_7 = \frac{\mu_h + \alpha_h}{\alpha_h} \cdot \frac{\mu_m}{N_m \alpha_m} \cdot \frac{2(\mu_s + \mu_s)}{\alpha_s} \cdot \frac{\mu_w + \alpha_w}{\alpha_w} \cdot \frac{\mu_M \phi_w \mu_H L_0}{\beta_H (\Lambda_H - \mu_H)}, \\ v_8 = \frac{\mu_L + \alpha_L}{N_H \alpha_L} \cdot \frac{\mu_h + \alpha_h}{\alpha_h} \cdot \frac{\mu_m}{N_m \alpha_m} \cdot \frac{2(\mu_s + \mu_s)}{\alpha_s} \cdot \frac{\mu_w + \alpha_w}{\alpha_w} \cdot \frac{\mu_M \phi_w \mu_H L_0}{\beta_H (\Lambda_H - \mu_H)}, \\ v_9 = 1. \end{array} \right. \quad (3.7.92)$$

Calculating non-zero second order of \mathbf{f} with respect to each variable in order to calculate the sign of \mathbf{a} .

$$\left\{ \begin{array}{l} \frac{\partial^2 f_1}{\partial x_9^2} = \frac{2\beta^* \Lambda_H}{L_0^2 \mu_H}, \\ \frac{\partial^2 f_2}{\partial x_9^2} = -\frac{2\beta^* \Lambda_H}{L_0^2 \mu_H}, \\ \frac{\partial^2 f_3}{\partial x_9^2} = \frac{-\beta^* (\Lambda_H - \mu_H)}{\mu_H (\phi_w L_0)^2}. \end{array} \right. \quad (3.7.93)$$

The non-zero partial derivative with respect to β^* and the variables is being used to calculate the sign of b, as follows

$$\left\{ \begin{array}{l} \frac{\partial^2 f_1}{\partial x_9 \partial \beta^*} = -\frac{\Lambda_H}{L_0 \mu_H}, \\ \frac{\partial^2 f_2}{\partial x_9 \partial \beta^*} = \frac{\Lambda_H}{L_0 \mu_H}, \\ \frac{\partial^2 f_3}{\partial x_9 \partial \beta^*} = \frac{(\Lambda_H - \mu_H)}{\mu_H \phi_w L_0}. \end{array} \right. \quad (3.7.94)$$

Substituting equation (3.7.93) and equation (3.7.94) into equation (3.7.90) to give us the sign of a and b.

Therefore,

$$\left\{ \begin{array}{l} a = \sum_{k,i,j=1}^9 u_k v_i v_j \frac{\partial^2 f_k}{\partial x_i \partial x_j}, \\ = u_1 v_9 v_9 \frac{\partial^2 f_1}{\partial x_9^2} + u_2 v_9 v_9 \frac{\partial^2 f_2}{\partial x_9^2} + u_3 v_9 v_9 \frac{\partial^2 f_3}{\partial x_9^2}, \\ = -\frac{2\beta^{2*} \Lambda_H^2}{\mu_H^3 L_0^3} - \frac{2\beta^{2*} \Lambda_H^2}{\mu_H^2 L_0^3 (\mu_H + \delta_H)} - \frac{\beta^{2*} (\Lambda_H - \mu_H)^2}{(\mu_w + \alpha_w) \phi_w^2 \mu_H^2 L_0^3} < 0. \end{array} \right. \quad (3.7.95)$$

Similarly,

$$\left\{ \begin{aligned}
 b &= \sum_{k,i,j=1}^9 u_k v_i \frac{\partial^2 f_k}{\partial x_9 \partial \beta^*}(0, 0), \\
 &= u_1 v_9 \frac{\partial^2 f_1}{\partial x_9 \partial \beta^*}(0, 0) + u_2 v_9 \frac{\partial^2 f_2}{\partial x_9 \partial \beta^*}(0, 0) + u_3 v_9 \frac{\partial^2 f_k}{\partial x_9 \partial \beta^*}(0, 0), \\
 &= \frac{\beta^* \Lambda_H^2}{\mu_H^3 L_0^2} + \frac{\beta^* \Lambda_H^2}{\mu_H^2 L_0^2 (\mu_H + \delta_H)} + \frac{\beta^* (\Lambda_H - \mu_H)^2}{(\mu_w + \alpha_w) \phi_w^2 \mu_H^2 L_0^2} > 0.
 \end{aligned} \right. \quad (3.7.96)$$

Clearly, we observe that $a < 0$ and $b > 0$, Therefore the Hookworm endemic state is locally asymptotically stable.

3.8 Numerical solutions

This section presents the numerical simulations of the model system 3.4.9. These simulations illustrate the influence of various within-host disease parameters on between-host model variables and in turn the influence of the between-host disease parameter on within-host model variables.

The values of model parameters are either from published literature or from estimates as values of some parameters not reported in the literature. The model system is simulated using python Version V2.7. We import the odeint function in the scipy.integrate package in python software using Runge kutta 4th order.

3.8.1 Sensitivity analysis

Sensitivity analysis was conducted on the multiscale model system (3.4.9). The analysis evaluated the sensitivity of the two disease dynamics metrics to all twenty-one parameters of the basic multiscale model for the hookworm infection. The two disease dynamics metrics are (1.) The reproductive number, R_0 (2.) Endemic value of the disease L_M^* . We used the sensitivity analysis to study the relative importance of different input factors on the model output. We make use of the sensitivity index with respect to the

parameter I of the two disease dynamics metrics (R_0, L_M^*) is given by

$$S_{J_i}^I = \frac{\partial J_i}{\partial I} \times \frac{I}{J_i}, \quad i = 1, 2. \quad (3.8.97)$$

Where,

$$\begin{cases} J_1 = R_0, \\ J_2 = L_M^*, \end{cases} \quad (3.8.98)$$

with L_M^* and the reproductive number given in equation (3.8.99). with

$$\begin{cases} L_M^* = \frac{1}{2} \left[-E_M \pm \sqrt{E_M^2 - 4F_M} \right], \\ E_M = \left[1 + \left(\frac{\beta_H}{\Lambda_H - \mu_H} - 1 \right) \frac{\mu_H(\mu_H + \delta_H)}{\beta_H + 2\mu_H} R_0 \right] (\beta_H + \mu_H), \\ F_M = [1 - (\mu_H + \delta_H)R_0] \mu_H L_0^2, \\ R_0 = \frac{1}{2} \frac{N_H N_m \alpha_L \alpha_H \alpha_h \alpha_m \alpha_s \alpha_w \beta_H (\Lambda_H - \mu_H)}{L_0 \mu_m \mu_M \mu_H \eta (\mu_H + \delta_H) (\mu_L + \alpha_L) (\mu_h + \alpha_h) (\mu_s + \alpha_s) (\mu_w + \alpha_w) (\mu_P + \alpha_H)}. \end{cases} \quad (3.8.99)$$

Table (3.3) show the results of the sensitivity assessment of the two hookworm transmission metrics to the baseline multiscale model system (3.4.9) parameters. Parameter number 7 to parameter 15 in Table (3.3) are associated with within-host scale disease parameters with the other parameters for the between-host scale. We noticed from these values that there are two within-host parameters, α_m, N_m being the most sensitive to R_0 . The between-host parameters that are sensitive to R_0 are Λ_H, β_H and N_H . Furthermore, R_0 was observed to be sensitive to natural death rates $\mu_w, \mu_s, \mu_m, \mu_h$. Parameters that are sensitive to the endemic point L_M^* are $\lambda_H, \alpha_m, N_m, N_H$ and α_L of which two of them are within-host scale parameters and the other three are between-host scale parameters. This sensitivity analysis should be taken into consideration when improving the accuracy of between-host scale parameters during data collection. Since L_M^* is more sensitive to the between-host parameters this implies that wearing shoes and improving sanitation facilities are more effective in controlling the hookworm infection and when the disease is at endemic in population level.

Both L_M^* and R_0 are significantly sensitive to β_H, N_H , we noticed β_H is modified by educating people about hookworm and changing a behavioral practice which implies wearing shoes. Overall, we note the assessment of the sensitivity of all the two hookworm transmission metrics which are the reproductive number and the endemic point L_M^* of the multiscale model parameters was useful with respect to guiding data collection for model parameterisation and to identify parameters which are crucial in the control of hookworm epidemics.

Figure (3.6) - (3.9) illustrates the solution profile of the population Infected human host (I_H), Hookworm eggs in the environment (E_L), Immature non-infective worms (L_H) and infective worms in environment (L_M) while varying the within-host parameters namely; $\alpha_w, \alpha_h, \mu_h$ and N_m .

Parameter	Description	Initial value value	Units	Source
β_H	Exposure rate of humans	0.028	day^{-1}	[29]
Λ_H	Human birth rate	0.5	humans day^{-1}	Estimated
L_0	Saturation constant	2×10^6	—	Estimated
μ_H	Human natural death rate	0.0000384	day^{-1}	[30]
δ_H	Death induced	0.0013699	day^{-1}	[10]
μ_w	Natural decay rate of within human host infective worm	0.009	day^{-1}	Estimated
α_w	Migration rate of infective worm to small intestine	0.09	day^{-1}	Estimated
μ_s	Natural decay rate of worms in the small intestine	0.0097	day^{-1}	Estimated
μ_m	Natural decay rate of fertilised	0.000183	day^{-1}	[10]
N_m	Average number of immature hookworms hatched	300	day^{-1}	Estimated
α_m	Rate at which the hookworm eggs are produced	0.1	day^{-1}	[10]
μ_h	Natural decay of hookworm eggs in the human host	0.0004	day^{-1}	[10]
μ_L	Natural decay rate of hookworm eggs in environment	0.0025	day^{-1}	[10]
α_L	Rate at which eggs hatch	0.009	day^{-1}	Estimated
μ_P	Natural decay of immature worms in environment	0.000685	day^{-1}	Estimated
α_H	Rate at which immature worms become infective worms	0.005	day^{-1}	Estimated
μ_M	Natural decay of infective larvae	0.05	day^{-1}	Estimated
N_H	Average number of immature hookworms hatched	1000	day^{-1}	Estimated
η_w	Proportionality constant	0.05	—	Estimated

Table 3.2: Parameter values used in simulation.

Number	Parameter	R_0	L_M^*
1	Λ_H	1.0000	0.7204
2	L_0	-1	0.5542
3	η	-1	-0.7204
4	δ_H	-1	0
5	β_H	1	0.4458
6	μ_H	-1	-0.0831
7	μ_w	-0.9027	-0.6503
8	α_w	0.9027	0.6503
9	μ_s	-0.5	-0.3602
10	α_s	0.5	0.3602
11	μ_m	-1	-0.7204
12	α_m	1	0.7204
13	μ_h	-0.00001	-0.000006
14	α_h	0.00001	0.000006
15	N_m	1	0.7024
16	N_H	1	0.7204
17	α_L	0.99990	0.7203
18	μ_L	-0.99990	-0.7203
19	α_H	0.9901	0.7132
20	μ_P	-0.99010	-0.7132
21	μ_M	-1	-0.7204

Table 3.3: Sensitivity index for all parameters

Parameters that can reduce R_0 are $L_0, \eta, \delta_H, \mu_H, \mu_w, \mu_s, \mu_m, \mu_h, \mu_L, \mu_P$, and μ_M with $L_0, \eta, \mu_m, \mu, \mu_M$ being the most sensitive. Parameters that can reduce L_M^* are $\eta, \mu_w, \mu_s, \mu_m, \mu_h, \mu_L, \mu_P, \mu_M$ with η and μ_m being the most sensitive and α_s being the least sensitive compared to all the other parameters.

3.9 Results

The simulations for the model system (3.4.9) is represented in graphical form. The initial value conditions used for the simulations of the behaviour of the experimental model system (3.4.9) are given by $S_H(0)=10000$, $I_H(0)=0$, $L_w(0)=5000$, $L_s(0)=0$, $L_m(0)=0$, $E_h(0)=0$, $E_L(0)=0$, $L_H(0)=0$ and $L_M(0)=5000$. The disease parameter values are represented in Table (3.1) and Table (2.2) respectively. Figure (3.2) to Figure (3.5) illustrates the solution profile of the population of infective worm within-host (L_w), worms in small intestine (L_s), matured worm (L_m) and Hookworm eggs within human host (E_h) varying the people host parameters namely; β_H , Λ_H , N_H and α_H . This is done to check the influence these between-host parameters have on the within-host variables.

3.9.1 The influence of between-host scale on within-host scale of the hookworm infection

In this section, we vary the between-host parameters on within-host variables. The multiscale model system (3.4.9) is bi-directionally coupled with the between-host scale submodel influencing the within-host scale submodel and the other way round. This section presents the numerical simulations are conducted using the baseline parameter values in Table (3.3). We illustrate the influence of key between-host parameters β_H , Λ_H , N_H , α_H on within-host scale variables L_w , L_s , L_m , E_h . Therefore, wearing shoes can reduce the infective worms L_w at the within-host scale are likely to reduce transmission of hookworm.

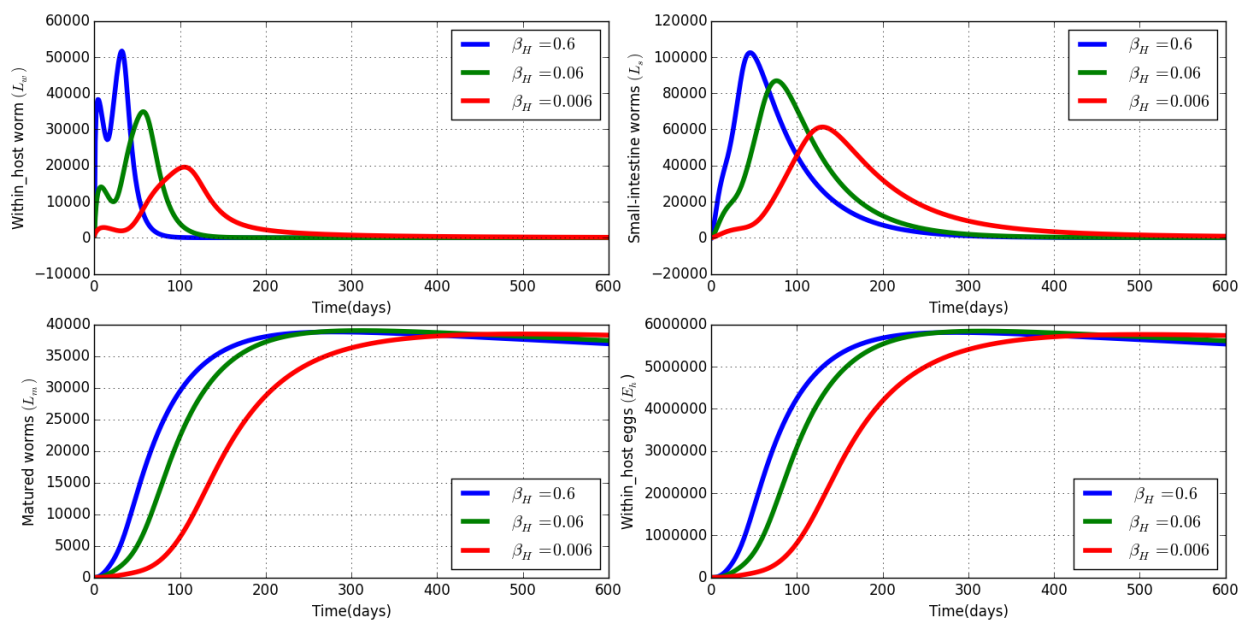


Figure 3.2: Graphs of numerical solutions of the model system (3.4.9). Top left to right showing propagation of Infective larvae within a human host L_w and worms in the small intestine L_s , respectively. Bottom left to right showing propagation of matured worms and hookworm eggs within the human host, respectively. The solutions are presented for different values of the infective contact rate, β_H : $\beta_H = 0.6$, $\beta_H = 0.06$ and $\beta_H = 0.006$.

The graphs simulated demonstrates that there is a correlation between within-host disease processes and the between-host disease transmission. Figure (3.2) shows graphs of numerical solutions of model system showing propagation for infective worms within an infected individual L_w , worms in the small intestine L_s , matured worms within an infected human L_m , worm eggs within an infected human E_h ; From top left to right and bottom left to right respectively for different values of the infection rate of human by parasite, β_H : $\beta_H = 0.6$, $\beta_H = 0.06$, $\beta_H = 0.006$. Results show an influence of the between-host disease processes on within-host infection dynamics. The increase in transmission rate for the disease has an increase in the within-host infection intensity. These solutions illustrate that the transmission rate at the population level has an influence on the within-host dynamics of an infected individual. This implies that the human behavioral changes like wearing shoes to reduce contact with the infective larvae reduce the intensity of the infection at the individual level.

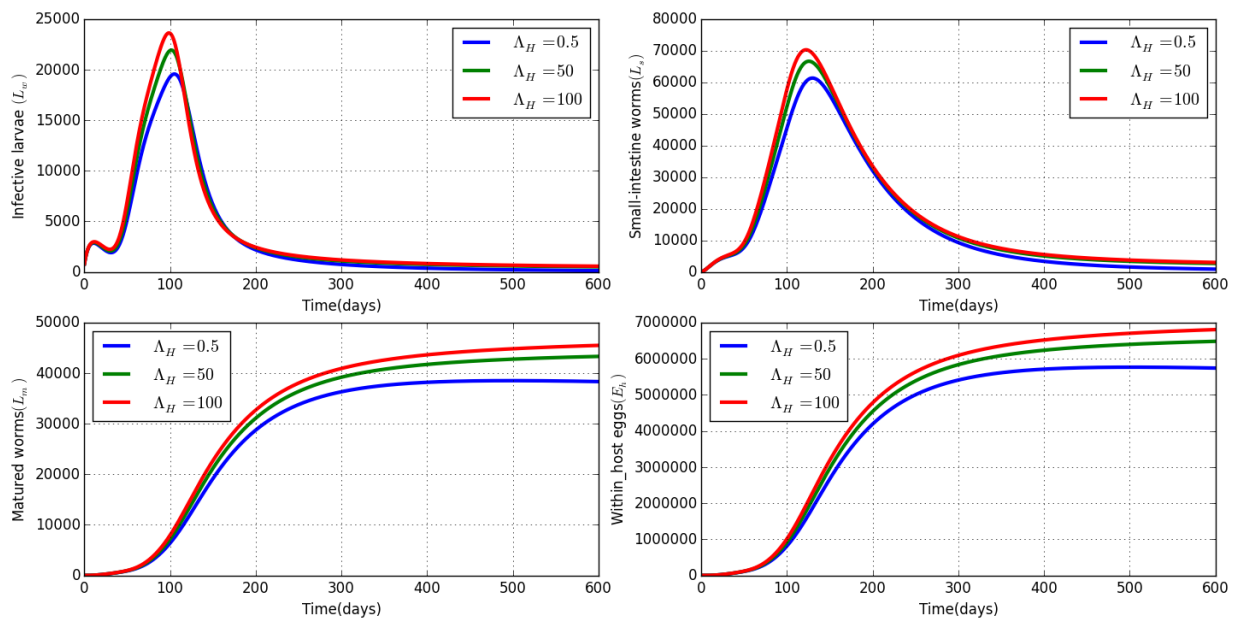


Figure 3.3: Graphs of numerical solutions of the model system (3.4.9). Top left to right showing propagation of Infective larvae within a human host L_w and worms in the small intestine L_s , respectively. Bottom left to right showing propagation of matured worms and hookworm eggs within the human host, respectively. The solutions are presented for different values of recruitment rate of new susceptible humans,

$$\Lambda_H: \Lambda_H = 10, \Lambda_H = 100 \text{ and } \Lambda_H = 1000.$$

Figure (3.3) demonstrates numerical solutions of within-host processes from top left to right is population of infective worms within an infected individual L_w , worms in the small intestine L_s and from bottom left to right matured worms within an infected human L_m , worm eggs within an infected human E_h respectively for different values of recruitment rate of new susceptible individuals Λ_H , $\Lambda_H = 0.5$, $\Lambda_H = 50$, $\Lambda_H = 100$. It is observed that the increase in new susceptible humans increases intensity of infection at individual level. The Figure (3.3) confirms the influence that between-host parameters have on within-host diseases processes.

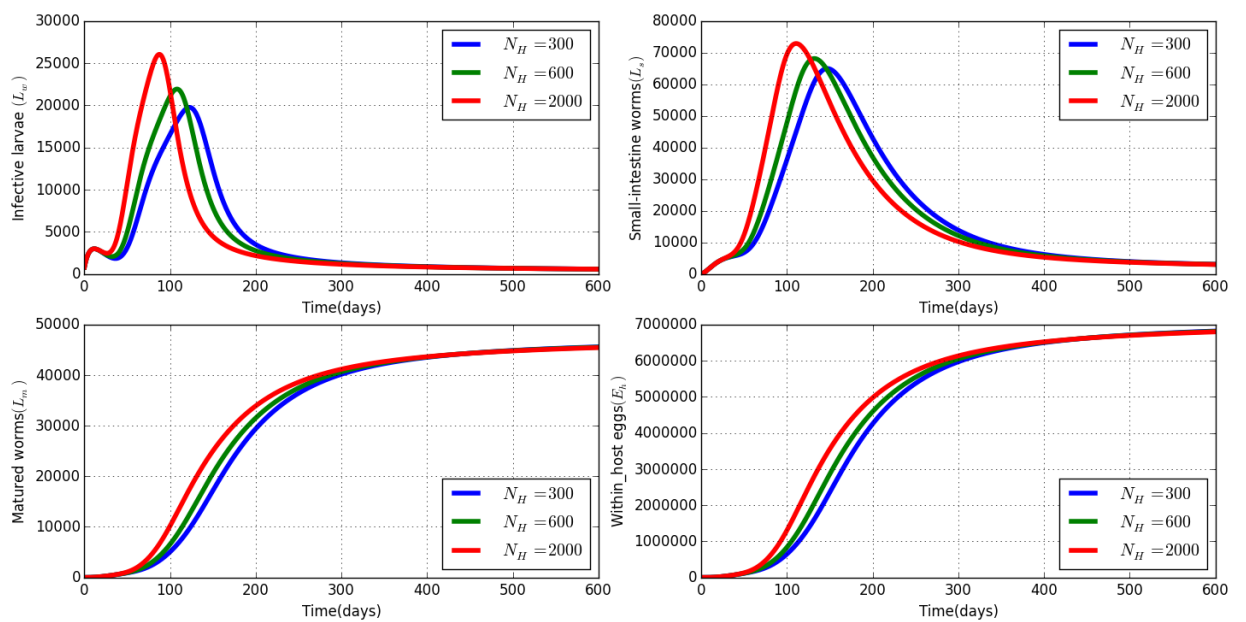


Figure 3.4: Graphs of numerical solutions of the model system (3.4.9). Top left to right showing propagation of Infective larvae within a human host L_w and worms in the small intestine L_s , respectively. Bottom left to right showing propagation of matured worms and hookworm eggs within the human host, respectively. The solutions are presented for different values of recruitment rate of new susceptible humans,

$$N_H: N_H = 300, N_H = 1200 \text{ and } N_H = 2000.$$

Figure (3.4) illustrates the numerical solutions of within-host processes. Solutions From top left to right and bottom from left to right respectively; infective worms within an infected individual L_w , worms in the small intestine L_s and from bottom left to right matured worms within an infected human L_m , worm eggs within an infected human E_h for different values for average number of non-infective worms in the environment N_H : $N_H = 300$, $N_H = 1200$, $N_H = 2000$. We observe from Figure (3.4) that an increase in the production of non-infective worms per day by eggs increases the transmission risk of human infection. Therefore, reducing the number of non-infective worms reduces the infection intensity within an infected individual.

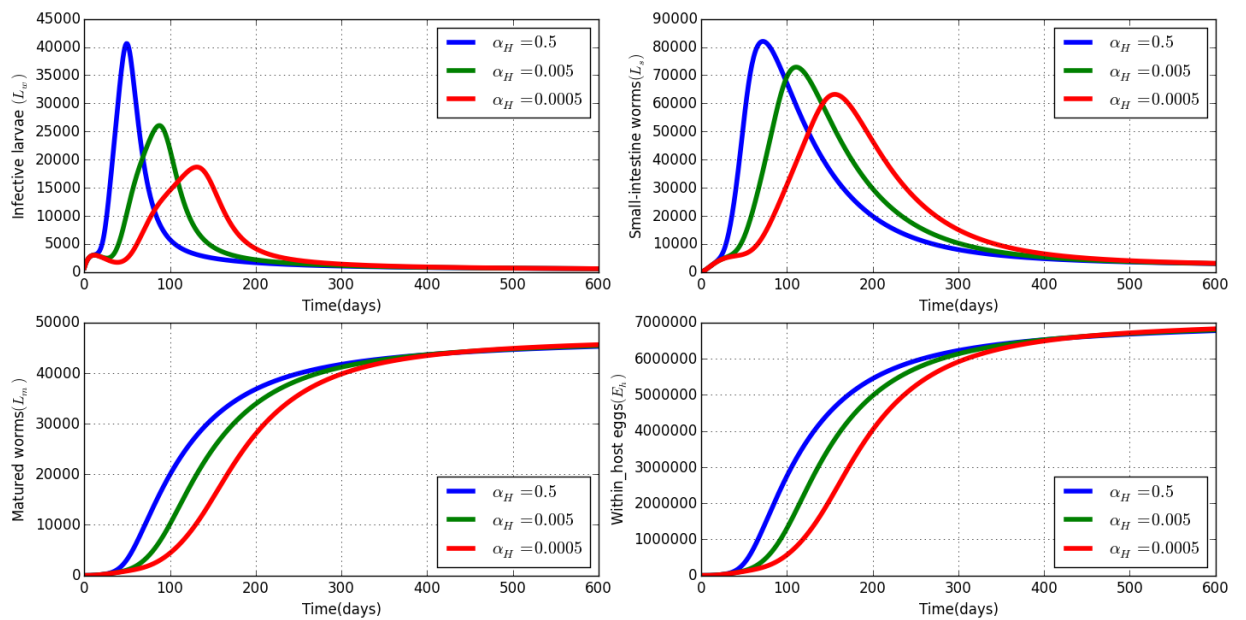


Figure 3.5: Graphs of numerical solutions of the model system (3.4.9). Top left to right showing propagation of Infective larvae within a human host L_w and worms in the small intestine L_s , respectively. Bottom left to right showing propagation of matured worms and hookworm eggs within the human host, respectively. The solutions are presented for different values of recruitment rate of new susceptible humans,

$$\alpha_H: \alpha_H = 0.0006, \alpha_H = 0.05 \text{ and } \alpha_H = 0.005.$$

Figure (3.5) demonstrates the numerical solutions of within-host processes of within-host processes; from top left to right infective worms within an infected individual L_w , worms in the small intestine L_s and from bottom left to right and from bottom left to right is matured worms within an infected human L_m , worm eggs within an infected human E_h for different values of developmental changes of the non-infective worms to infective worms in the environment α_H : $\alpha_H = 0.05$, $\alpha_H = 0.005$, $\alpha_H = 0.0006$. The numerical solution results show that the between-host processes affect the infection intensity within an infected human. Therefore, stopping the process of growth for worms going to infective stage will reduce the within the infected humans.

3.10 The influence of With-host scale parameters on between-host scale variables

In this section we vary the within-host parameters on between-host variables.

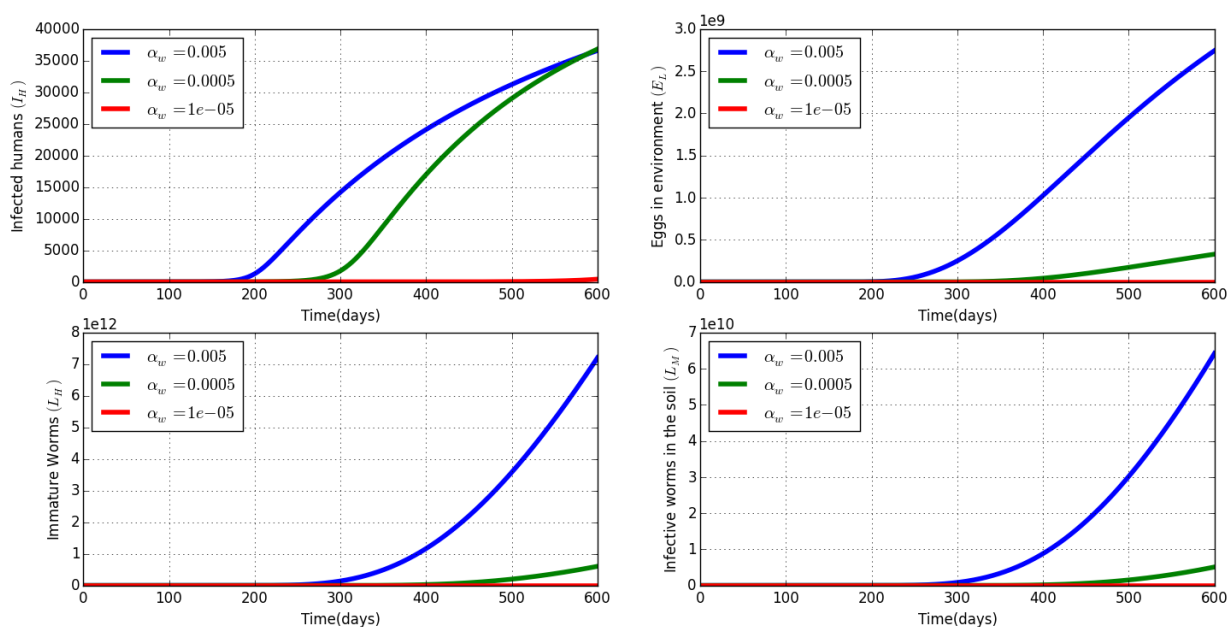


Figure 3.6: Graphs of numerical solutions of the model system (3.4.9). Top left to right showing propagation of Infected individuals I_H and hookworm eggs in the environment E_L , respectively. Bottom left to right showing propagation of immature worms in the environment E_L and infective larvae in the environment L_M , respectively. The solutions are presented for different values of migration rate of infective worm to small intestine, α_w : $\alpha_w = 0.005$, $\alpha_w = 0.0005$ and $\alpha_w = 0.0001$.

Figure (3.6) illustrates the solution of the population of Infected humans I_H , Eggs in the physical environment E_L , non-infective worms L_H , infective larvae in the physical environment L_M from top left to right and bottom left to right respectively; for different values of movement rate to small intestine α_w : $\alpha_w = 0.005$, $\alpha_w = 0.0005$, $\alpha_w = 0.00001$. The results show that higher rates of movement rate results affects transmission of the disease in the population level. When reduced there is a delay in transmission in the between-host processes.

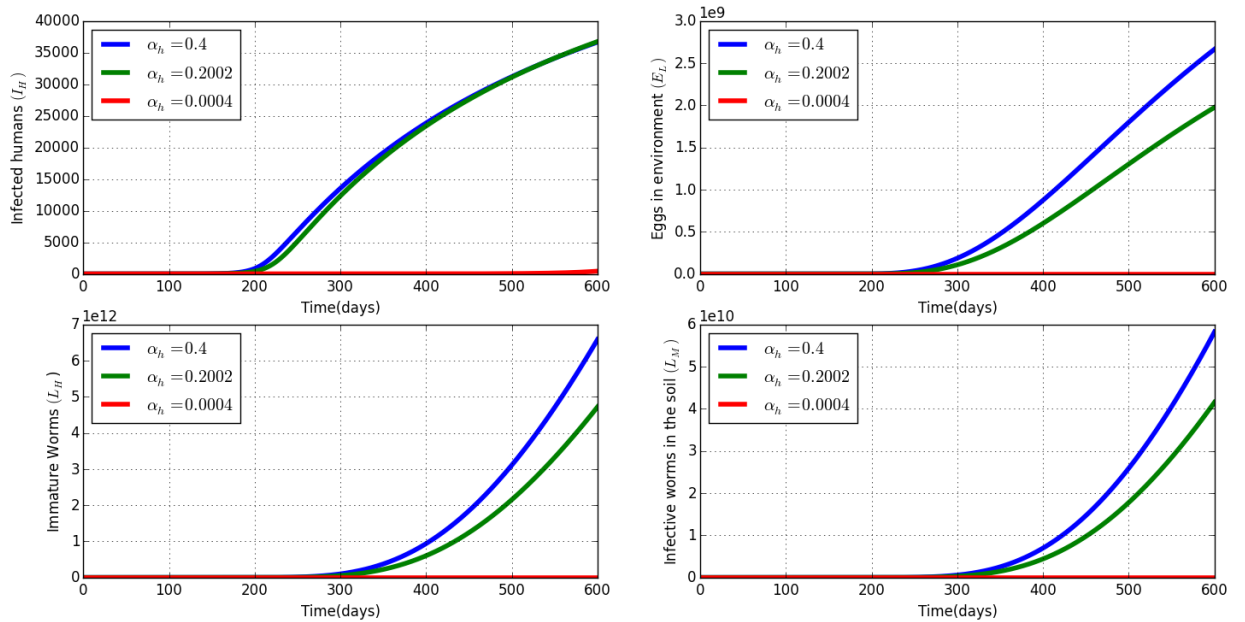


Figure 3.7: Graphs of numerical solutions of the model system (3.4.9). Top left to right showing propagation of Infected individuals I_H and Hookworm eggs in the environment E_L , respectively. Bottom left to right showing propagation of immature worms in the environment E_L and infective larvae in the environment L_M , respectively. The solutions are presented for different values of excretion rate of hookworm eggs to the environment, α_h : $\alpha_h = 0.5$, $\alpha_h = 0.01$ and $\alpha_h = 0.003$.

Figure (3.7) shows graphs of numerical solutions of model system showing the profiles of infected humans I_H , eggs in the physical environment E_L , non-infective worms L_H , Infective larvae in the physical environment L_M from top left to right and bottom left to right respectively; for different values for excretion rates of worm eggs α_h , $\alpha_h = 0.05$, $\alpha_h = 0.001$, $\alpha_h = 0.0003$. The graphs show that higher rates of worm eggs excretion results in increased transmission in population level. Figure (3.7) shows that reducing α_h reduces environmental contamination by improving sanitation practices within the community reduce the infection intensity at within-host level.

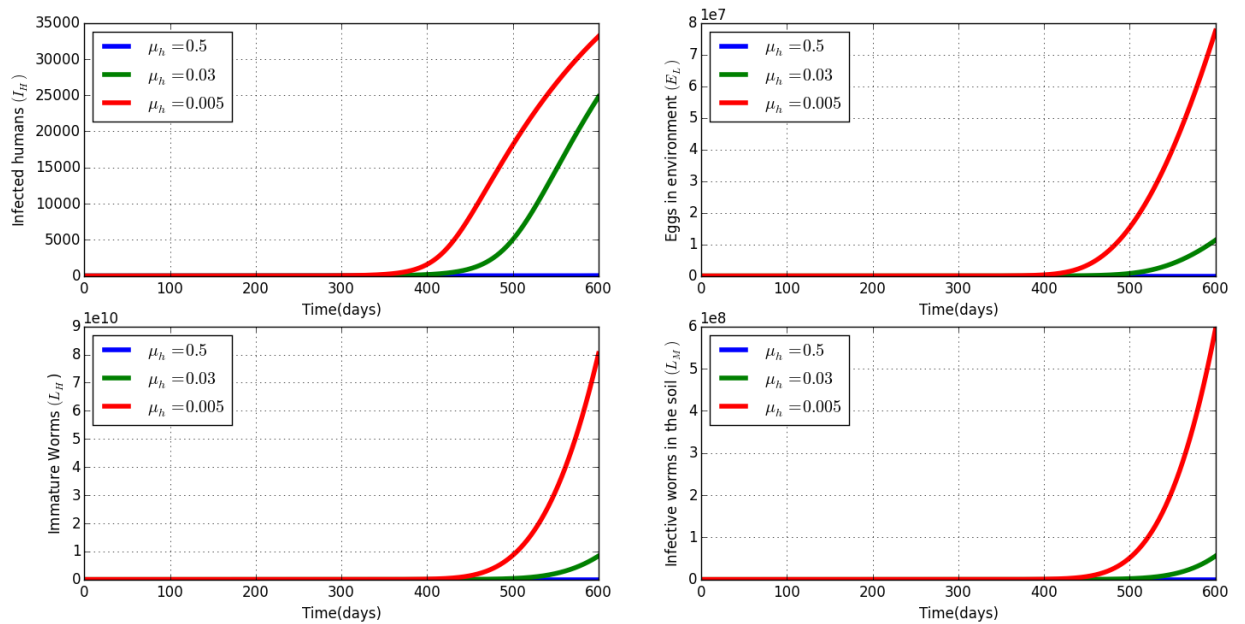


Figure 3.8: Graphs of numerical solutions of the model system (3.4.9). Top left to right showing propagation of Infected individuals I_H and hookworm eggs in the environment E_L , respectively. Bottom left to right showing propagation of immature worms in the environment E_L and Infective larvae in the environment L_M , respectively. The solutions are presented for different values of natural death of eggs in within-host, μ_h : $\mu_h = 0.0005$, $\mu_h = 0.003$ and $\mu_w = 0.05$.

Figure (3.8) demonstrates the profiles of the population of infected humans I_H , eggs in the physical environment E_L , non-infective worms L_H , infective larvae in the physical environment L_M from top left to right and bottom left to right respectively; for different values for natural death of worm eggs, μ_h : $\mu_h = 0.5$, $\mu_h = 0.03$, $\mu_h = 0.005$. The numerical results show that when we increase the death rate of worm eggs reduces the transmission of the disease at population level. Therefore, the killing of worm eggs within-host reduce transmission risk of the infection within a community.

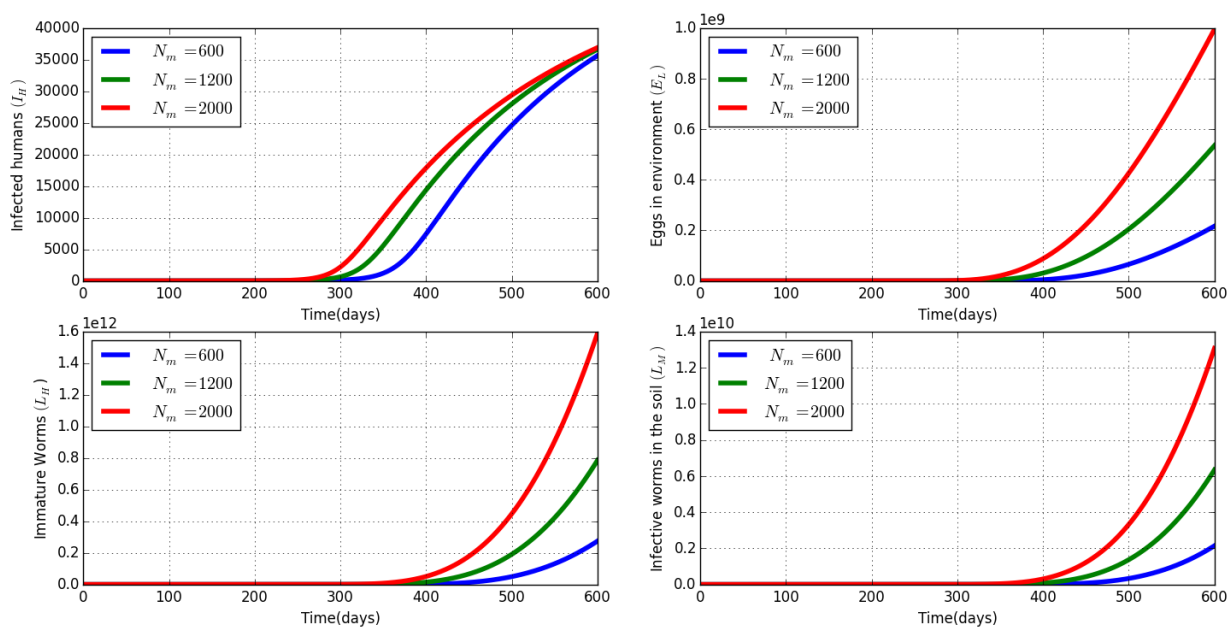


Figure 3.9: Graphs of numerical solutions of the model system (3.4.9). Top left to right showing propagation of infected individuals I_H and Hookworm eggs in the environment E_L , respectively. Bottom left to right showing propagation of immature worms in the environment E_L and infective larvae in the environment L_M , respectively. The solutions are presented for different values of average number of hookworm eggs produced within the human host, N_m : $N_m = 600$, $N_m = 1200$ and $N_m = 2000$.

Figure (3.9) shows graphs of numerical solutions of model system (3.4.9) showing propagation of infected individuals I_H and Hookworm eggs in the environment E_L , respectively. Bottom left to right showing propagation of immature worms in the environment E_L and Infective larvae in the environment L_M , respectively; for different values of average number of eggs produced in a day N_m : $N_m = 600$, $N_m = 1200$ and $N_m = 2000$. The results show that the reduction in the number of eggs produced then the transmission dynamics at population level is reduced. Figure (3.9) show the increase in production of worm eggs per day by each pairing of worms increase transmission in the community.

Chapter 4

HOOKWORM MULTI-SCALE MODEL WITH INTERVENTION

4.1 The Multi-scale model for hookworm with health intervention combinations

In this chapter, we implement intervention measures on the model system (3.4.9) for hookworm infection taking into account the effects of vaccination, chemotherapy, sanitation and wearing shoes on the reduction and controlling of hookworm infection. The parameters of the extended multi-scale model are all constant and their description remains the same as in Table (3.1) except for those intervention parameters incorporated into the model tabulated in Table (4.1). The description of the new parameters are as follows

- ★ Wearing shoes (behavioral practice) is modeled by a quantity $\beta_H(1 - w_s)$, $0 \leq w_s \leq 1$, where w_s is the efficacy of wearing shoes intervention and it is a parameter that measures the probability of

reducing of susceptible human contact with infective larvae of hookworm infection from the physical environment. This behavioral practice aims to reduce the transmission risk of the hookworm infection.

- ★ Vaccination is modeled by a quantity $L_0(1 + v)$ with $0 \leq v \leq 1$, where v is the efficacy of vaccine intervention and that the parameter typically relates to increasing the susceptibility of humans to the infection. Vaccines increases resistance of the susceptible humans to the infection. Thus $L_0(1 + v)$ measures the probability that reduces the infection rate. The aim of the vaccine induce anti-enzyme antibodies that will fight off the infection when an individual becomes infected.
- ★ Chemotherapy is used in the treatment of an infection using a single drug or a combination of drugs. This is an intervention that is administered at within-host scale. We assume that treatment with Albendazole (ALB) or Mebendazole (MEB) kills a given fraction of adult worms. We further assume that the proportion of worms killed by ALB or MEB is equal to reductions in mean egg counts. Drug treatment which is modelled by a quantity $(1 + d)\mu_m$, with $0 \leq d \leq 1$, where d is the efficacy of drug treatment and the parameter increase the death rate of matured worms. This intervention aims at using different drugs in reducing the worms in the human body.
- ★ Sanitation modeled by a quantity $\alpha_h(1 - s)$ with $0 \leq s \leq 1$ where s is the efficacy of sanitation intervention and this parameter prevents contamination of the physical environment due to improved environmental sanitation practices which is associated with the construction and the use of sanitation facilities such as latrines at the household or community level by individuals in the endemic areas. Thus, $\alpha_h(1 - s)$ measures the probability of preventing individuals contaminating the environment.
- ★ The emergent property for drug intervention is modelled by a quantity $(1 - p)\delta_H$ with $0 \leq p \leq 1$, where q is the efficacy of emergent properties that transpire after using the drug treatment because we expect the induced death rate of infection to be reduced.
- ★ The emergent property for vaccination intervention v , modelled by $(1 + q)\mu_M$; with $0 \leq q \leq 1$ where q is the efficacy of the emergent property that transpires after using the vaccination intervention we expect that the infective worms in the environment will be reduced by increasing susceptibility of the humans.

The model presented herein is the multiscale model implementing intervention for hookworm infection;

$$\left\{ \begin{array}{l}
 \frac{dS_H}{dt} = \Lambda_H - \hat{\lambda}(t)_H S_H - \mu_H S_H, \\
 \frac{dI_H}{dt} = \hat{\lambda}(t)_H S_H - \mu_H I_H + (1-p)\delta_H I_H, \\
 \frac{dL_w}{dt} = \frac{\hat{\lambda}_H(S_H - 1)}{\phi_w(I_H + 1)} - (\mu_w + \alpha_w)L_w, \\
 \frac{dL_s}{dt} = \alpha_w L_w - (\mu_s + \alpha_s)L_s, \\
 \frac{dL_m}{dt} = \frac{\alpha_s}{2} L_s - (1+d)\mu_m L_m, \\
 \frac{dE_h}{dt} = N_m \alpha_m L_m - \mu_h E_h - (1-s)\alpha_h E_h, \\
 \frac{dE_L}{dt} = (I_H + 1)(1-s)\alpha_h E_h - (\mu_l + \alpha_l)E_L, \\
 \frac{dL_H}{dt} = N_H \alpha_L E_L - (\mu_P + \alpha_H)L_H, \\
 \frac{dL_M}{dt} = \alpha_H L_H - (1+q)\mu_M L_M.
 \end{array} \right. \quad (4.1.1)$$

where,

$$\hat{\lambda}_H(t) = \frac{(1-w_s)\beta_H L_M(t)}{L_0(1+v) + L_M(t)}, \quad (4.1.2)$$

with w_s is wearing shoes, s is the sanitation, v denotes vaccination and d is the drug treatment.

Intervention	Transformation	Efficay levels
Intervention whose efficacy is modeled by wearing shoes w_s	$\beta_H \longrightarrow (1 - w_s)\beta_H$	0.3, 0.6, 0.95
Intervention whose efficacy is modeled by vaccination v	$L_0 \longrightarrow (1 + v)L_0$	0.3, 0.6, 0.95
Emergent property related to the sanitation intervention s	$\mu_M \longrightarrow (1 + q)\mu_M$	0.2
Intervention whose efficacy is modeled by drug treatment (d)	$\mu_m \longrightarrow (1 + d)\mu_m$	0.3, 0.6, 0.95
Emergent property related to drug intervention d	$\delta_H \longrightarrow (1 - p)\delta_H$	0.2
Intervention whose efficacy is modeled by sanitation (s)	$\alpha_h \longrightarrow (1 - s)\alpha_h$	0.3, 0.6, 0.95

Table 4.1: Intervention parameter values used in simulation

4.2 Endemic points

In this section we find the endemic points of the model system (4.1.1) with interventions. The Endemic equilibrium point is denoted by

$$\tilde{E}_2 = (\tilde{S}_H, \tilde{I}_H, \tilde{L}_w, \tilde{L}_s, \tilde{L}_m, \tilde{E}_h, \tilde{E}_L, \tilde{L}_H, \tilde{L}_M), \quad (4.2.3)$$

$$\left\{ \begin{array}{l}
 \tilde{S}_H(\tilde{L}_M) = \frac{\Lambda_H[(1+v)L_0 + L_M^*]}{\mu_H(1+v)L_0 + ((1-w_s)\beta_H + \mu_H)L_M^*}, \\
 \tilde{I}_H(\tilde{L}_M) = \frac{(1-w_s)\beta_H\Lambda_H L_M^*}{[\mu_H + (1-p)\delta_H][[(1-w_s)\beta_H + \mu_H]L_M^* + \mu_H(1+v)L_0]}, \\
 \tilde{L}_w(\tilde{L}_M) = \frac{1}{(I_H^* + 1)}Z_H, \\
 \tilde{L}_s(\tilde{L}_M) = \frac{\alpha_w}{(\mu_s + \alpha_s)(I_H^* + 1)}Z_H, \\
 \tilde{L}_m(\tilde{L}_M) = \frac{\alpha_w\alpha_s}{2\mu_m(1+d)(\mu_s + \alpha_s)(I_H^* + 1)}Z_H, \\
 \tilde{E}_h(\tilde{L}_M) = \frac{\alpha_w\alpha_s N_m\alpha_m}{2\mu_m(1+d)(\mu_s + \alpha_s)[\mu_h + (1-s)\alpha_h](I_H^* + 1)}Z_H, \\
 \tilde{E}_L(\tilde{L}_M) = \frac{\alpha_w\alpha_s N_m\alpha_m(1-s)\alpha_h}{2\mu_m(1+d)(\mu_s + \alpha_s)[\mu_h + (1-s)\alpha_h](\mu_L + \alpha_L)(I_H^* + 1)}Z_H, \\
 \tilde{L}_H(\tilde{L}_M) = \frac{\alpha_w\alpha_s N_m\alpha_m(1-s)\alpha_h N_H\alpha_L}{2\mu_m(1+d)(\mu_s + \alpha_s)[\mu_h + (1-s)\alpha_h](\mu_L + \alpha_L)(\mu_P + \alpha_H)(I_H^* + 1)}Z_H,
 \end{array} \right. \quad (4.2.4)$$

where,

$$Z_H = \frac{(\Lambda_H - \mu_H)(1-w_s)\beta_H L_M^*[L_0(1+v) + L_M^*] - (1-w_s)\beta_H^2 L_M^{*2}}{\eta(\mu_w + \alpha_w)[(1+v)L_0 + L_M^*][[(1-w_s)\beta_H + \mu_H]L_M^* + \mu_H L_0(1+v)](I_H^* + 1)}. \quad (4.2.5)$$

Now using the parasite equation given by,

$$\alpha_H \tilde{L}_H - \mu_M \tilde{L}_M = 0. \quad (4.2.6)$$

Which reduces to

$$A.\tilde{L}_M[\tilde{L}_M^2 + E_M\tilde{L}_M + F_M] = 0. \quad (4.2.7)$$

Therefore,

$$\begin{cases} E_{M1} &= \left[1 + \left(\frac{(1-w_s)\beta_H}{\Lambda_H - \mu_H} - 1 \right) \frac{\mu_H[\mu_H + (1-p)\delta_H]}{(1-w_s)\beta_H + 2\mu_H} R_{0E} \right] [(1-w_s)\beta_H + \mu_H], \\ F_{M1} &= [1 - [\mu_H + (1-p)\delta_H] R_{0E}] \mu_H L_0^2 (1+v), \end{cases} \quad (4.2.8)$$

$$\tilde{L}_M = \frac{1}{2} \left[-E_{M1} \pm \sqrt{E_{M1}^2 - 4F_{M1}} \right], \quad (4.2.9)$$

where,

$$R_{0E} = \frac{N_H \alpha_H \alpha_L (1-s) \alpha_h N_m \alpha_w \alpha_m \alpha_s (1-w_s) \beta_H (\Lambda_H - \mu_H)}{2\mu_H \mu_m \mu_M \eta (1+d) L_0 (1+v) [\mu_h + (1-s)\alpha_h] (\mu_P + \alpha_H) (\mu_L + \alpha_L) (\mu_s + \alpha_s) (\mu_w + \alpha_w)}. \quad (4.2.10)$$

4.3 Evaluation of the comparative effectiveness of Hookworm interventions

Comparative effectiveness is part of research that focuses on the direct comparison of health interventions which works best, which treatment works best and under what circumstances. The benefit of modelling infectious disease is that it helps us identify what clinical and public interventions work best to improve health, which will help inform public health decision makers and policy makers. In this section we use the multi-scale mathematical model with intervention to evaluate the effectiveness of different interventions applied at different scales, that is, within-host scale interventions and between-host interventions at different efficacy values. Currently, assessment of the effectiveness of interventions has been applied to models in a single scale manner and lack of quantitative assessment. There still exists an efficacy-effectiveness gap due to lack of information [18] and [19].

In this study, comparative effectiveness of the four hookworm health interventions which include vaccination, wearing shoes, chemotherapy and sanitation improvements using indicators of intervention effectiveness (i) the reproductive number (R_0) and (ii) intervention induced endemic value \tilde{L}_M .

The indicators of intervention effectiveness are given by:

$$\left\{ \begin{array}{l} R_{0E} = \frac{N_H \alpha_H \alpha_L (1-s) \alpha_h N_m \alpha_w \alpha_m \alpha_s (1-w_s) \beta_H (\Lambda_H - \mu_H)}{2\mu_H \mu_m \mu_M \eta (1+d) L_0 (1+v) [\mu_h + (1-s) \alpha_h] (\mu_P + \alpha_H) (\mu_L + \alpha_L) (\mu_s + \alpha_s) (\mu_w + \alpha_w)}, \\ \tilde{L}_M = \frac{1}{2} \left[-E_{M1} \pm \sqrt{E_{M1}^2 - 4F_{M1}} \right], \\ E_{M1} = \left[1 + \left(\frac{(1-w_s) \beta_H}{\Lambda_H - \mu_H} - 1 \right) \frac{\mu_H [\mu_H + (1-p) \delta_H]}{(1-w_s) \beta_H + 2\mu_H} R_{0E} \right] [(1-w_s) \beta_H + \mu_H], \\ F_{M1} = [1 - [\mu_H + (1-p) \delta_H] R_{0E}] \mu_H L_0^2 (1+v). \end{array} \right. \quad (4.3.11)$$

We use these quantities (R_{0E} and \tilde{L}_M) as indicators of intervention effectiveness to relate individual level efficacy to population level effectiveness. In the subsections we present the assessment of the health interventions using the two indicators of intervention effectiveness.

4.4 Comparative effectiveness of Hookworm intervention using R_{0E} as indicator

In this section, we assess the comparative effectiveness of the hookworm intervention using the effective reproductive number R_{0E} as the indicator of intervention effectiveness. We calculate the percentage reduction of the basic reproductive number R_0 due to intervention combinations at three efficacy levels (i) low efficacy of 0.3, (ii) medium efficacy of 0.6, (iii) high efficacy levels of 0.95 for various intervention combination.

$$\text{Percentage reduction of } R_0 = \frac{R_0 - R_{0E}}{R_0} \times 100. \quad (4.4.12)$$

We use the intervention on R_0 to reduce any secondary infections, we then look at the effectiveness of different intervention combinations. We then rank the percentage reductions of the basic reproductive number R_0 in ascending order from 1 to 18 corresponding to the different combinations of the four health interventions.

Table (4.2) shows results of the assessment of the comparative effectiveness of the 18 different combinations of the four hookworm interventions corresponding to efficacy values 0.3, 0.6 and 0.95 obtained using the effective reproductive number R_{0E} as the indicator. In the Table (4.2) (1.) CEL stands for comparative effectiveness at low efficacy which is 0.3, (2.) CEM stands for comparative effectiveness at medium efficacy at 0.6 and (3.) CEH comparative effectiveness at high efficacy at 0.95.

No	Indicator of Intervention effectiveness	% age reduction of R_0 at low efficacy of 0.3	CEL	% age reduction of R_0 at medium efficacy of 0.6	CEM	% age reduction of R_0 at high efficacy of 0.95	CEH
1	R_0	0,00	1	0,00	1	0,00	1
2	R_{0ed}	21,70	2	38,35	2	47,80	2
3	R_{0ev}	23,08	3	39,50	3	48,72	3
4	R_{0es}	41.63	6	70.25	6	95.83	6
5	R_{0ew}	30,00	4	63.26	4	95,00	5
6	R_{0eved}	39,77	5	63.51	5	73,23	4
7	R_{0esed}	46.23	9	79.09	9	97.44	4
8	R_{0ewed}	45,19	7	78.60	7	97,39	7
9	R_{0esev}	47.18	10	79.56	10	97.48	10
10	R_{0ewev}	46,15	8	79.07	8	97,44	8
11	R_{0ewes}	51.93	11	88.87	12	99.75	15
12	$R_{0evedes}$	58.64	13	88.97	13	98.69	12
13	$R_{0edevev}$	57,84	12	88.66	11	98,66	11
14	$R_{0esedev}$	58.64	13	88.97	13	98.69	12
15	$R_{0ewedev}$	58.66	15	88.99	15	98.69	14
16	$R_{0esedew}$	61.61	16	94.69	16	99.87	16
17	$R_{0esvdew}$	63.02	17	95.08	17	99.87	17
18	$R_{0edevesew}$	71.05	18	98.85	18	99.93	18

Table 4.2: Results of the assessment of comparativeness of Hookworm interventions using the reproductive number R_{0E} as an indicator of intervention effectiveness when each of the four interventions have (i) low efficacy of 0.3, (ii) medium efficacy of 0.6, and (iii) high efficacy level at 0.95.

From Table (4.2), we deduce the following results:

- Comparing the single interventions comprising of the drug from chemotherapy treatment and vaccine have more or less the same comparative effectiveness at the medium efficacy and high efficacy. We notice that from Table (4.2) that the wearing shoes has the most comparative effectiveness in percentage reductions of R_0 at all efficacy levels.
- Comparing the two interventions at a time, any combination which has wearing shoes as an intervention has the highest percentage reduction and those combinations approximately has approximately more or less the same effectiveness at the three efficacy levels.
- Comparing the three intervention combinations we notice that combination number 13th, ranked at 13th has the second highest comparative effectiveness.
- Comparing three and four intervention combinations have approximately more or less the same percentage reductions or R_0 at all the efficacy levels respectively.

4.5 Comparative effectiveness of Hookworm intervention using \tilde{L}_M as indicator

In this section, we present the results of the comparative effectiveness of hookworm health interventions using the intervention induced endemic value \tilde{L}_M as the indicator of intervention effectiveness. Similarly to the previous section, we calculate the percentage reduction at the three different efficacy levels; low efficacy at 0.3, medium efficacy at 0.6 and high efficacy at 0.95 respectively using the following formula:

$$\text{Percentage reduction of } \tilde{L}_M = \frac{\tilde{L}_M - \tilde{L}_{ME}}{\tilde{L}_M} \times 100. \quad (4.5.13)$$

The comparativeness of these interventions is ranked on a scale from 1 to 18 with 1 denoting the lowest comparative effectiveness while 18 denotes the highest comparative effectiveness. Table (4.3) shows the results of the comparative effectiveness of the 18 different hookworm health intervention combination obtained using intervention induced endemic value, \tilde{L}_M , as an indicator of intervention effectiveness. Abbreviations (CEL, CEM, CEH) in Table (4.3) still remains the same as in Table (4.2).

No	Indicator of Intervention effectiveness	% age reduction of \tilde{L}_M at low efficacy of 0.3	CEL	% age reduction of \tilde{L}_M at medium efficacy of 0.6	CEM	% age reduction of \tilde{L}_M at high efficacy of 0.95	CEH
1	\tilde{L}_M	0,00	1	0,00	1	0,00	1
2	\tilde{L}_{Med}	12.30	3	20.96	3	28.41	3
3	\tilde{L}_{Mev}	0.01	2	0.02	2	0.03	2
4	\tilde{L}_{Mes}	23.62	8	42.27	8	79.72	8
5	\tilde{L}_{Mew}	16.35	5	36.79	5	77.78	5
6	\tilde{L}_{Mevded}	12.31	4	20.98	4	28.46	4
7	\tilde{L}_{Mesed}	27.34	11	50.51	11	84.34	10
8	\tilde{L}_{Mewed}	26.64	9	50.05	9	84.19	9
9	\tilde{L}_{Mesev}	17.16	7	37.40	7	78.13	7
10	\tilde{L}_{Mewev}	16.36	6	36.82	6	77.92	9
11	\tilde{L}_{Mewes}	30.69	15	60.44	15	95.77	15
12	$\tilde{L}_{Mevdedes}$	27.36	12	50.55	12	84.54	12
13	$\tilde{L}_{Medevev}$	26.65	10	50.09	10	84.39	11
14	$\tilde{L}_{Mesedev}$	27.36	12	50.55	12	84.54	12
15	$\tilde{L}_{Mewedev}$	27.38	14	50.58	14	84.55	14
16	$\tilde{L}_{Mesedew}$	38.62	17	68.45	17	97.51	17
17	$\tilde{L}_{Mesevev}$	30.71	16	60.49	16	96.59	16
18	$\tilde{L}_{Medevevew}$	39.24	18	68.83	18	98.56	18

Table 4.3: Results of the assessment of comparativeness of Hookworm interventions using the endemic point \tilde{L}_M as an indicator of intervention effectiveness when each of the four interventions have (i) low efficacy of 0.3, (ii) medium efficacy of 0.6, and (iii) high efficacy level at 0.95.

From Table (4.3), we deduce the following results regarding the 18 different intervention combinations:

- When considering single intervention at a time, wearing shoes shows high comparative effectiveness for all different efficacy levels and sanitation having the lowest effectiveness with approximately less or more the same at the different levels.

- When considering two interventions at a time from the six individual hookworm health interventions. We note that intervention combination that includes wearing shoes and an intervention applied at the within-host scale (vaccines and drugs) have the highest comparative effectiveness.
- From the three and using all the intervention combination have approximately more or less the same comparative effectiveness for all the different efficacy levels.

Chapter 5

DISCUSSION AND CONCLUSION

In this study, we developed multiscale model linking the within-host scale and the between-host scale dynamics of hookworm. We choose to to follow the multiscale modelling approach because it allows us to simultaneously assess the effectiveness of the intervention when controlling and reducing the spread of the infection. From following the life cycle of the hookworm infection we noticed the transmission dynamics can be modelled using the embedded framework due to the fact that the within-host scale which is the lower/micro scale is embedded in the upper/macro scale referred to as between-host scale. The whole idea of this study was to establish the influence that each scale have on each other and then evaluate the effectiveness of each intervention combination that controls, eliminate and eradicate the spread of an infection. We can conclude that the main aim was achieved because we proved that there exist a bi-directional relationship between the within-host scale and between-host scale for hookworm infection. We first established a model exhibiting between-host dynamics, it was established that even though the mathematical model is well posed, globally stable and the endemic state exist but having followed the life cycle suggested that there the within-host scale is fed the pathogen load from the physical environment. Due to that discovery we then extended the single model to a multiscale model that expresses both the within-host and the between-host dynamics simultaneously. The multiscale model

was analysed and found to be epidemiologically well posed. We also established the stability analysis of both the disease free equilibrium and the endemic equilibrium. The sensitivity analysis was conducted on the multiscale model to evaluate the sensitivity of the two disease metrics (reproductive number and endemic equilibrium point) on all twenty-one model parameters. The sensitivity analysis suggested that the parameters that are most sensitive and capable of reducing the number of secondary infections are saturation constant, L_0 ; proportionality constant, η_w and disease induced, δ_H also reduce the persistence of the infection in the population. When conducting the numerical simulations of the multiscale model is then easy to know which parameters to target when showing the influence of within-host parameters on between-host variable and also how the between-host parameters on within-host variables. Furthermore, the numerical simulations of the multiscale model supported our initial claim of bi-directional relationship of the within-host scale on between-host scale and vice versa. Having found out that there is a relationship amongst the scales, then we incorporated intervention measures aimed in controlling and reducing the spread of the hookworm infection. The comparative effectiveness of the intervention combination suggests that at different efficacy values 0.3, 0.6 and 0.95 when considering a single intervention, sanitation and wearing shoes to be the most effective. Then considering the combination of two interventions showed that combining wearing shoes with sanitation intervention are most effective at 0.3, 0.6 and 0.95. The analysis also showed that the combination of wearing shoes, sanitation intervention and vaccination has the most effectiveness at all the explored efficacy values. We can then conclude that any combination containing wearing shoes shows to be effective in reducing the spread of the infection. The use of all intervention ensures the highest comparative effectiveness in controlling and reducing the spread or persistence of hookworm at all efficacy levels. There is a need for improve the parameter values which in turn means advancement in data collection. The results presented in this study have efforts to improve the level of understanding of the hookworm infection transmission dynamics in humans and with the aim to inform decision and policy makers on how to control, eliminate and eradicate soil-transmitted helminths.

Bibliography

- [1] Bethony, J., Brooker, S., Albonico, M., Geiger, S.M., Loukas A., Diemert, D. and Hotez, P.J. 2006. Soil-transmitted helminths: Ascariasis, Trichuriasis and Hookworm. *The Lancet. Elsevier*. 367(9521):1521-1532.
- [2] Yakob, L., Magalhães, Ricardo, J., Soares, G., Darren, J., Gabriel, W., Nicola, D., Rebecca, B., Jan, B., Franziska, W., Gail, M. and Archie, C.A. 2014. Modelling parasite aggregation: disentangling statistical and ecological approaches. *International Journal for Parasitology*. 44(6):339-342.
- [3] Fenwick, A. 2012. The global burden of neglected tropical diseases. *Public Health*. 126(3):233-236. doi:10.1016/j.puhe.2011.11.015. PMID 22325616.
- [4] Global Health - Division of parasitic diseases, Centers for disease control and prevention. 2013. <https://www.cdc.gov/dpdx/trichuriasis/index>. Accessed on 04 December 2018.
- [5] Starr, M.C. and Montgomery, S.P. 2011. Soil-transmitted helminthiasis in the United States: a systematic review—1940–2010. *The American journal of tropical medicine and hygiene*, 85(4):680-684.
- [6] WHO. 2018. Soil-transmitted helminth infections Fact sheet of Soil Transmitted Helminths. World Health Organisation. Accessed on 20 February 2018.
- [7] De Sirra, N.R., Brooker, S., Hotez, P.J, Montresor, A., Angelo, D. and Saviolli, L. 2003. Soil transmitted helminth infections: updating the global picture. *Trends Parasitol*. 19(2003):547-551.
- [8] Bleakley, H. 2003. Disease and development: evidence from American south. *Eurpe Association*. 1(2003):376-386.

- [9] Anderson, R. and May, R.M. 1991. *Infectious Diseases of Humans: Dynamics and control*. Oxford University Press.
- [10] Garira, W. , Mathebula, D. and Netshikweta, R. 2014. A Mathematical modelling framework for linked within-host and between-host dynamics for infections with free-living pathogens in the environment. *Mathematical Biosciences*. 256(2014):58-78.
- [11] Hotez, P.J., Brooker, S., Bethony, J.M., Bottazzi, M.E., Loukas, A. and Xiao, S. 2004. Hookworm infection. *New England Journal of Medicine*. 351(8):799-807.
- [12] Sabatelli, L.,Rhani, A.C, Rodrigues, L.C, Hotez, P.J. and Brooker, S. 2008. Modelling heterogeneity and the impact of chemotherapy and vaccination against human hookworm. *Journal of the Royal Society Interface*.The Royal society. 5(28):1329-1341.
- [13] Garira, W. 2017. A complete categorization of multiscale models of infectious disease systems. *Journal of biological dynamics*. 11(1):378-435.
- [14] Chan, M.S., Bradley, M. and Bundy, D.A., 1997. Transmission patterns and the epidemiology of hookworm infection. *International Journal of Epidemiology*, 26(6):1392-1400.
- [15] Pawelek, L.A., Liu, S. and Lolla, M.U. 2016. Modelling the spread of hookworm disease and assessing chemotherapy programs: Mathematical analysis and comparison with surveillance data.*Journal of Biological Systems*. 24(01): 167-191.
- [16] Garira, W. 2018. A primer on multiscale modelling of infectious disease systems. *Infectious Disease Modelling*, 3:176-191.
- [17] Shi, B., Xia, S. and Liu, J. 2013. A complex systems approach to infectious disease surveillance and response. In *International Conference on Brain and Health Informatics*. Springer. 8211:524-535.
- [18] Santaguida, P.L., Helfand, M. and Raina, P. 2005. Challenges in systematic reviews that evaluate drug efficacy or effectiveness. *Annals of internal medicine*, 142(12), pp.1066-1072.
- [19] Allotey, P., Reidpath, D.D., Ghalib, H., Pagnoni, F. and Skelly, W.C., 2008. Efficacious, effective, and embedded interventions: implementation research in infectious disease control. *BMC Public Health*. 8(1):pp.343.

- [20] Hotez, P.J., Brooker, S., Bethony, J.M., Bottazzi, M.E., Loukas, A. and Xiao S. 2004. Hookworm infection. *New England Journal of Medicine*. 351(8):799-801.
- [21] Van den Driessche, P.J. and Watmough, P.J. 2002. Reproduction numbers and sub-threshold endemic equilibria for compartmental models of disease transmission. *Mathematical Bio-sciences*. 180(1):29-48.
- [22] Brakken-Thal, S. 2007. Gershgorin's theorem for estimating eigenvalues. Source: < <http://buzzard.ups.edu/courses/2007spring/projects/brakkenthal-paper.pdf>. Accessed 06 December 2018.
- [23] McCluskey, C.C. 2006. Lyapunov functions for tuberculosis models with fast and slow Progression. *Mathematical Bio-sciences*. 3(2006):603-614.
- [24] Miller, T.A. 1979. Hookworm infection in man. *Advances in Parasitology*. 17:315-384.
- [25] Brooker, S., Bethony, J. and Hotez, P. J. 2004. Human hookworm infection in the 21st century. *Advances in Parasitology*. 58(2004), pp. 197.
- [26] Carlos-Chavez, C., Zhilan, F. and Huang, W. 2002. On the computation of R_0 and its role on global stability. In *Mathematical Approaches for Emerging and Re-emerging Infectious Diseases Part 1: An Introduction to Model, Methods and Theory*. *Institute for Mathematics and its Application*. 125:229-250.
- [27] Ugwa, K.A. and Agwu, I.A. 2013. Mathematical Analysis Of The Endemic Equilibrium Of The transmission Dynamics Of Tuberculosis. *International Journal of Scientific and Technology Research*. 2(12):263-269.
- [28] Hookworm in Humans. symptoms. Treatment. Life cycle. Prevention. <http://rajn.co/hookworms-in-humans-symptoms-treatment-life-cycle-prevention>. Accessed on 06 December 2018.
- [29] Mangal, T.D., Paterson, S. and Fenton, A. 2008. Prediction the impact of long-term temperature changes on the epidemiology and control of schistosomiasis: a mechanistic model. *Plos One*, 3(1), pp.1438.
- [30] Milner, F.A. and Zhao, R. 2008. A deterministic model of schistosomiasis with spartial structure. *Bio-sciences*. Eng. 5 (3), pp.505-522.

- [31] Chiyaka, E.T. and Garira, W. 2009. Mathematical analysis of the transmission dynamics of schistosomiasis in the human–snail hosts. *Biological Systems*. 17 (03) (2009):397-423.